

EFFECT OF CAPILLARY DIMENSIONS ON
DIE SWELL OF MOLTEN POLYMERS

27
55
72

EFFECT OF CAPILLARY DIMENSIONS ON
DIE SWELL OF MOLTEN POLYMERS

By

Dang, Huu Thanh, B. Sc.

Sunmark

A Project
Submitted to the Faculty of Graduate Studies
In Partial Fulfilment of the Requirements
For the Degree
Master of Engineering

McMaster University

January, 1974

MASTER OF ENGINEERING (1974)
(Chemical Engineering)

McMaster University
Hamilton, Ontario

TITLE: EFFECT OF DIE DIMENSIONS ON DIE SWELL OF
MOLTEN POLYMERS

AUTHOR: *Surname* Dang Huu Thanh, B. Sc.

SUPERVISOR: Dr. J. Vlachopoulos

NUMBER OF PAGES: 95

ABSTRACT

The effect of capillary dimensions on the die swell of molten polymers is investigated. Low and high density polyethylene, polypropylene, polystyrene are used to make investigation. It is found the die swell decreases with L/D . The plot of die swell index (d/D) vs. L/D has the shape of an exponential decay curve.

Bagley's decaying equation is used to fit the data. The effect of Deborah number on die swell phenomenon is also studied. The relationship between the recoverable shear strains of infinitely long capillary and the one with dimensions ratio L/D is obtained. This relationship could be used to estimate the die swell of short capillary from its value at equilibrium and polymer characteristics.

ACKNOWLEDGEMENTS

The author wishes to express his gratitude to his research advisor, Dr. John Vlachopoulos for his constant guidance and advice in data interpretation, and most of all, for his encouragement.

Gratitude is also due to the Department of Chemical Engineering, McMaster University, for its financial support to the author.

TABLE OF CONTENTS

	PAGE
I Introduction	1
II Literature Survey	
2.1) Experimental Observations	4
2.2) Some proposed mechanisms for die swell	6
III Theoretical Background	
3.1) Expressions predicting die swell	9
3.2) Capillary flow	12
3.3) Errors in Capillary flow	16
3.3.1) End effects	
3.3.2) Slip at the wall	
3.3.3) Heat effects	
IV Experimental Procedure	19
4.1) Equipment	19
4.2) System operation	21
4.3) Materials	21
4.4) Treatment of Data	23
4.4.1) Shear diagram	23
4.4.2) Melt fracture	28
4.4.3) Extrudate swelling	
4.4.4) Molten polymers behave as power law fluids	
V Results	
5.1) Reproducibility	33
5.2) Effect of temperature on die swell	34
5.3) Effect of shear stress and shear rate on die swell	36
5.4) Effect of molecular weight distributions on die swell	36
5.5) Effect of capillary dimensions on die swell	43
VI Analysis and Discussion	
6.1) Bagley's suggestion	49
6.2) Effect of Deborah number on die swell	
6.2.1) Time constant	57
6.2.2) Definition of Deborah number	60
6.2.3) Effect of Deborah number on polymer processing	60
6.3) Relationship between average recoverable shear strain of a short and long capillary	61
VII Conclusions	78
VIII Suggestions	79
IX Nomenclature	80
X References	83
XI Appendices	86
Experimental Data	86

LIST OF FIGURES

		PAGE
Figure 1.1	Schematic illustration of die swell phenomenon.	3
Figure 1.2	Decay of die swell with capillary dimensions	3
Figure 3.1	Schematic illustration of the flow in a capillary tube	13
Figure 3.2	Correction of tube length, L, by the addition of length ND	17
Figure 4.1	Plot of pressure vs. L/D of capillary	24
Figure 4.2	Plot of true shear stress versus pseudo shear rate	25
Figure 4.3	Plot of true shear rate versus true shear stress (LDPE)	26
Figure 4.4	Plot of true shear rate versus true shear stress (HDPE)	27
Figure 4.5	Plot of pseudo shear rate versus true shear stress on logarithmic scale	
	.1) Low density polyethylene	30
	.2) High density polyethylene	30
	.3) Polypropylene	31
	.4) Polystyrene	31
Figure 4.6	Velocity profiles for the isothermal flow of power law fluids through tubes	32
Figure 5.1	Effect of temperature on die swell	35
Figure 5.2	Effect of shear stress on die swell	
	.1) Low density polyethylene	37
	.2) High density polyethylene	38
	.3) Polypropylene	39
	.4) Polystyrene	40
Figure 5.3	Effect of molecular weight distribution on die swell	42
Figure 5.4	Effect of L/D on die swell of LDPE	44
Figure 5.5	Effect of L/D on die swell of HDPE	45
Figure 5.6	Effect of L/D on die swell of Polypropylene	46
Figure 5.7	Effect of L/D on die swell of Polystyrene	47
Figure 5.8	Effect of L/D on die swell of standard Polystyrene	48

Figure 6.1	Bagley's exponential decay equation is used to fit data for LDPE	52
Figure 6.2	Bagley's exponential decay equation is used to fit data for HDPE	53
Figure 6.3	Bagley's exponential decay equation is used to fit data for Polypropylene.	54
Figure 6.4	Bagley's exponential decay equation is used to fit data for Polystyrene.	55
Figure 6.5	Definition of time constant of a polymeric system.	59
Figure 6.6	Plot of die swell index vs. average residence time, LDPE	62
Figure 6.7	Plot of die swell index vs. average residence time, HDPE	63
Figure 6.8	Plot of die swell index versus average residence time, Polypropylene	64
Figure 6.9	Plot of die swell index versus average residence time, Polystyrene	65
Figure 6.10	Plot of average recoverable shear strain vs. pseudo shear rate, LDPE	67
Figure 6.11	Plot of average recoverable shear strain vs. pseudo shear rate, HDPE	68
Figure 6.12	Plot of average recoverable shear strain vs. pseudo shear rate, Polypropylene	69
Figure 6.13	Plot of average recoverable shear strain vs. Pseudo shear rate, Polystyrene	70
Figure 6.14	Plot of $\ln \left(\frac{\sigma_{L/D}}{\sigma_0} \right)$ vs. L/D for LDPE	73
Figure 6.15	Plot of $\ln \left(\frac{\sigma_{L/D}}{\sigma_0} \right)$ vs. L/D for HDPE	74

LIST OF TABLES

		PAGE
Table 4.1	Table of Capillaries used	20
Table 4.2	Table of Materials used	22
Table 6.1	Table of parameters of Equation (6.5) for LDPE (0701)	50
Table 6.2	Table of parameters of Equation (6.5) for LDPE (0118)	50
Table 6.3	Table of parameters of Equation (6.5) for HDPE(7930)	51
Table 6.4	Table of parameters of Equation (6.5) for Polypropylene	51
Table 6.5	Table of parameters of Equation (6.5) for Polystyrene(HF-55)	51
Table 6.6	Table of parameters of Equation (6.5) for Polystyrene (HT42.1)	56
Table 6.7	Table of exponent of power law fluid and slope of plot $\bar{\sigma}$ vs. G.	71
Table 6.8	Table of parameters of Equation (6.11) for LDPE	72
Table 6.9	Table of parameters of Equation (6.11) for HDPE	75
Table 6.10	Table of parameters of Equation (6.11) for Polypropylene	75
Table 6.11	Table of parameters of Equation (6.11) for Polystyrene	75

I INTRODUCTION

It is generally observed that when a molten polymer is forced from a reservoir, through a capillary, the extrudate diameter is not equal to the capillary diameter. (Figure 1.1). This phenomenon is known as "die swell", alternatively termed "memory", "puff up", or "Barus effect". This effect is usually described experimentally in terms of the swelling ratio (d/D) which is the ratio of extrudate diameter over the die diameter. The reasons for increased interest in this behaviour are numerous ranging from the desire to define the viscoelastic response of polymeric systems to the need to obtain direct relations between die swell and such polymer processing characteristics as swell in bottle blowing, thickness in extruded wire and cable insulation, "neck-in" in sheet extrusion, etc.

In spite of the importance of extrusion in polymer processing, there has not been much progress in relating die swell to the structure of the polymer.

It should be remembered that even non-elastic fluids will emerge from a capillary with a diameter different from that of the tube itself. Experiments indicated that for such non-elastic liquids at low Reynold's number, the emergent stream will exhibit a die swell (d/D) of about 1.10. For high Reynold's number flow, the emergent stream contracts giving a value (d/D) of about 0.87. There is a smooth transition between the two extreme limits, however, this effect is small compared to the large die swell observed with viscoelastic polymer melts.

Much effort has been devoted to find the expressions for polymer swell from a long capillary, assuming the capillary long enough, such that the effect of capillary length is excluded.

However, it has been observed that die swell greatly depends on the capillary dimensions. It is found that the swelling ratio decays exponentially with L/D (Figure 1.2). Although some work has been done to investigate the phenomenon, the explanation still remains unclear. The objectives of this project are:

- 1) To investigate the effect of capillary length on die swell for some types of commercial polymers low and high density polyethylene, polypropylene, polystyrene.
- 2) To examine the effects of extrusion variables, shear stress, shear rate, temperature, etc. on die swell phenomenon.

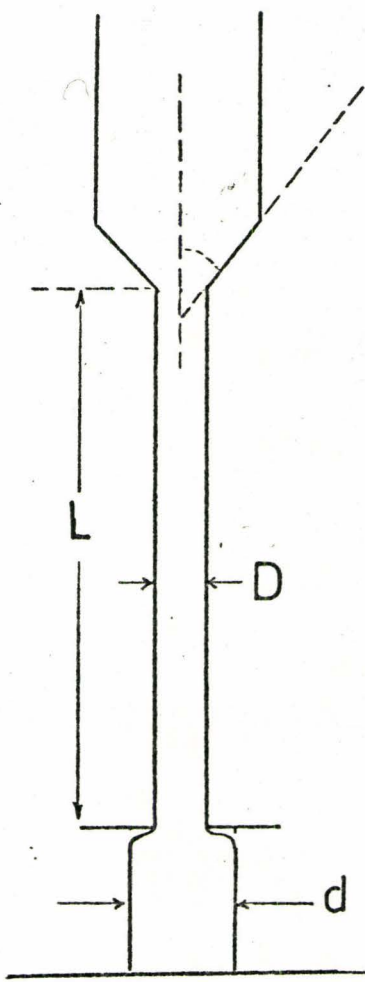


Fig.(1-1) Schematic illustration of the flow in a capillary.

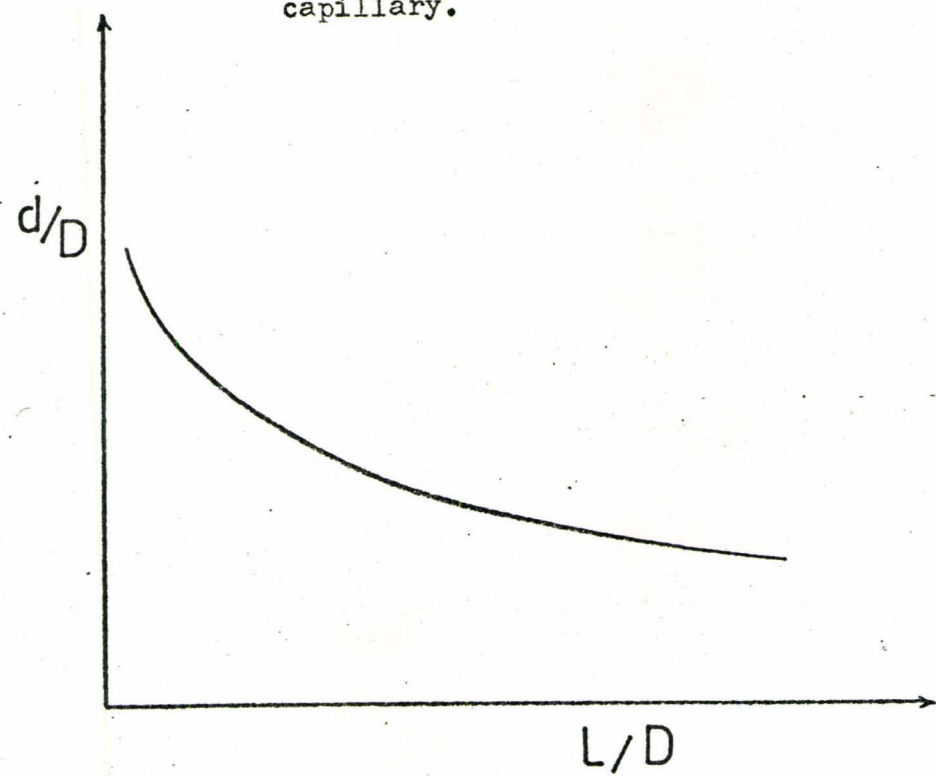


Fig.(1-2) Decay of die swell with capillary dimensions

II LITERATURE SURVEY

2.1 Experimental Observations

With the rapid growth of the polymer processing industry, the importance of die swell becomes evident. One area in which die swell investigations have proven useful is in the field of bottle blowing of thermoplastic materials. Wechsler and Bayliss⁽³⁶⁾ investigated the effect of die swell in this flow molding process. In extending this work, Beynon and Glyde⁽⁷⁾ studied (d/D) as a function of shear rate and found that (d/D) increased with shear rate up to the critical rate at which certain flow defects appeared. At this point (d/D) went through a maximum and then decreased. One problem in determining (d/D) at high output rate arises because extrudate distortion makes it difficult or impossible to measure extrudate diameter, but experimentally the distortion can be minimized by using tapered dies. Beynon and Glyde⁽⁷⁾ agreed with Dillon and Johnston⁽¹³⁾ that the swell did decrease with increasing temperature, but the maximum attainable swell also increased with temperature.

The importance of die swell as a variable in the extrusion blowing of polyethylene bottles is also discussed by Wilson⁽³⁷⁾ who noted that die swell tends to increase the diameter and depends on the extrusion rate, die design, and polymer composition.

Burgess and Lewis⁽¹⁰⁾ discussed the importance of die swell in die design, and noted that the actual amount of swell depended on the melt index of the polymer, the temperature and rate of extrusion, and die length, agreeing with others that the higher the temperature and the longer the die land the lower the swell, and the higher

the molecular weight the higher the swell. Actually, both melt index and die swell are complex functions of molecular weight, molecular weight distribution and branching. Thus a correlation between die swell and melt index may, in fact, be misleading. In the case of certain polymers, the generalizations given above may not be valid. In polyvinylchloride the degree of swell decreases with increasing molecular weight at a given shear rate⁽²⁹⁾.

In the past years, several fundamental investigations were made and these are described briefly below. According to Goren, Middleman, and Gavis⁽¹⁶⁾ swelling of jets of viscoelastic fluid might be due to relaxation of axial stresses.

Sieglaff⁽²⁹⁾ measured and correlated the effect of die geometry and polymer molecular weight on the post-extrusion of Polyvinylchloride resins but the experiments did not elucidate a mechanism.

Along with experimental data on die swell in polymer melts, Arai and Aoyama⁽¹⁾ discussed die wall restriction on the elastic shear deformation in steady flow. The shear modulus in steady flow must be a function of elastic shear stress, and the modulus increases with the molecular weight.

Huseby and Gogos⁽¹⁹⁾ pointed out that when recoverable strain in tube flow is plotted versus swelling ratio, the resulting curves are consistent with the observation that swelling ratio is an increasing function of normal stress.

Kruse⁽²¹⁾ measured extrudate swelling for polypropylene (mol. wt. 540,000) in a N_2 -pressurized rheometer at 400°F. The amount of swelling decreased with residence time in the die.

Bagley, Storey, and West⁽⁵⁾ also pointed out in their experiments with polyethylene that (d/D) depends, at constant pseudo shear rate, on the length-to-radius ratio of the capillary even though the viscosity does not.

2.2 Some Proposed Mechanisms for Die Swell

Spencer and Dillon⁽³¹⁾ considered the orientation - relaxation of polymer molecules on leaving the die as a major factor in the swelling phenomenon. Clegg⁽¹¹⁾ has disqualified this by stressing the necessity of comparing die transit time with relaxation time.

Metzner⁽²⁵⁾ has derived an expression for the expansion ratio (d/D) , that contains both axial and radial normal stresses.

In 1966, Nakajima and Shida⁽²⁷⁾ emphasized that elastic recovery is the most important factor in the swelling process in polymer melts. They derived an equation using the concept of rubber elasticity to calculate the tensile stress for the elastic deformation of the extrudate until its diameter becomes that of the capillary.

Following the analysis of Nakajima and Shida⁽²⁷⁾, Bagley and Duffey⁽³⁾ obtained an expression using a one-constant stored energy function for a Mooney material⁽²⁶⁾.

Bagley and Duffey⁽³⁾ also carried out an energy balance analysis along Graessley's lines⁽¹⁷⁾ and arrived at another equation.

Graessley, Glasscock and Crawley⁽¹⁷⁾ assumed that the increase in the diameter of the extrudate is due to the release of elastic energy stored in the fluid inside the capillary. They introduced a modulus of elasticity estimated from the theory of rubber elasticity in terms of the average molecular weight between entanglements.

Recently Tanner⁽³²⁾ has proposed another expression relating recoverable shear at the wall to the swelling ratio based on the elastic recovery concept of a Poiseuille flow of a BKZ fluid. The BKZ fluid obeys the constitutive equation postulated by Bernstein, Kearsley and Zapas⁽⁶⁾. This constitutive equation is one of the integral type representations which can take the strain history into account.

To explain the effect of die dimensions on die swell of extruded polymers, Bagley⁽⁴⁾ proposed that the swell is considered as the unretarded recovery of elastic strain imparted to polymer by two parts:

- a) Elastic deformation at the entrance
- b) Elastic deformation during shearing flow through the die due to the steady normal stresses

In long land die (e.g. large L/D capillaries) the entrance strain decays along the length of the die, and the die swell may be viewed as a consequence of the deformation due to normal stress generated in the shearing field. In a very short die the entrance deformation predominates.

The decay of swelling with capillary length might be expected to be a typical relaxation process, showing an exponential dependence on the time of transit through the die. If B is defined as the ratio of extrudate diameter to die diameter and t_a is the average time of transit through the die, then Bagley⁽⁵⁾ proposed the following decaying equation:

$$(B - B_\infty) = (B_0 - B_\infty) \exp(-kt_a) \quad (2.1)$$

where B_0 and B_∞ are values of B at zero and infinite transit times respectively and k is a decay rate constant.

Kawasaki, Tat Susaka and Ono⁽²⁰⁾, in a recent paper, considered the extruding process as a series of deformation mechanisms

- 1) Elongation from the reservoir to the entrance of the capillary

2) The release of inner stress proceeding under a constant elongation

3) Recovery of remaining strain after leaving the capillary

Next, an Oldroyd model (series of a dash pots (μ_1) and Voigt elements (μ_2 and G_2)) are employed as the representative rheological model for molten polymers. This led them to an equation presenting die swell as function of polymer characteristics and die dimensions.

$$\text{Log} \left\{ 1 - \frac{1}{(B-\Delta)^2} \right\} = - \text{Log} \left\{ \frac{\gamma(t_1)}{\gamma_2(t_1)} \right\} - \frac{1.74}{\dot{\gamma}_a^\tau} \left(\frac{L}{R} \right)$$

in which $\tau = \frac{\mu_1 + \mu_2}{G_2}$, $\dot{\gamma}_a$ is pseudo shear rate, B is die swell index $\left(\frac{d}{D}\right)$, Δ is die swell index of infinitely long capillary.

By varying the capillary length (L/R) while fixing the apparent shear rate $\dot{\gamma}_a$, a linear relation exists between $\text{Log} \left\{ 1 - \frac{1}{(B-\Delta)^2} \right\}$ versus (L/R).

III THEORETICAL BACKGROUND

3.1 Expressions Predicting Die Swell

Several expressions have been proposed for the prediction of die swell, centered on the concept of elastic recovery of the swelling process. These expressions relate the swelling ratio (d/D) to the recoverable shear (σ).

The recoverable shear strain is usually defined from Hooke's law which seems to hold for most polymers:

$$\sigma = \tau_{12} J_o \quad (3.1)$$

where τ_{12} is the shear stress and J_o the shear compliance ($J_o = 1/G_o$ where G_o is the shear modulus).

Coleman and Markovitz⁽¹²⁾ have shown that:

$$\tau_{11} - \tau_{22} = 2J_o \tau_{12}^2 \quad (3.2)$$

where τ_{11} and τ_{22} are the first and second normal stress respectively.

From Equation (3.1) and (3.2)

$$\frac{\tau_{11} - \tau_{22}}{2\tau_{12}} = \sigma \quad (3.3)$$

This expression led some authors to the definition of σ as "Stress Ratio".

Nakajima and Shida⁽²⁷⁾ used the concepts of rubber elasticity. They assumed that the polymer, in a capillary, is in an elongated state in the direction of the capillary axis. Consequently, the polymer in the capillary has the elastic energy in the same sense as the potential energy of a stretched spring. This energy will recover after passing through the capillary and this causes the die swell.

Assuming the molecular network of polymer is a Gaussian one⁽²²⁾, Nakajima and Shida⁽²⁷⁾ calculated the tensile stress for the elastic

deformation of the extrudate until its diameter becomes that of the capillary:

$$\frac{\tau_t}{NakT} = (\lambda - \lambda^{-2}) \quad (3.4)$$

where $\lambda = (d/D)^2$, τ_t is the tensile stress, Na & k are the number of chains per unit volume, and Boltzmann's constant respectively.

Elastic modulus G_o , is given ⁽³⁵⁾ by:

$$G_o = NakT \quad (3.5)$$

Therefore, $\frac{\tau_t}{NakT}$ has a meaning of tensile strain. Here Nakajima

made a bold assumption that the tensile strain is taken as the quantitative expression for the recoverable strain in the flow:

$$\bar{\sigma} = \frac{\tau_t}{NakT} = \left(\frac{d}{D}\right)^2 - \left(\frac{d}{D}\right)^{-4} \quad (3.6)$$

Assuming the parabolic velocity profile, it has been shown ⁽²²⁾ that:

$$\sigma_w = \sqrt{3} \bar{\sigma} \quad (3.7)$$

In case of a flat velocity profile:

$$\sigma_w = \sqrt{2} \bar{\sigma} \quad (3.8)$$

in which $\bar{\sigma}$ and σ_w are the average recoverable shear strain and at the wall respectively. If the parabolic velocity profile is assumed then:

$$\sigma_w = \sqrt{3} \left\{ \left(\frac{d}{D}\right)^2 - \left(\frac{d}{D}\right)^{-4} \right\} \quad (3.9)$$

Bagley and Duffey ⁽³⁾ followed the analysis of Nakajima ⁽²⁷⁾ and used one constant stored energy function for a Mooney material ⁽²⁶⁾.

$$\bar{W} = C_1 (I_1 - 3) \quad (3.10)$$

where I_1 is the first strain invariant and C_1 is a constant i.e.,

$$I_1 = \lambda_1^2 + \lambda_2^2 + \lambda_3^2 \quad (3.11)$$

$\lambda_1, \lambda_2, \lambda_3$ are the principal extension ratios which are given as:

$$\lambda_1 = \lambda \quad (3.12)$$

$$\lambda_2 = \lambda_3 = \lambda^{-1/2} \quad (3.13)$$

then

$$\bar{W} = C_1 (\lambda^2 + (2/\lambda) - 3) \quad (3.14)$$

and force f_b which is defined as:

$$f_b = \frac{d\bar{w}}{d\lambda} = 2C_1 (\lambda - \lambda^{-2}) \quad (3.15)$$

The tensional stress t_{xx} acting on the cylinder in the final elongated state is then:

$$t_{xx} = \lambda f_b = 2C_1 (\lambda^2 - \lambda^{-1}) \quad (3.16)$$

on the other hand⁽³⁵⁾

$$G_o = 2C_1 \quad (3.17)$$

therefore, assuming

$$\bar{\sigma} = t_{xx} / G_o \quad (3.18)$$

Bagley obtained the relation:

$$\bar{\sigma}^2 = \left(\frac{d}{D}\right)^4 - \left(\frac{d}{D}\right)^{-2} \quad (3.19)$$

Bagley and Duffey⁽¹⁹⁾ also carried out an energy balance analysis along Graessley's⁽¹⁷⁾ lines. The strain energy function in shear inside the capillary is given⁽²⁶⁾

$$\bar{W}_{\text{shear}} = \frac{1}{2} G_o \bar{\sigma}^2 \quad (3.20)$$

in the elongational case, in passing from the unstrained material to the strained case the stored strain energy per unit volume is:

$$\bar{W}_{\text{elongation}} = \frac{1}{2} G_o (\lambda^2 + \frac{2}{\lambda} - 3) \quad (3.21)$$

Since $\bar{W}_{\text{elongation}}$ must equal \bar{W}_{shear} at the die exit, we obtain (for

$$\lambda = (d/D)^2)$$

$$\bar{\sigma}^2 = (d/D)^4 + 2/(d/D)^2 - 3 \quad (3.22)$$

Another expression relating recoverable shear at the wall to the swelling ratio has been proposed by Tanner⁽³²⁾ based on the elastic recovery concept of a Poiseuille flow of BKZ fluid⁽⁶⁾.

He made the following assumptions:

- 1) The flow is isothermal and incompressible
- 2) The die is long enough
- 3) Inertial effects in the flow are ignored
- 4) Gravity, other body forces, and surface tension forces are ignored
- 5) The flow at exit may be approximated by a sudden strain which takes the fluid from the viscometric stress state inside the tube instantaneously to the zero stress state outside the tube
- 6) As a constitutive equation, BKZ form⁽⁶⁾ is assumed

On the basis of these assumptions, Tanner got the expression

$$\sigma_w^2 = 2\left[\left(\frac{d}{D}\right)^6 - 1\right] \quad (3.23)$$

Since (d/D) approaches a value of $1.10^{(17)}$ for slow Newtonian flow,

Tanner suggested a modification to the previous equation

$$\sigma_w^2 = 2\left[\left(\frac{d}{D}\right) - 0.1\right]^6 - 1 \quad (3.24)$$

An evaluation of the above equation predicting die swell has been carried out by Vlachopoulos, Horie, and Lidorikis⁽³⁵⁾.

3.2 Capillary Flow:

The three basic equations which describe the flow of a fluid in a capillary are the equations of continuity, momentum, and energy. The momentum equation in its most general form is:

$$\frac{D\bar{v}}{Dt} = -\nabla P - \nabla \cdot \bar{\tau} + \Sigma \rho F \quad (3.25)$$

In cylindrical co-ordinates (r, θ, z) Equation (3.25) may be represented in terms of τ , by the following equation. Assuming gravity to be the only field force present, so only z component is important.

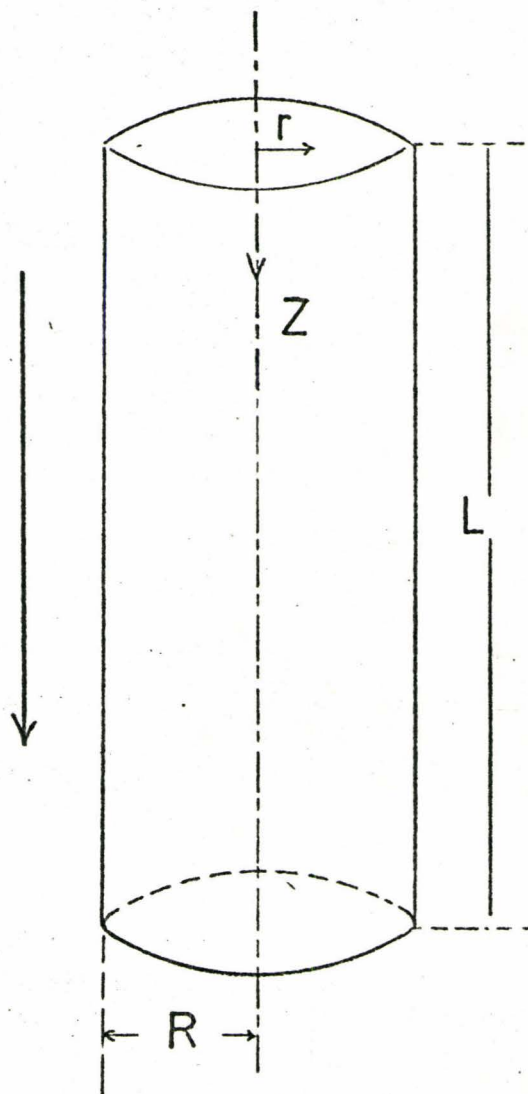


Fig. (3-1) Schematic illustration of flow in a capillary tube

z component:

$$\rho \left(\frac{\partial V_z}{\partial t} + \frac{V_r \partial V_z}{\partial r} + \frac{V_\theta}{r} \frac{\partial V_z}{\partial \theta} + \frac{V_z \partial V_z}{\partial z} \right) = -\frac{\partial P}{\partial z} - \left\{ \frac{1}{r} \frac{\partial}{\partial r} (r \tau_{rz}) + \frac{1}{r} \frac{\partial \tau_{\theta z}}{\partial \theta} + \frac{\partial \tau_{zz}}{\partial z} \right\} + \rho g_z \quad (3.26)$$

The following assumptions will be made for the capillary flow:

- 1) The flow is steady
- 2) The axial component of the velocity (V_z) is assumed to be a function of the radial distance (r) alone
- 3) There are no radial and tangential components of the velocity
- 4) There is no slippage at the wall
- 5) The tube is sufficiently long so that end effects are negligible
- 6) The fluid is incompressible
- 7) Isothermal conditions prevail throughout
- 8) Viscosity doesn't change appreciably with change in pressure down the tube

Then the Equation (3.26) reduces to

$$0 = -\frac{\partial P}{\partial z} - \frac{1}{r} \frac{\partial}{\partial r} (r \tau_{rz}) \quad (3.27)$$

which becomes upon integration;

$$\tau_{rz} = -\frac{r}{2} \frac{\partial P}{\partial z} \quad (3.28)$$

At the wall, since $r = R$ and $\tau_{rz} = \tau_w$

$$\tau_w = -\frac{R}{2} \frac{dP}{dz} \quad (3.29)$$

From Equations (3.28) and (3.29)

$$\tau_{rz} = \frac{r}{R} \tau_w \quad (3.30)$$

For laminar steady flow through a capillary of radius R , the volume flow rate Q is given by the integral:

$$Q = 2\pi \int_0^R r V_z(r) dr$$

Using Equation (3.30) one gets:

$$Q = 2\pi \left(\frac{R}{\tau_w} \right)^2 \int_0^{\tau_w} \tau_{rz} V_z d\tau_{rz} \quad (3.31)$$

The velocity can be given by

$$v_z = \int_r^R \left(- \frac{dv_z}{dr} \right) dr = \frac{R}{\tau_w} \int_{\tau}^{\tau_w} \left(- \frac{dv_z}{dr} \right) d\tau_{rz} \quad (3.32)$$

Combining Equation (3.31) and (3.32) gives:

$$\frac{4Q}{\pi R^3} = \frac{8}{\tau_w^3} \int_0^{\tau_w} \tau_{rz} \int_{\tau_{rz}}^{\tau_w} \left(- \frac{dv_z}{dr} \right) d\tau_{rz} d\tau_{rz} \quad (3.33)$$

Integrate by parts

$$\frac{4Q}{\pi R^3} = \frac{4}{\tau_w^3} \int_0^{\tau_w} \tau_{rz}^2 \left(- \frac{dv_z}{dr} \right) d\tau_{rz} \quad (3.34)$$

which is the general equation that relates the flow to the velocity gradient in the system.

* For a Newtonian fluid Equation (3.34) becomes:

$$\frac{4Q}{\pi R^3} = \frac{\tau_w}{\mu} = - \frac{R}{2\mu} \frac{dP}{dz} \quad (3.35)$$

This equation can be used to define a capillary shear diagram as $4Q/\pi R^3$ versus τ_w . The term $4Q/\pi R^3$ is called "pseudo-shear rate".

A simple relation between the flow rate and the wall shear rate was obtained by Rabinowitsch differentiation of Equation (3.34)

$$\frac{d \left[(\tau_w^3 (4Q/\pi R^3)) \right]}{d\tau_w} = 4\tau_w^2 \left(- \frac{dv_z}{dr} \right)_w \quad (3.36)$$

which results in:

$$\left(- \frac{dv_z}{dr} \right)_w = \frac{3}{4} \left(\frac{4Q}{\pi R^3} \right) + \frac{\tau_w}{4} \frac{d(4Q/\pi R^3)}{d\tau_w} \quad (3.37)$$

This equation can be used directly to reduce the capillary shear diagram to the basic shear diagram as follows:

- 1) For a given value of τ_w , the value of $4Q/\pi R^3$ can be obtained from the data
- 2) The slope of the curve can also be obtained at that point.
- 3) Thus $\left(-\frac{dV_z}{dr}\right)_w$ is calculated from Equation (3.37)
- 4) Both τ_w and $\left(-\frac{dV_z}{dr}\right)_w$ are measured at the same point and thus are the terms of the basic diagram.

3.3 Errors in Capillary Flow:

3.3.1 End effects:

Equation (3.30) was derived from the assumption that there is no entrance and exit of the tube, however, the end effects cause an appreciable amount of pressure drop, the estimation of τ_w by Equation (3.30) is in error. One way to eliminate the entrance effect is to use large length-to-diameter ratio of the capillary to reduce the error but it is difficult to work with long capillaries.

An empirical method of correcting for entrance effects has been suggested by Bagley⁽²⁾. The procedure developed by Bagley is outlined below.

Following Figure (3.2), P_s is the pressure gradient in the region of steady flow then:

$$P_s = \frac{\Delta P}{ND+L} \quad (3.38)$$

where ND , as shown by Figure (3.2), represents a fictitious tube length that, when added to the actual length, enables one to use the over-all pressure drop in calculating the gradient in the steady flow section.

The expression for the shear stress at the wall in the steady flow section of the tube can now be written:

$$\tau_w = \frac{D}{4} \left(\frac{\Delta P}{L+ND} \right) \quad (3.39)$$

1. Tapered entrance
2. Entrance region
3. Region of steady flow
4. Exit region

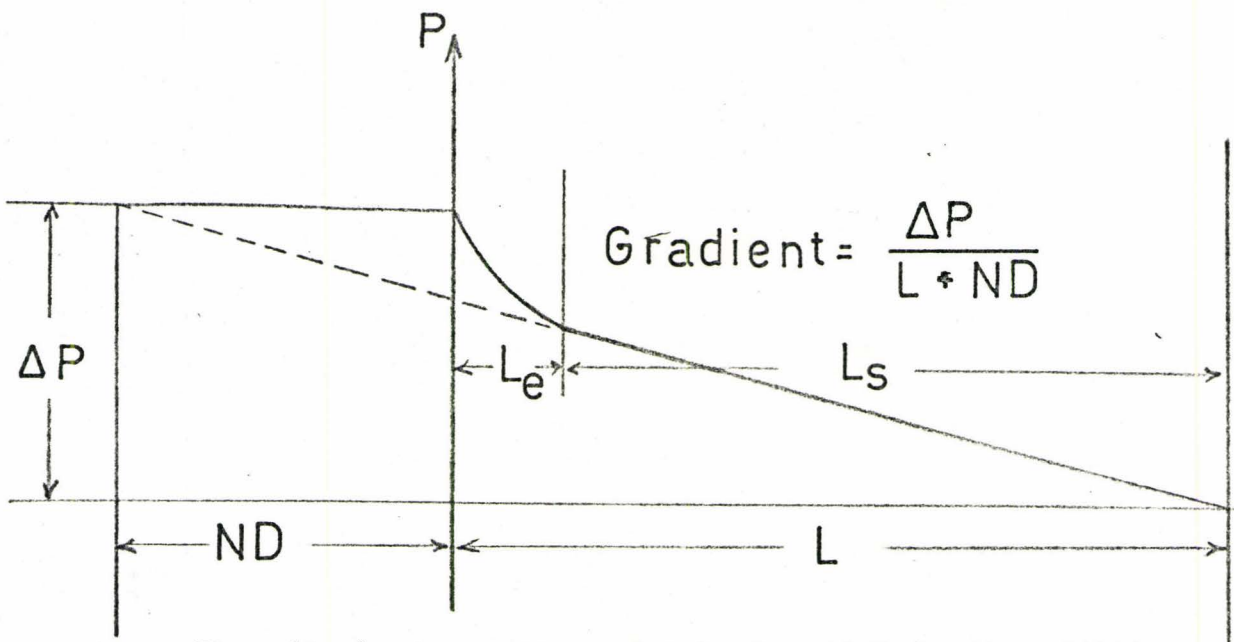
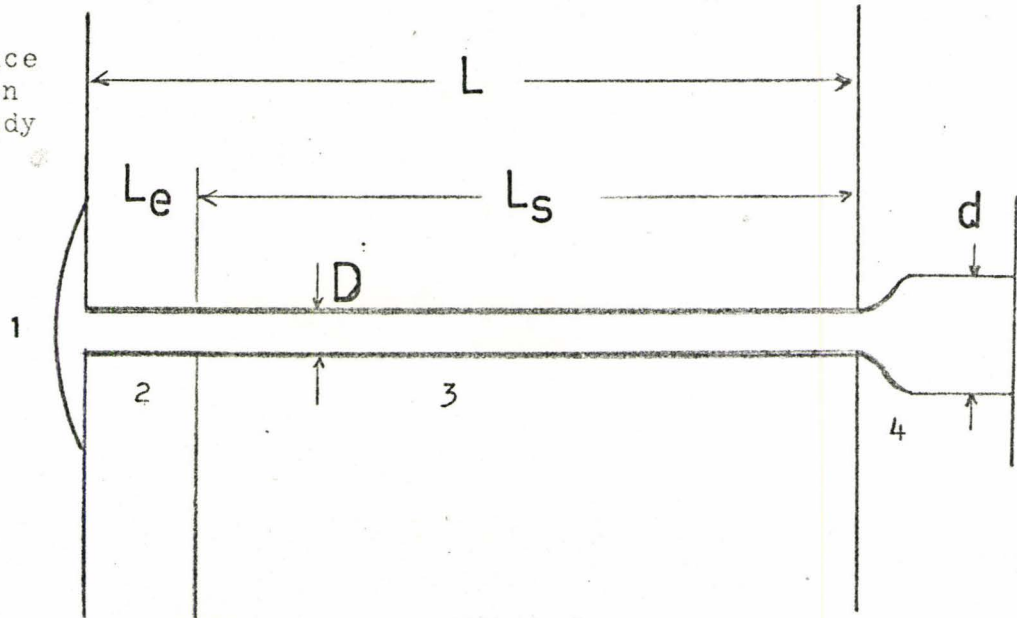


Fig. (3-2) Correction of tube length L by the addition of length ND

τ_w is a unique function of Γ , which is defined as:

$$\Gamma = \frac{4Q}{\pi R^3}$$

$$\tau_w = g(\Gamma)$$

Rearranging Equation (3.39) becomes:

$$\frac{L}{D} = -N + \frac{\Delta P}{4g(\Gamma)} \quad (3.40)$$

N: is the total end correction.

Equation (3.40) suggests that the value of N might be determined from flow measurements made with a series of capillary tubes having different L/D ratios. For each tube, the pressure drop ΔP giving some specific value of pseudo shear rate would be determined. Then, by plotting (L/D) versus ΔP , a straight line having $-N$ as an intercept would be obtained. The corrected value of τ_w will be calculated from (3.39).

3.3.2 Slip at the Wall

The derivation of Equation (3.30) is based on the assumption that velocity is zero at the wall of the capillary. Brodkey⁽⁸⁾ has shown that a plot of $4Q/\pi R^3$ versus τ_w will determine the existence or absence of slip. For a system with slip, $4Q/\pi R^3$ must decrease at constant τ_w , with increasing diameter of the capillary. It is often found that in the flow of molten polymers, a no-slip condition can be assumed.⁽⁹⁾

3.3.3 Heat Effects

It is assumed that the flow is in isothermal condition. Gerrard and Appeldoorn⁽¹⁵⁾ have shown that the use of an average temperature is unimportant as it is insensitive to changes that can occur because of temperature gradient. Lidorikis⁽²³⁾ has shown that heat effect is negligible under the usual operating conditions of viscometer.

IV EXPERIMENTAL PROCEDURE

4.1 Equipment

The experiment was carried out by using the Instron capillary rheometer model 3211.

The model 3211 Rheometer has a synchronous motor and gearbox which drives the plunger at a constant rate, independent of load on the plunger. Thus, the volumetric flow rate through the capillary will be constant, making it unnecessary to collect extrudate, weigh it and back - calculate through the density to obtain the volumetric rate of flow.

The push button drive system of the 3211 Rheometer makes it simple to instantaneously select from six shear rates (plunger speeds) for testing a single load of material in the barrel. The maximum and minimum shear rates span a 333:1 range with a given capillary, and the plunger speeds are adjustable from 20 inches/minute to 0.006 inches/minute by means of changing gears.

Since the viscosity of many materials is extremely temperature dependent, the model 3211 Rheometer is designed to control absolute temperature within $\pm 1^{\circ}\text{C}$ and the temperature profile from the top to the bottom of the rheometer barrel can be controlled to within $\pm 2^{\circ}\text{C}$.

To investigate the effect of capillary dimensions on die swell, nine capillaries were used, most capillaries are made of brass, all have the entry angle of 90 degrees. The length to diameter ratios of these capillaries vary from zero to twenty five. Table(4-1) gives the specifications of these capillaries.

TABLE OF CAPILLARIES USED

NO.	MATERIAL	ENTRANCE ANGLE	DIAMETER (INCHES)	LENGTH (INCHES)	L/D
1	Brass	90°	0.0525	1.300	24.8
2	Brass	90°	0.0525	1.050	20.0
3	Brass	90°	0.0525	.839	16.0
4	Brass	90°	0.0525	.519	9.9
5	Brass	90°	0.0525	.418	7.9
6	Stainless Steel	90°	0.0525	.281	5.01
7	Brass	90°	0.0525	.157	2.99
8	Stainless Steel	90°	0.0525	.0517	0.99
9	Brass	90°	0.0525	~0	~0

Table 4.1

4.2 System Operation:

The material to be tested is loaded into the extrusion barrel, allowed to come up to temperature and is forced, at constant speed, through the capillary. The plunger forces, corresponding to selected plunger speeds, are indicated on a recorded paper. The forces and corresponding plunger speeds can be converted to shear stress and shear rate by a simple mathematical calculation involving the geometry of the barrel and capillary as discussed in Section (4.4).

4.3 Materials

The commercial samples of four polymers are used to make the investigation:

- (1) Low density (Branched) polyethylene (Union Carbide Canada Limited)
- (2) High density (Linear) polyethylene (Union Carbide Canada Limited)
- (3) Polypropylene (Shell Canada Limited)
- (4) Commercial Polystyrene (Monsanto Company, Limited)
- (5) Standard Polystyrene (Pressure Chemical Company, Pittsburgh Pa.)

The blent polystyrene was prepared by mixing and dissolving the narrow distribution polystyrene in tetrahydrofuran (at room temperature), then precipitating and filtering with purified methanol, and evaporating the remaining in a vacuum oven.

The average molecular weight of blent polymer is calculated from the following equations:

$$\bar{M}_w = \frac{\sum W_i (M_w)_i}{\sum W_i}$$

$$\bar{M}_n = \frac{\sum W_i}{\sum (W_i / (\bar{M}_{ni}))}$$

$$\bar{M}_z = \frac{\sum_i W_i \bar{M}_{wi}^2}{\sum_i W_i \bar{M}_{wi}}$$

$$\bar{M}_{z+1} = \frac{\sum_i W_i \bar{M}_{wi}^3}{\sum_i W_i \bar{M}_{wi}^2}$$

POLYMER SAMPLES USED

TRADE NAME	\bar{M}_w^*	\bar{M}_w / \bar{M}_n^*	POLYMER	SUPPLIER
DFDY-0701	51,300	3.72	L.D.Polyethylene	Union Carbide
DFDQ-0118	53,500	3.00	L.D.Polyethylene	Canada, Ltd.
DFDY-6005	82,800	3.96	L.D.Polyethylene	
DMDA-7930	69,590	4.17	H.D.Polyethylene	Union Carbide
PP-5820	287,000	--	Polypropylene	Canada, Ltd.
LUSTREX HF-55	320,000	3.10	Polystyrene	Shell Canada
LUSTREX HT 42.1	---	--		Ltd.
BLENT POLYSTYRENE (mixing two standard Polystyrenes, one having $\bar{M}_w = 1,800,000$	498,000	2.21	Polystyrene	Monsanto Company, Limited
				Pressure Chemical Company

$$\frac{\bar{M}_w}{\bar{M}_n} < 1.2$$

and another having

$$\bar{M}_w = 200,000$$

$$\frac{\bar{M}_w}{\bar{M}_n} = 1.06 \quad) \quad \text{BLENT POLYSTYRENE having } \frac{\bar{M}_z \bar{M}_{z+1}}{\bar{M}_w^2} = 11.04$$

* Determined by Suppliers

TABLE 4-2

4.4 Treatment of Data

4.4.1 Shear Diagram

The calculation of basic shear diagram in capillary rheometer requires the measurements of volumetric flow rate and the pressure drops through the capillary. Shear stress and shear rate at the wall are obtained as follows:

- 1) From the volumetric flow rates, pseudo shear rate ($4Q/\pi R^3$) is obtained.
 - 2) At a value of pseudo shear rate, the corresponding pressure is obtained and cross plotted versus the L/D ratio (Fig. 4.1)
 - 3) The intersections of these lines with x-axis are used to calculate the corrected shear stresses.
 - 4) From the plot of corrected shear stress versus pseudo shear rate (Fig. 4.2), the slope is obtained, thus $-dV_z/dr (= \dot{\gamma}_w)$ is calculated by using Rabinowitsh Equation (Eq. 3.37)
 - 5) The plot of $\dot{\gamma}_w$ versus τ_w gives the basic shear diagram (Fig. 4.3)
- Value of Pressure, $4Q/\pi R^2$, τ_w , $\dot{\gamma}_w$ and swelling ratio for all polymers are given in Appendix I.

4.4.2 Melt Fracture

The incipience of melt fracture was determined visually by the appearance of a pronounced distortion in the extrudate. This was fairly easy for most polymer samples. The Instron capillary rheometer is equipped with a chart recorder. At the incipience of melt fracture, the chart records a zig-zag line, however, the best way to recognize the on-set of melt fracture is by observing the extrudate distortion.

$G = 386 \text{ sec}^{-1}$

Fig. (4-1) Plot of pressure vs. L/D

Low Density Polyethylene

 $\bar{M}_w = 53,500$ $\bar{M}_w / \bar{M}_n = 3.00$

Temp. = 150°C

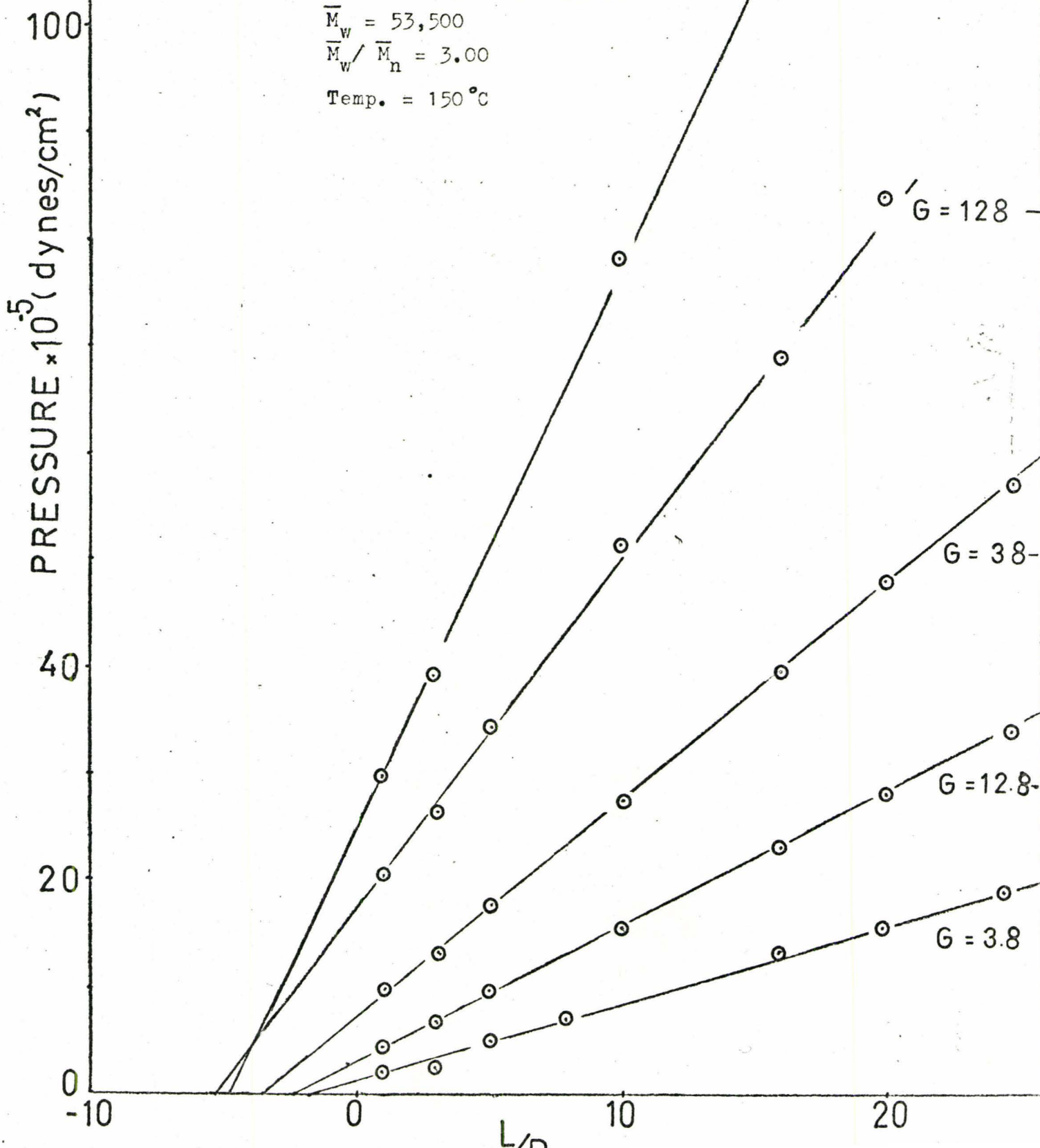


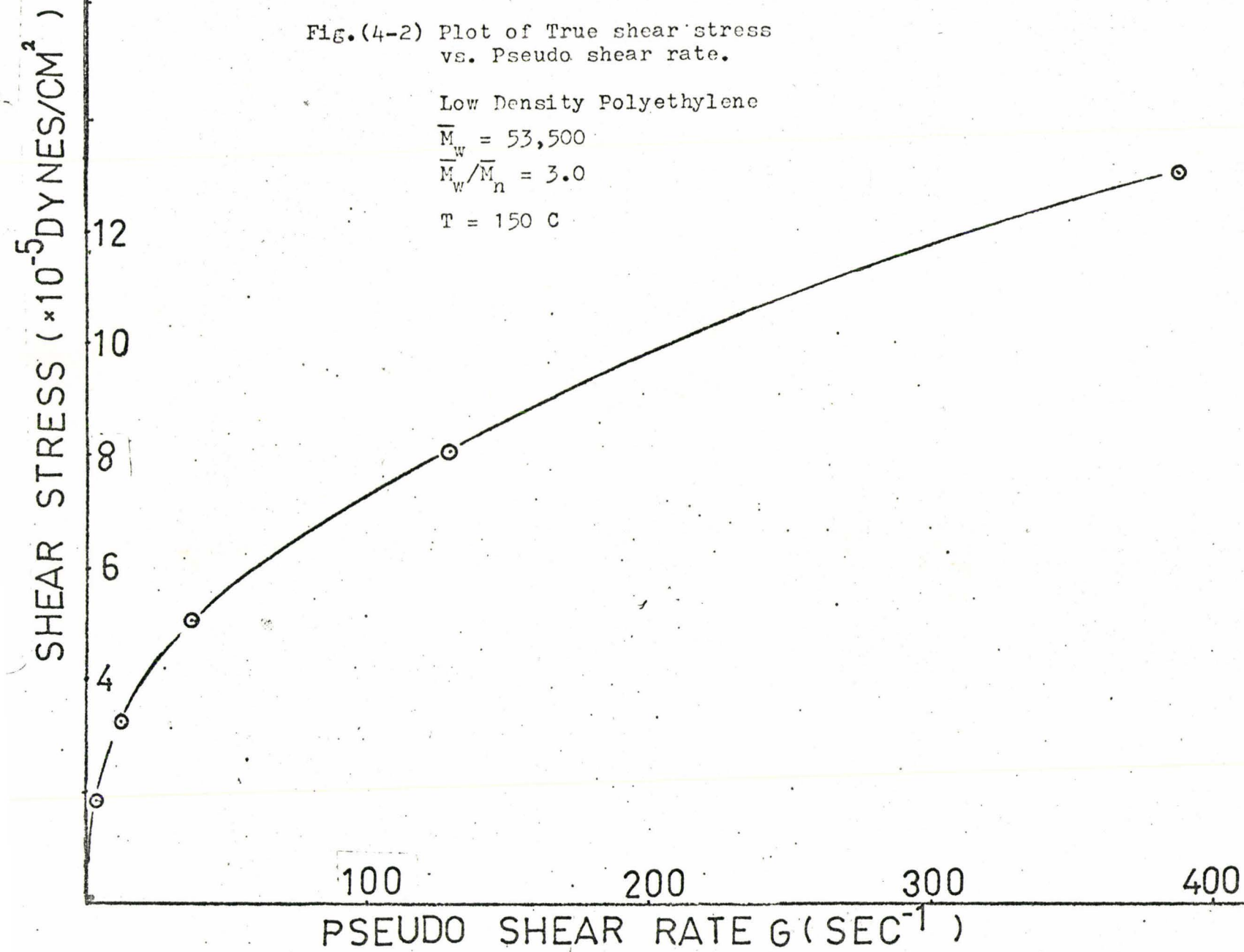
Fig.(4-2) Plot of True shear stress vs. Pseudo shear rate.

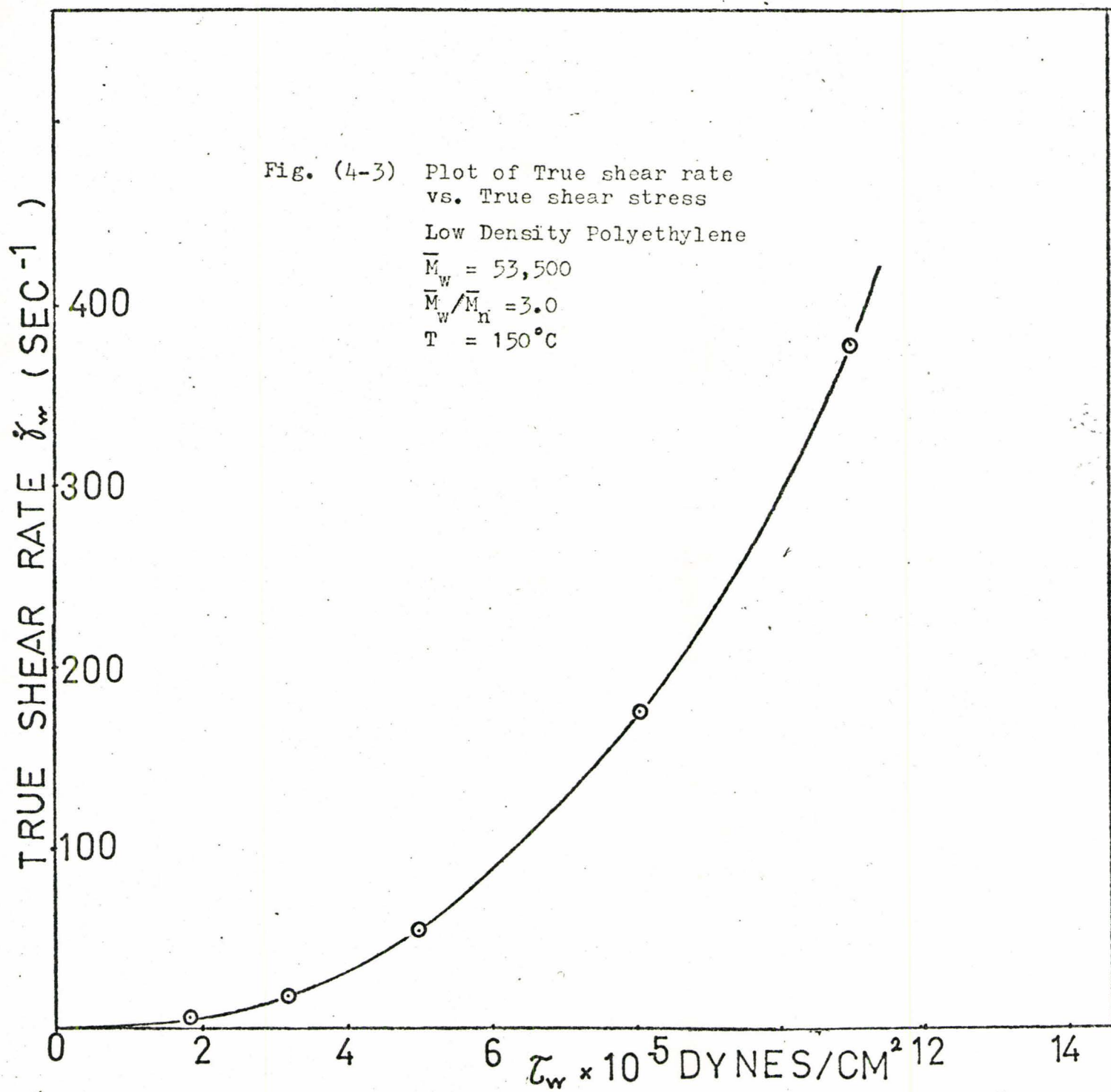
Low Density Polyethylene

$$\bar{M}_w = 53,500$$

$$\bar{M}_w/\bar{M}_n = 3.0$$

$$T = 150 \text{ C}$$





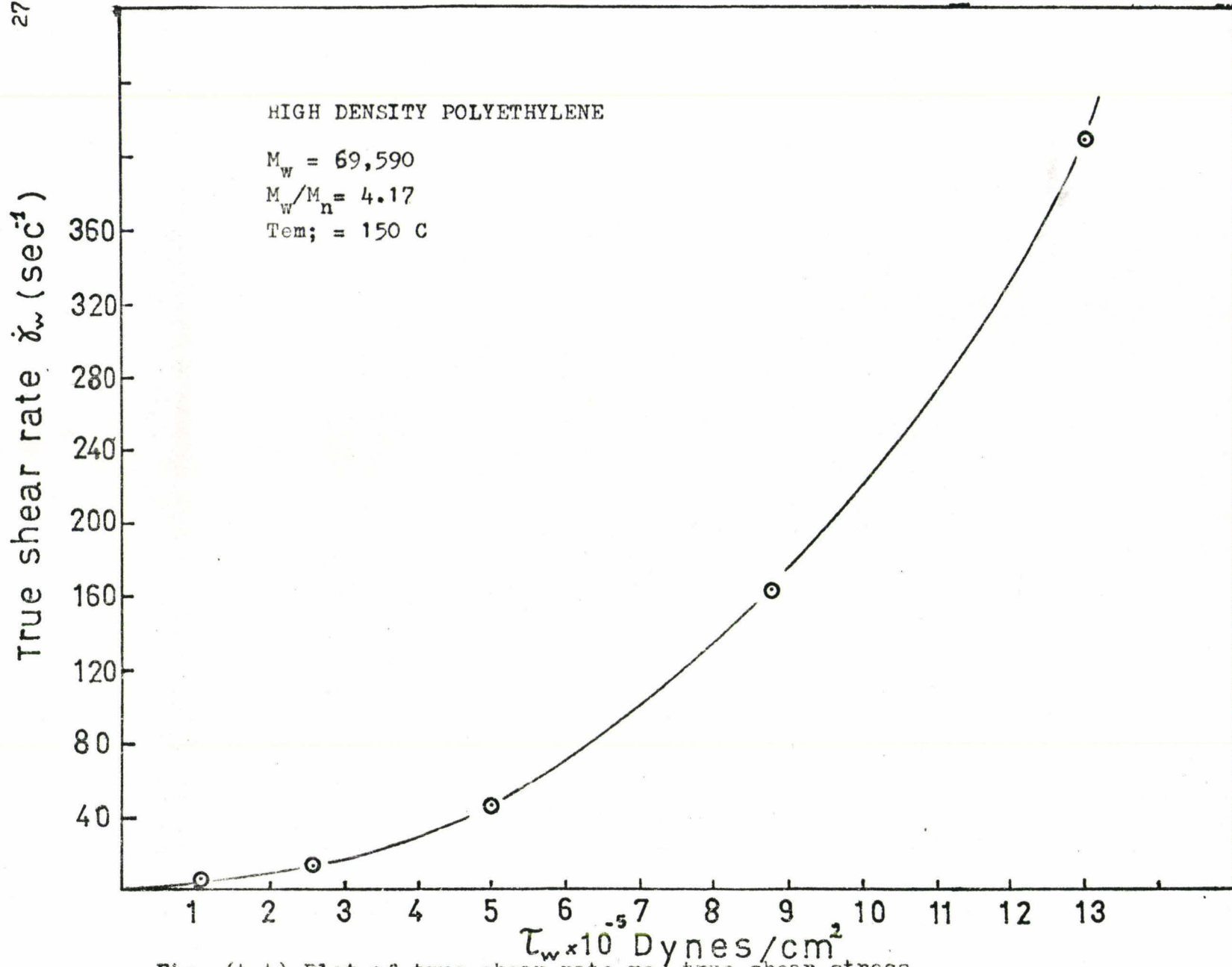


Fig. (4.4) Plot of true shear rate vs. true shear stress.

4.4.3 Extrudate Swelling

The diameter of the extrudate was obtained by extruding the polymer melt downward directly into the air. All experiments were made in this manner, and the diameter of hardened extrudate was measured with a micrometer to the nearest 0.001 inch.

To obtain a specimen for measurement, the extruding molten rod was first cut short at the capillary. As fresh extrudate emerged, it cooled and hardened in the first few inches beyond the exit. The diameter of the extrudate decreases because of elongation at the exit from the increasing weight of the extrudate. All diameter measurements were made approximately 1/4 inch back from the leading end where elongation was negligible. The extrudate was quite uniform in diameter at low shear stresses but lost their uniformity at the critical stresses due to the extrudate distortion.

All the diameters of extrudates have been corrected for the density difference between room temperature and extrusion temperature

$$\text{i.e. } \frac{d}{d_0} = (\rho_0^*/\rho^*)^{1/3}$$

where d = swelled diameter of melt at extrusion temperature

d_0 = swelled diameter of frozen polymer

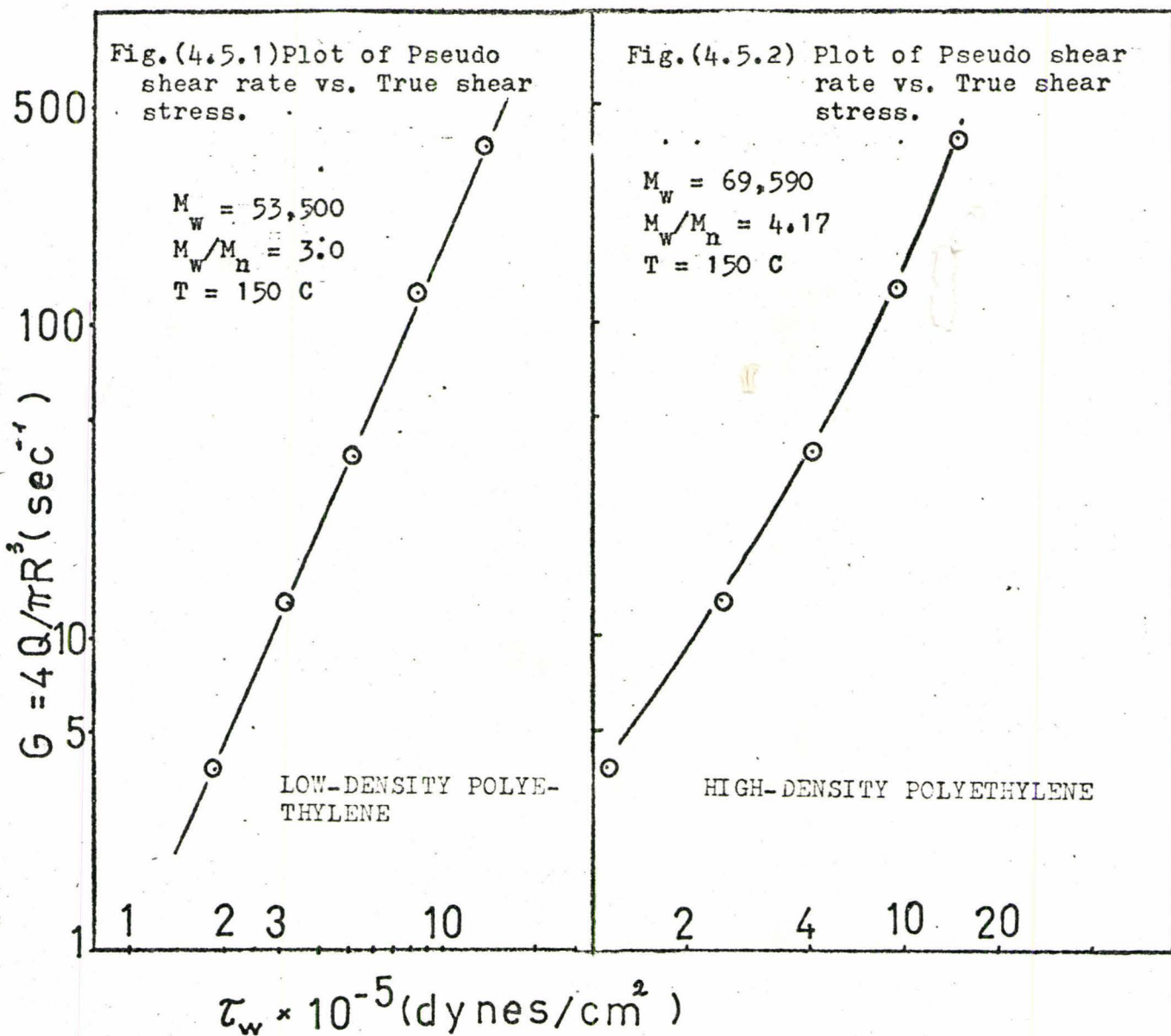
ρ^* = density of melt, ρ_0^* = density of frozen polymer

4.4.4. Molten Polymers Behave as a Power Law Fluid

Logarithmic flow curves of molten polymers often appear to be straight if restricted to one or two decades of shear rate, but when extended over several decades, they are usually not straight.

Logarithmic plots of shear rate versus shear stress for investigated polymers are shown in Figure (4.5.) It is observed that low density polyethylene, in the range of experimental data, follows the power-law fluid ($\tau = K\dot{\gamma}^n$) with n in the range of 0.4-0.5

The flow curves of high density polyethylene, polypropylene, and especially polystyrene somewhat deviate from power law. This deviation is what we would expect because molten polymer is viscoelastic material, its rheological equation is not exactly represented by the power law, every rheological model contains at least two parameters, one for viscosity and the other for elasticity characteristics.



Plot of Pseudo shear rate vs. True shear stress

Fig.(4-5.3) Plot of Pseudo shear rate vs. true shear stress

POLYPROPYLENE

$\bar{M}_w = 287,000$

$T = 180 \text{ C}$

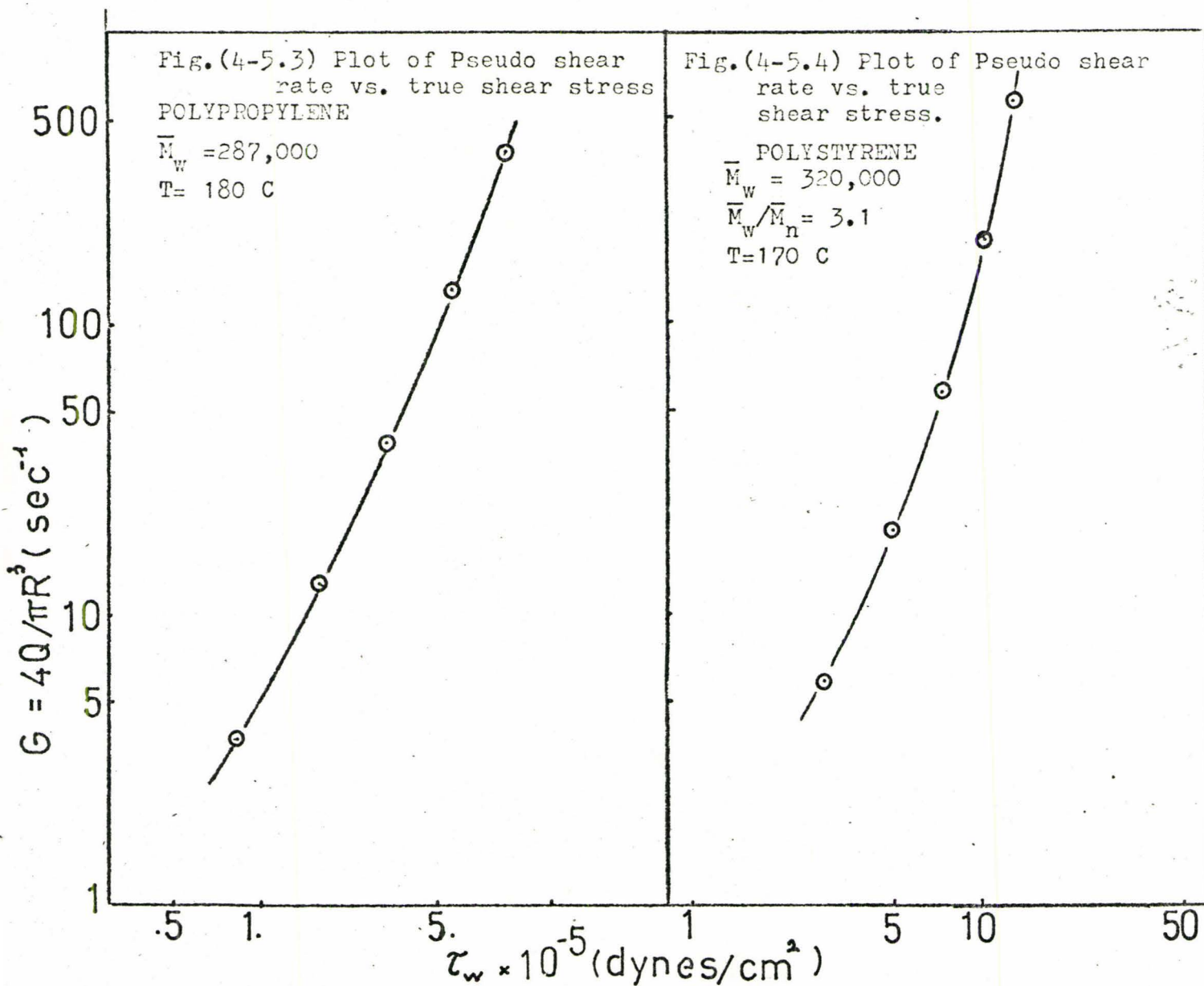


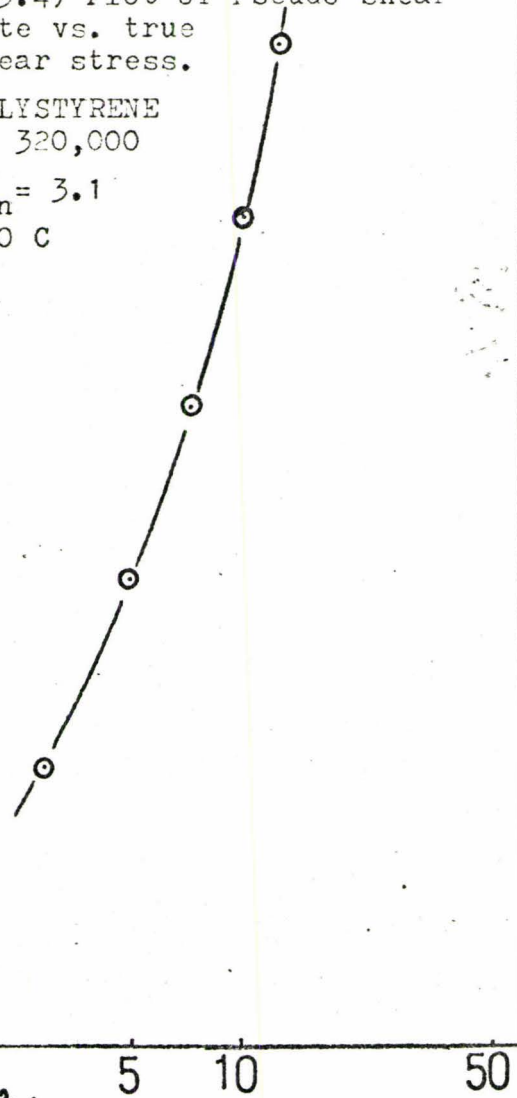
Fig.(4-5.4) Plot of Pseudo shear rate vs. true shear stress.

POLYSTYRENE

$\bar{M}_w = 320,000$

$\bar{M}_w/\bar{M}_n = 3.1$

$T = 170 \text{ C}$



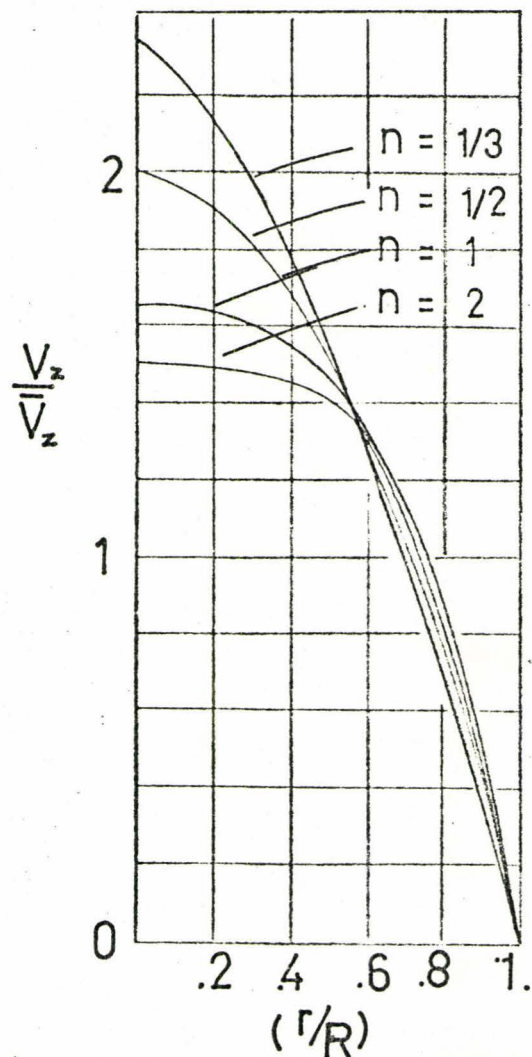


Fig. (4-6) Velocity profiles for the isothermal flow of power law fluid through tubes.

V RESULTS

5.1 Reproducibility

The measurements of extrudate diameters were repeated four times to check the reproducibility of these values. The applied pressures are obtained within 2% while the diameter of the extrudate was found reproducible within nearly 1 %. All measurements are taken in a standard way, in this way while the absolute diameter of the extrudate might be in doubt because of "frozen-in" mechanism but comparison between those values of different capillaries does make sense. It was observed that down drawing by weight does not affect the measurement of extrudate diameter, because the measurement is made at 1/4" from the leading end.

5.2 Effect of Temperature on Die Swell

Figure (5-1) is the plot of die swell(d/D) vs. true shear stress for low density polyethylene at four different temperatures ranging from 150°C to 210°C . It is found that swell is independent of temperature over this range. This agrees with Graessley⁽¹⁷⁾ and Smelkov⁽³⁰⁾ for Polystyrene and PMMA. This result, however, disagrees with Horie⁽²²⁾. Horie found that at a fixed true shear stress, die swell increases with temperature for low density polyethylene.

Investigating the effect of temperature on die swell of polystyrene, PMMA, Low density polyethylene, Horie⁽²²⁾ made the following conclusions:

- 1) At a fixed shear rate, die swell decreases with temperature for polystyrene and PMMA.
- 2) At a fixed shear rate, die swell increases with temperature for low density polyethylene.

Conclusion (1) is in agreement with Beynon and Glyde⁽⁷⁾, Brydson⁽⁹⁾, Dillon and Johnston⁽¹³⁾. Conclusion (2) disagrees with Beynon and Glyde⁽⁷⁾ and Dillon and Johnston⁽¹³⁾. Unfortunately, the reasons for the rather unconventional behaviour of these materials are not clear.

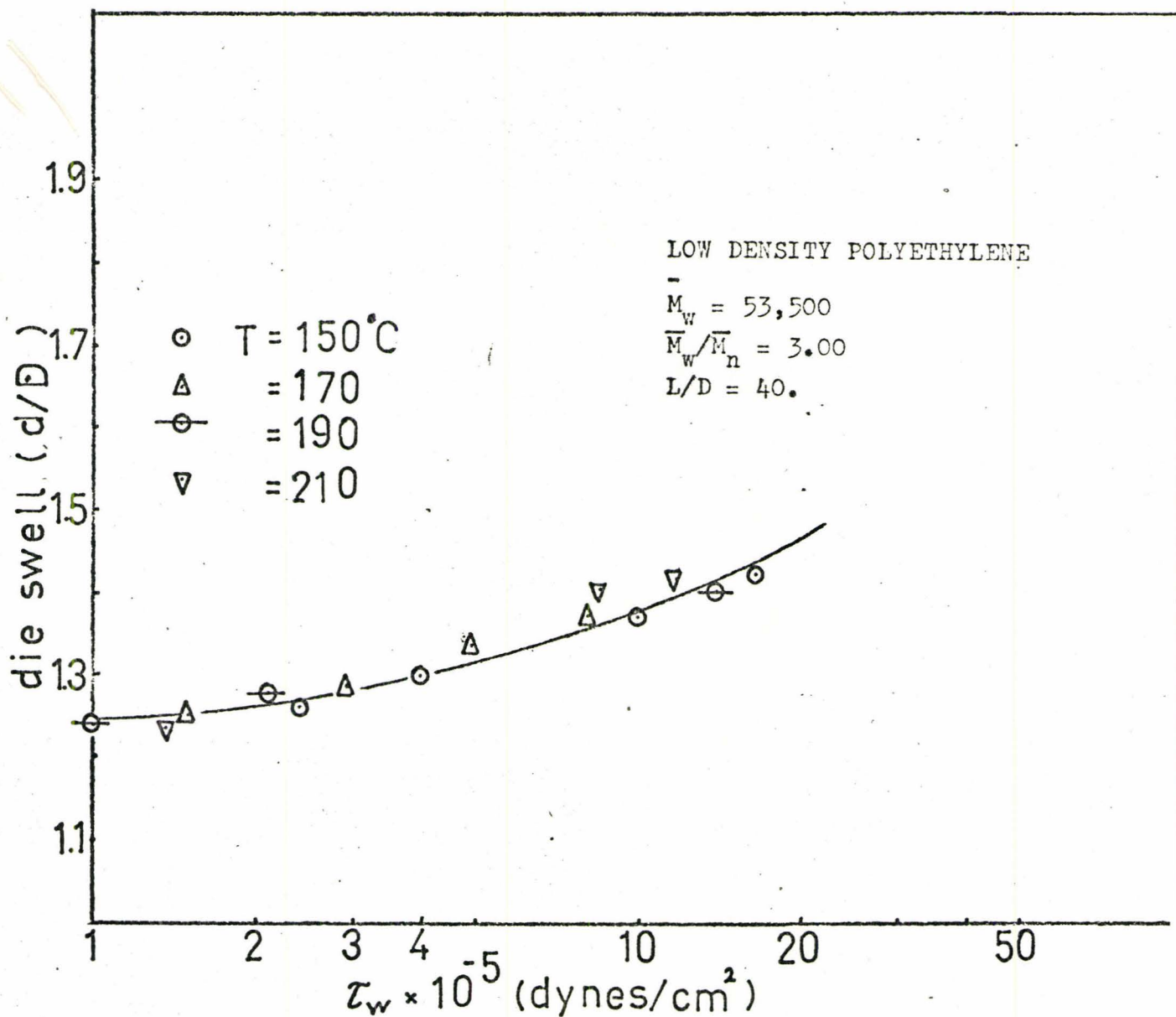


Fig.(5-1) Effect of temperature on die swell.

5.3 Effects of Shear Rate and Shear Stress on Die Swell

Figures (5.2.1 to 5.2.4) are the plots of die swell versus shear stress with different capillaries for all polymers studied.

The following conclusions could be drawn:

1) With a fixed capillary, die swell increases with shear stress for low, high density polyethylene, polypropylene

2) With a fixed capillary, die swell increases with shear rate for low, high density polyethylene, polypropylene, polystyrene

These results are definitely in agreement with Horie⁽²²⁾ and with the bulk of literature^{(7),(29)}.

It should be mentioned that extrudate swelling is only investigated up to critical stress, beyond that limit, measurements are impossible to carry on due to the zig-zag shape of extrudate. McInstosh⁽²⁴⁾ found that the plot of die swell versus shear stress increases to a maximum value then decreases beyond the critical shear stress.

5.4 Effect of Molecular Weight Distribution

The effect of molecular weight distribution on die swell has been carefully investigated by many former researchers^{(17),(22)}. The general

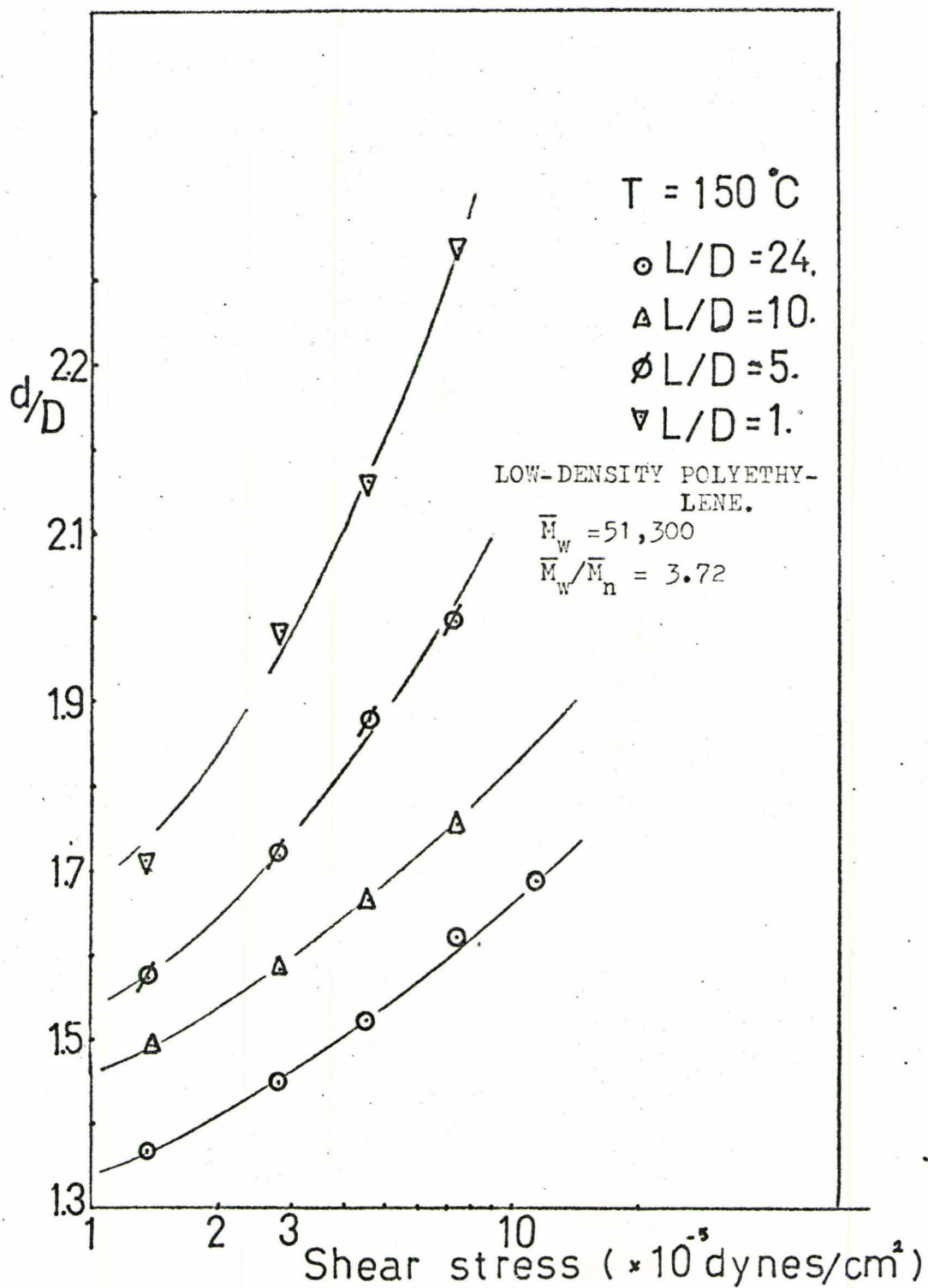


Fig. (5.2.1) Effect of shear stress on die swell

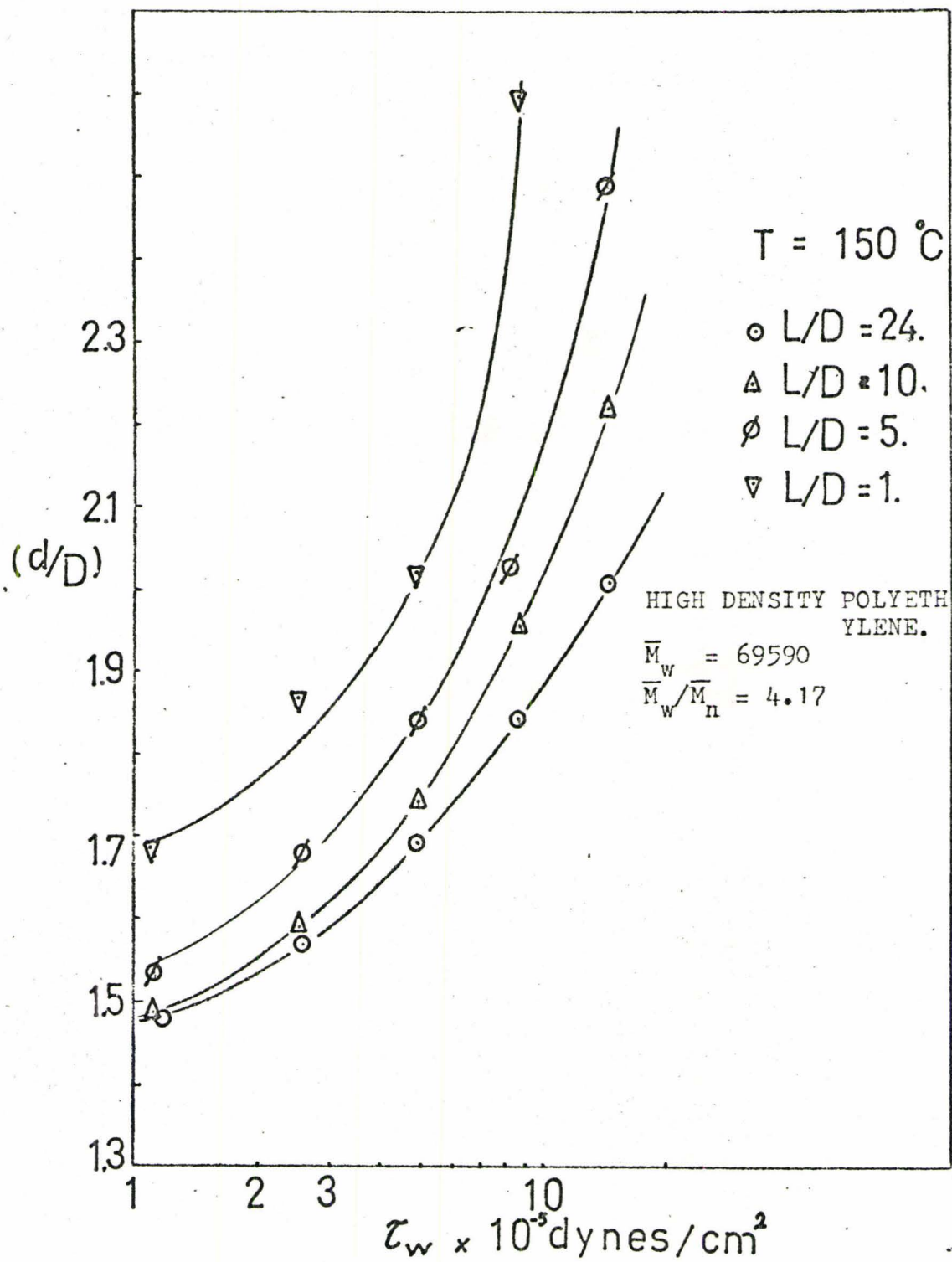


Fig. (5.2.2) Effect of shear stress on die swell of High density polyethylene.

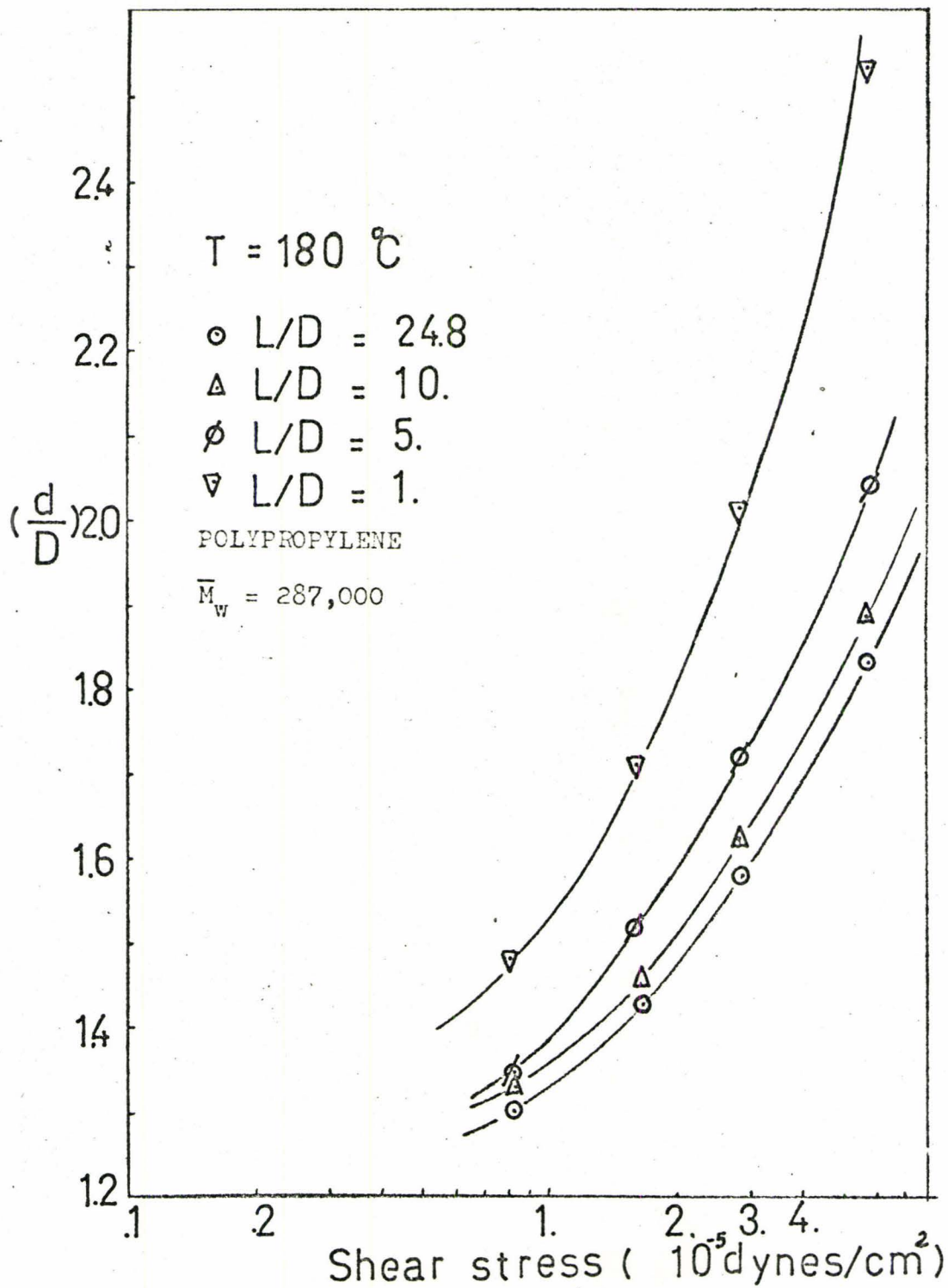


Fig. (5.2.3) Effect of shear stress on die swell of Polypropylene.

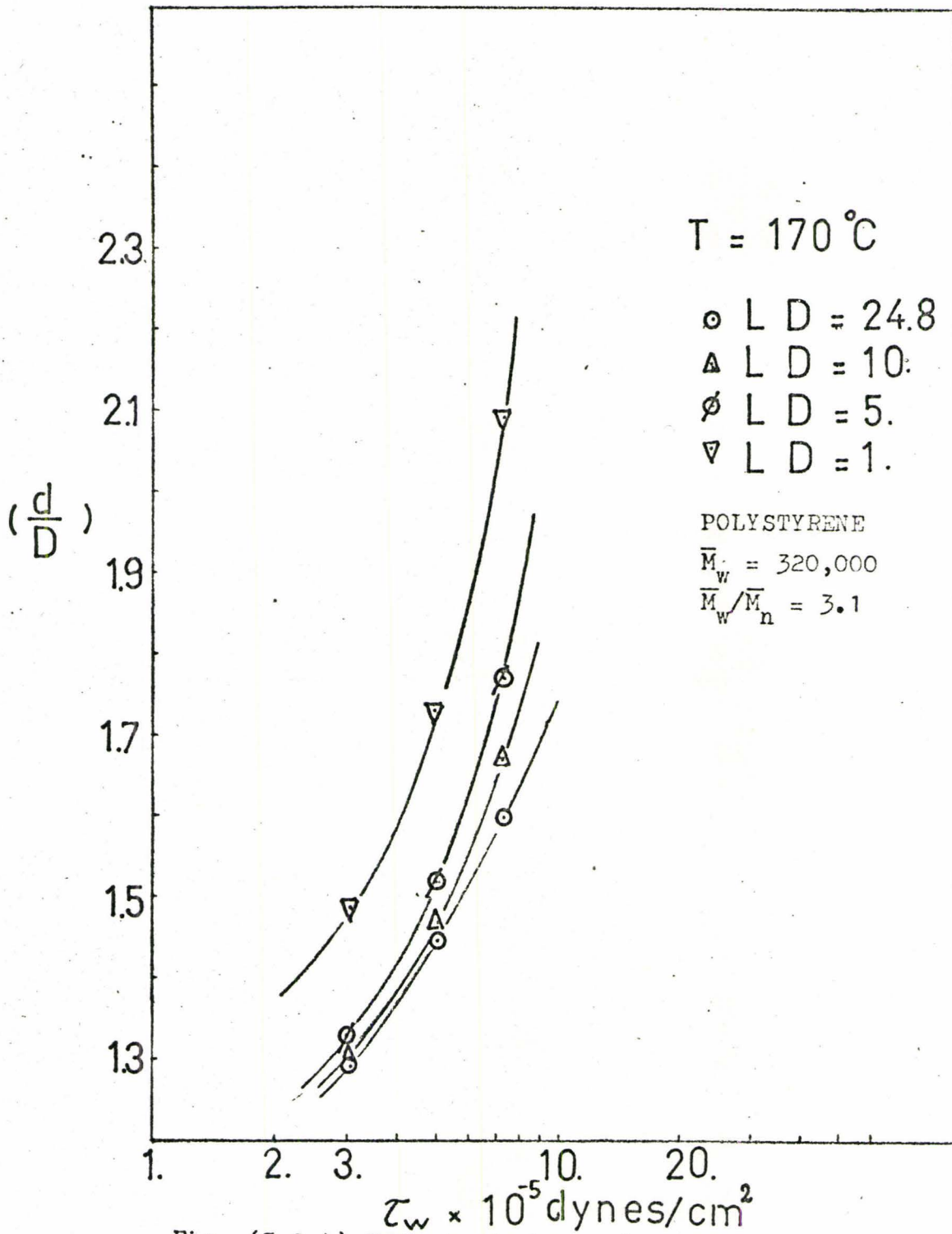


Fig. (5.2.4) Effect of shear stress on die swell of polystyrene.

conclusion is: Die swell increases with molecular weight distribution which is represented by the factor $(\bar{M}_z \bar{M}_{z+1} / \bar{M}_w^2)$.

In Figure (5.3) the plot of swelling ratio versus true shear stress for low density polyethylene with various polydispersity (\bar{M}_w / \bar{M}_n) is shown.

Dependence on factor $\bar{M}_z \bar{M}_{z+1} / \bar{M}_w^2$ implies that die swell is influenced by high molecular weight tail.

In Section (3.1), it has been stated that the swelling ratio (d/D) is a function of recoverable shear, and the recoverable shear is defined from Hooke's law in shear:

$$\sigma = \tau_{12} J_o \quad (5.1)$$

where J_o is the shear compliance of material. Graessley and co-workers⁽¹⁷⁾ carried out rheogoniometer measurements on concentrated solutions and melts of polystyrene and developed the following correlation between "true" and Rouse shear compliance at zero shear rate:

$$J_o = \frac{2.2 \times J_R}{1 + 0.347 \rho E_o} \quad (5.2)$$

where J_R is the Rouse shear compliance

$$J_R = \frac{2}{5} \frac{\bar{M}_z \bar{M}_{z+1}}{\bar{M}_w^2} \frac{\bar{M}_w}{\rho R_g T} \quad (5.3)$$

$E_o = \bar{M}_w / 16,000$ is the entanglement density at zero shear, ρ is the density, R_g is the ideal gas constant.

It is clear that shear compliance (J_o) is related to the molecular weight distribution $(\bar{M}_z \bar{M}_{z+1} / \bar{M}_w^2)$ through the Rouse shear compliance. That is the reason why the molecular weight distribution has great importance in polymer swell.

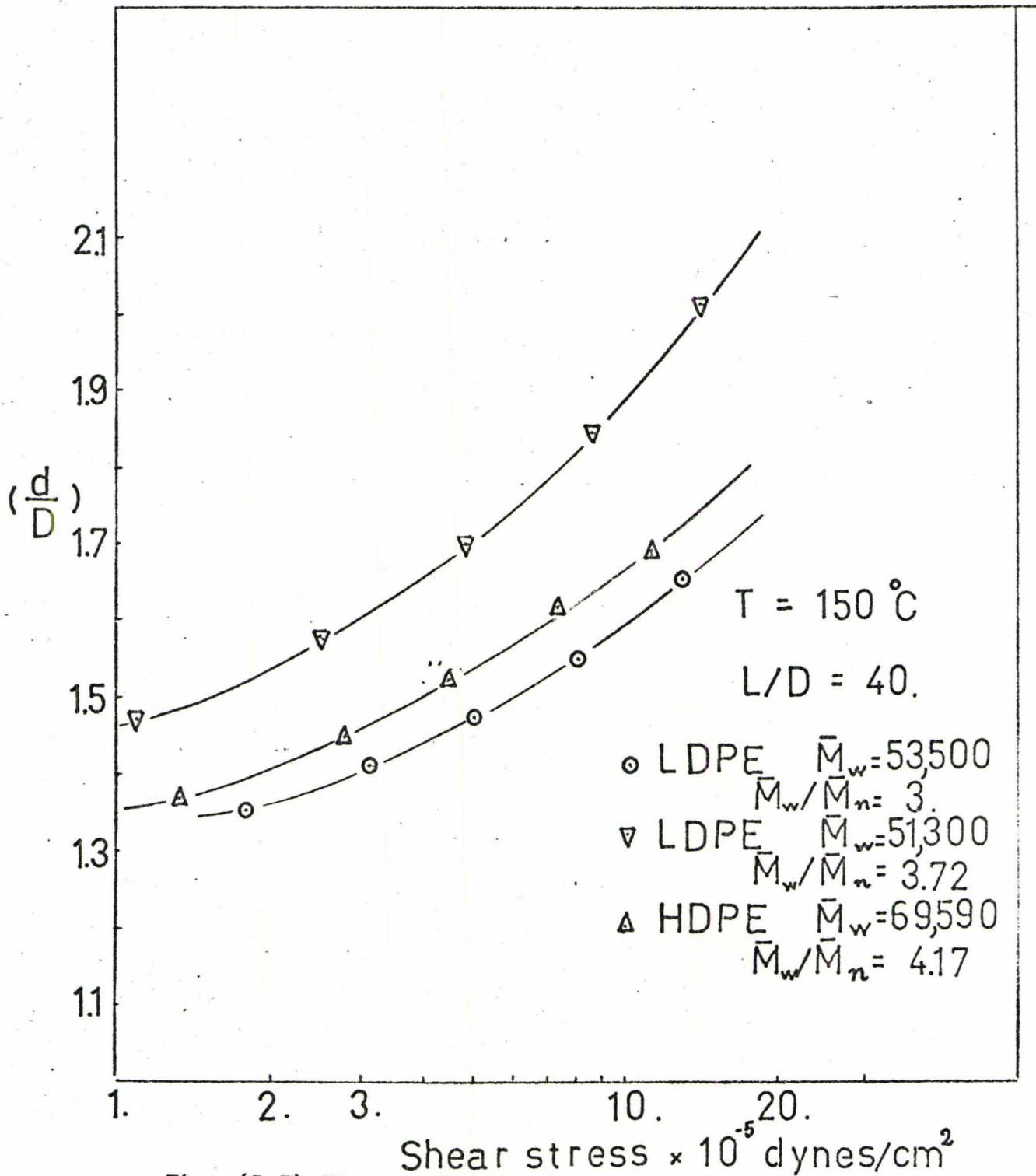


Fig. (5,3) Effect of molecular weight distribution on die swell

High density polyethylene which has linear chain molecules is compared with low density polyethylene (branched molecules), Figure (5.3). It can be concluded that: branched polyethylenes are less swelling than linear polyethylenes with similar molecular weight distributions.

This is in agreement with Horie⁽²²⁾ as well as Bengou and Glyde⁽⁷⁾.

5.5 Effect of Die Length on Swelling Ratio

The effect of die length on swelling ratio is investigated for low and high density polyethylene, polypropylene and polystyrene.

Figures (5.4 to 5.10) are plots of die swell versus L/D for different polymers. It is observed that low density polyethylene needs a long capillary to level off, in our data the swelling ratio seems still decreasing at the value of L/D equal 24.8. Die swell of high density polyethylene reaches equilibrium value relatively faster (L/D=15), the same behaviour is noticed for polypropylene and polystyrene which level off at L/D equal 15 and 12 respectively.

It should be recalled that high density polyethylene, polypropylene and polystyrene are linear polymers while low density polyethylene is a branched polymer. The equilibrium values change with different shear rates. These results are generally in agreement with Graessley⁽¹⁷⁾ (Polystyrene) and Bagley⁽⁵⁾ (Polyethylene)

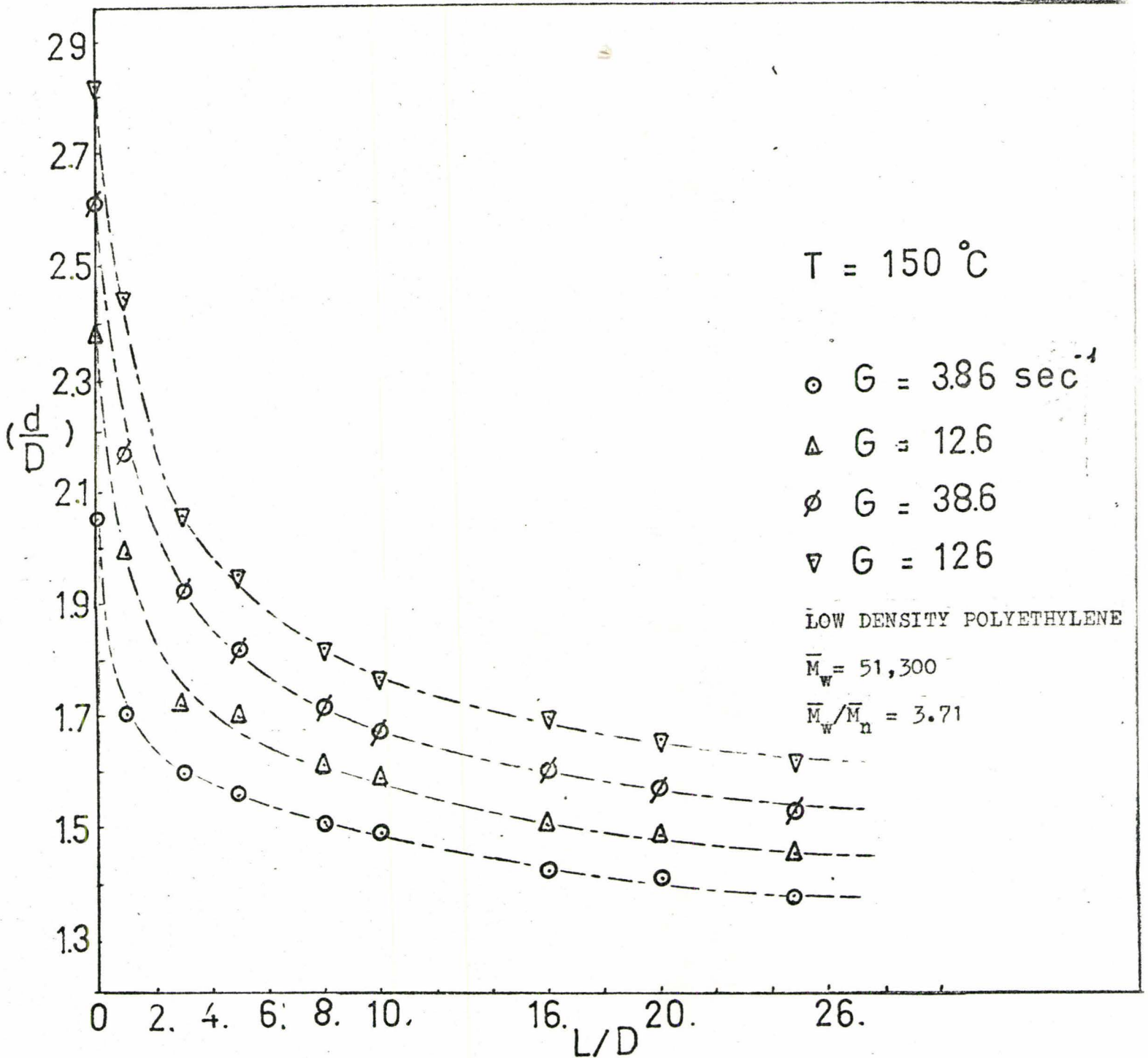


Fig. (5-4) Effect of die dimensions on die swell of LDPE.

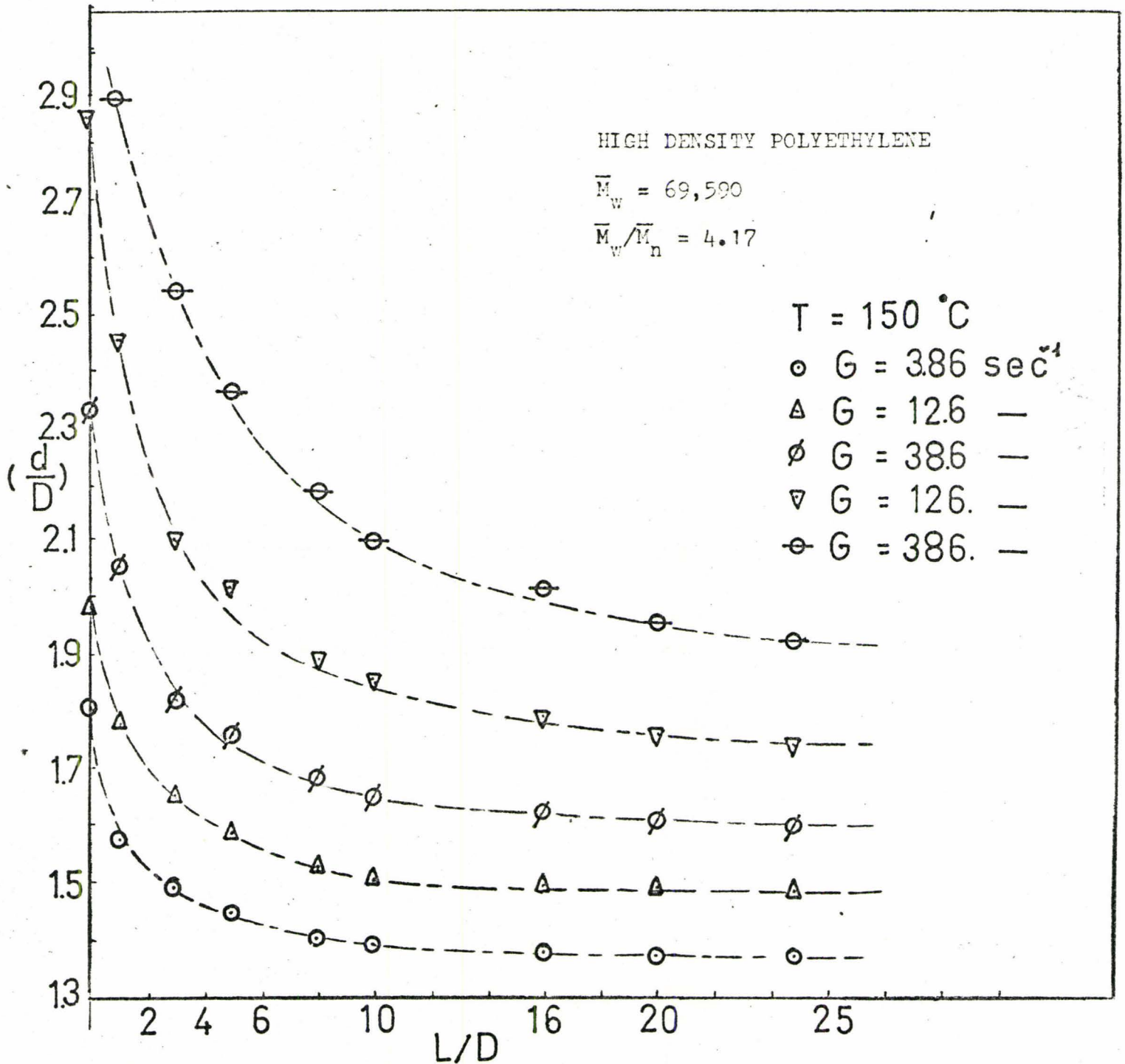


Fig.(5-5) Effect of L/D on die swell of HDPE

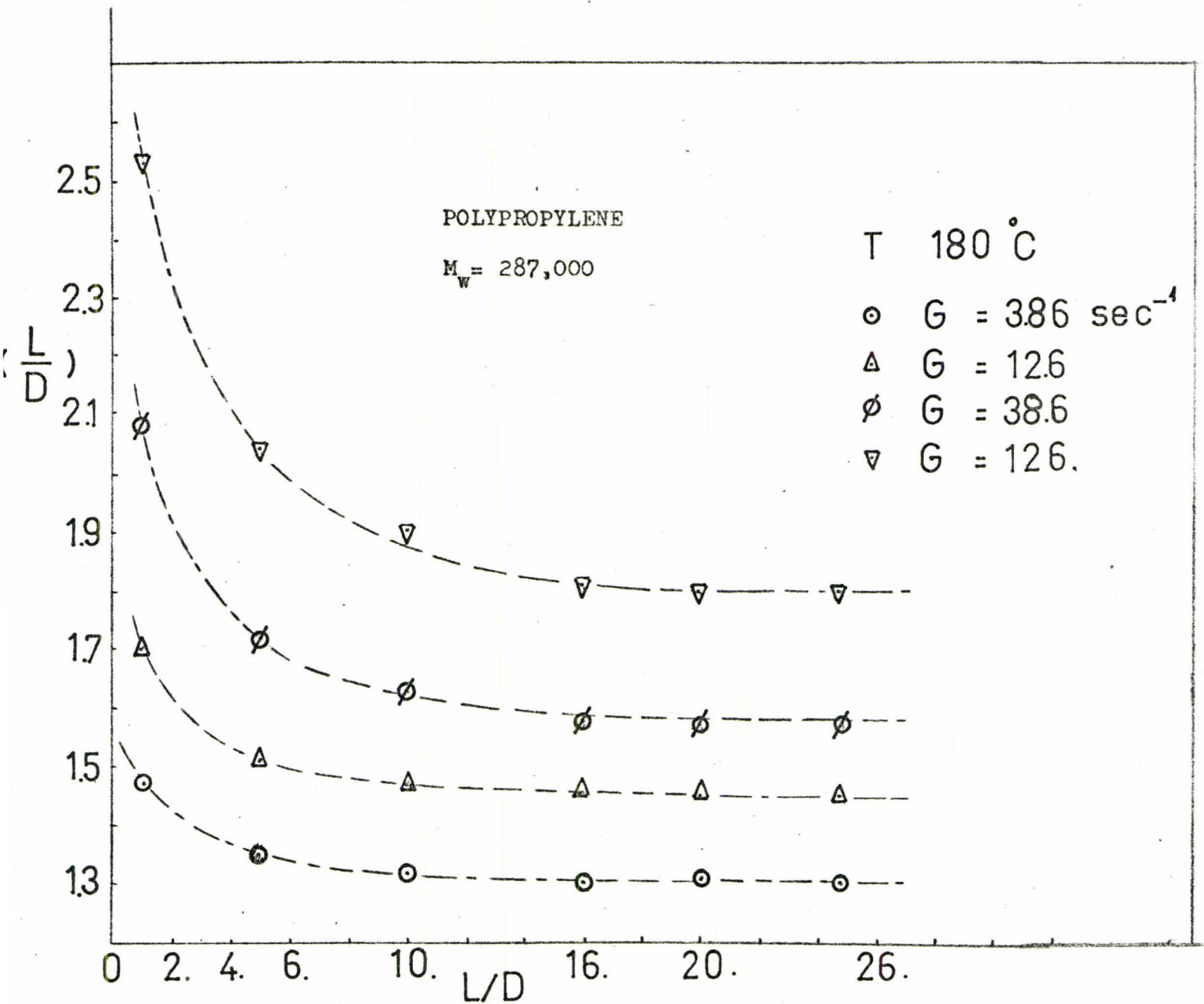


Fig.(5-6) Effect of L/D on die swell of polypropylene.

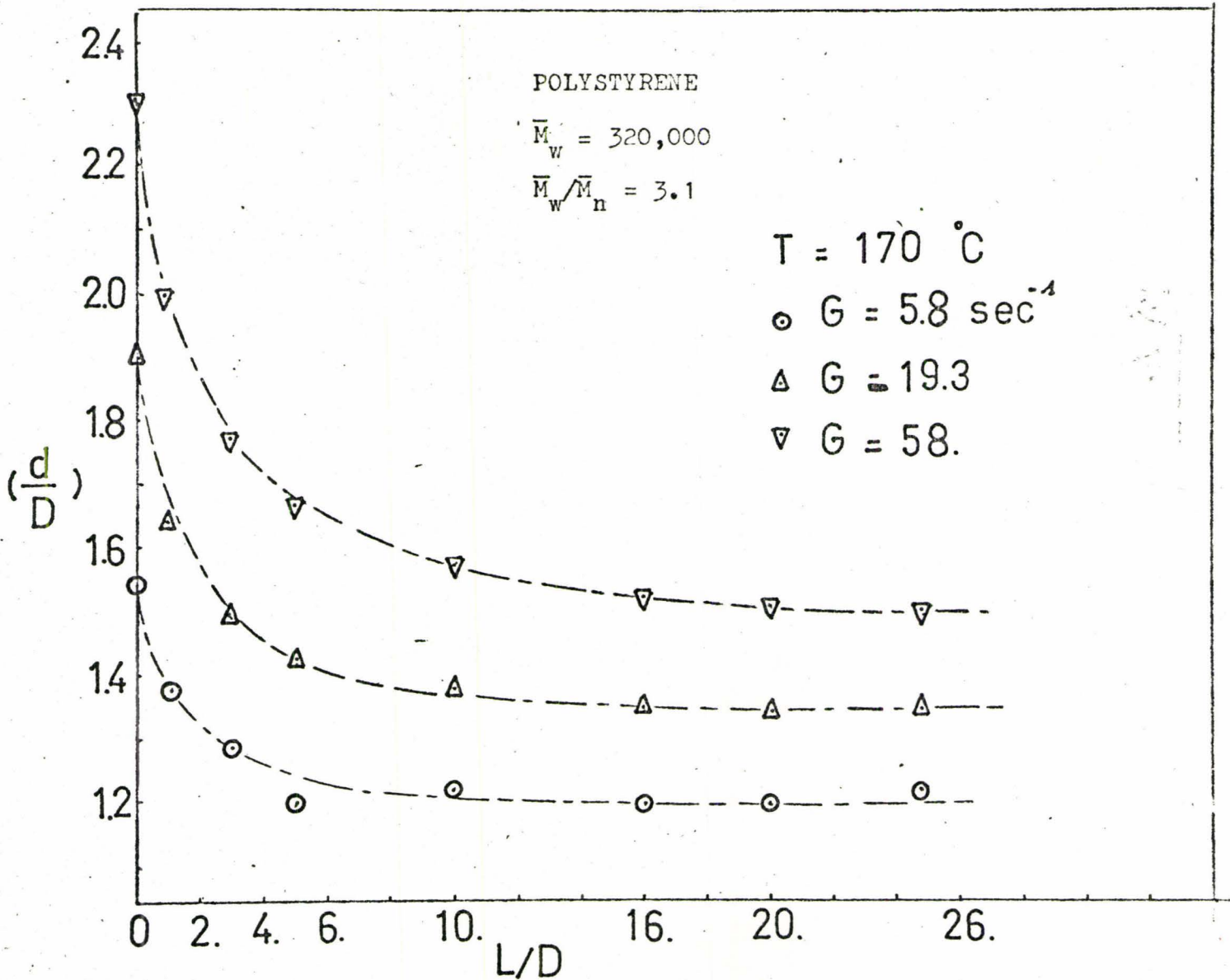


Fig.(5-7) Effect of L/D on die swell of polystyrene.

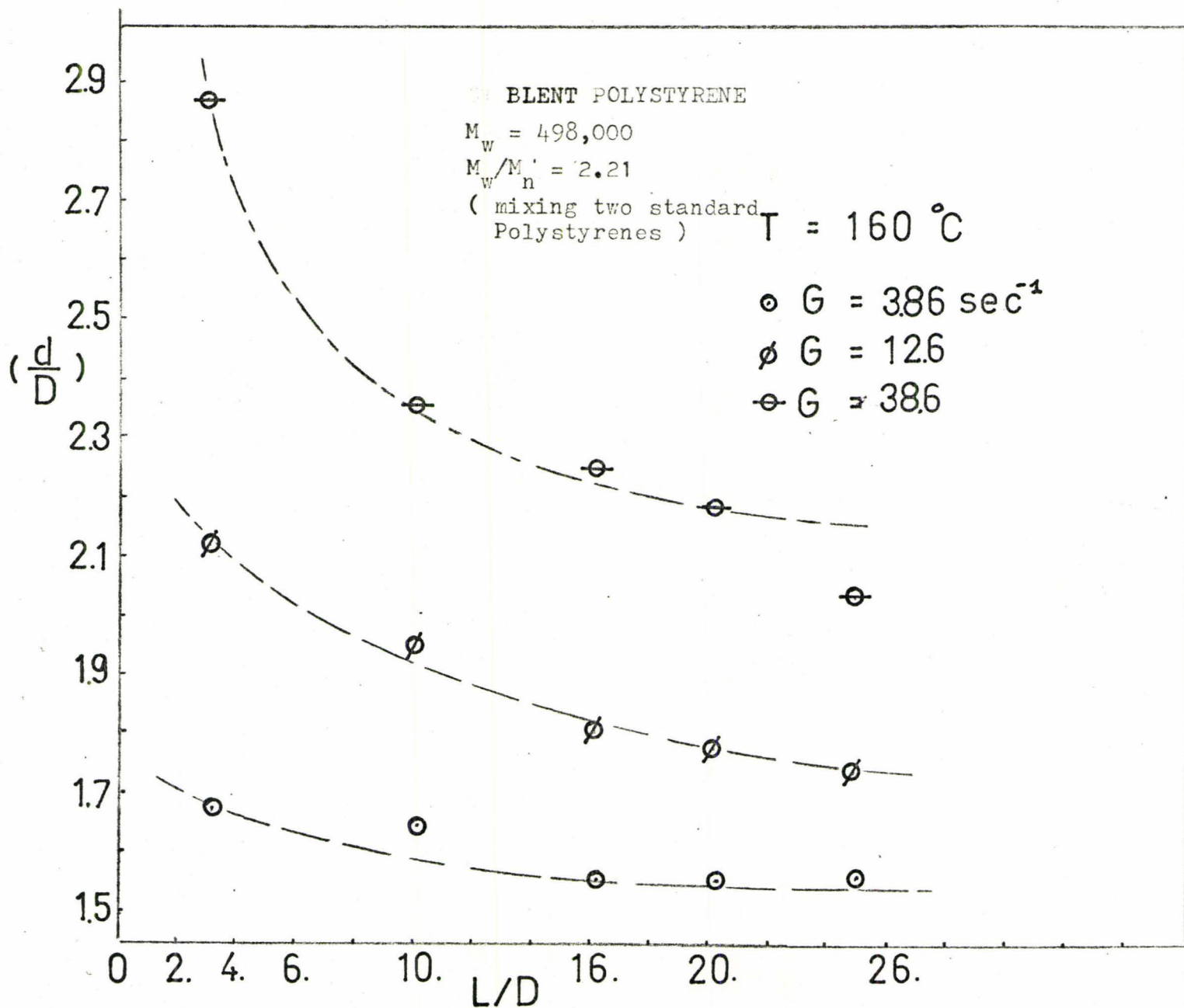


Fig.(5-8) Effect of L/D on die swell of standard polystyrene.

VI ANALYSIS

6.1 Bagley's Suggestion

It was suggested by Bagley⁽⁵⁾ (Section 2.2) that swelling of an extrudate decays exponentially with the shear strain put on the melt system. Bagley fitted his data to his suggested Equation (2.1) by a least-squares method:

$$(B-B_{\infty}) = (B_0 - B_{\infty}) \exp(-kt_a) \quad (2.1)$$

His most interesting relationship is the plot of k versus shear rate results in a straight line passing through the origin, so the following relationship can be written:

$$k = (c/4)G \quad (6.1)$$

If Q is the output rate through a capillary of radius R and length L then:

$$t_a = \pi R^2 L / Q \quad (6.2)$$

which may be written as:

$$t_a = 4(\pi R^3 / 4Q)(L/R) \quad (6.3)$$

or

$$t_a = 4(L/R)/G \quad (6.4)$$

where G is the pseudo shear rate. Combine Equation (6.1), (6.4) with Equation (2.1), we obtain:

$$(B-B_{\infty}) = (B_0 - B_{\infty}) \exp. (-c L/R) \quad (6.5)$$

c is called the decay rate of swelling with die length being independent of shear rate, shear stress or residence time, so c depends only on the kind of polymer used.

Equation (6.5) suggested by Bagley is used to fit data for five polymers studied: high and low density polyethylene, polypropylene, and polystyrene. The curves are shown from Figure (6.1) to (6.4) and the parameters are tabulated in the following tables.

TABLE 6.1

Parameters of Equation (6.5) found at 150°C for Low Density polyethylene (0701) $\bar{M}_w = 51,000$, $\bar{M}_w/\bar{M}_n = 3.72$, $T = 150^\circ\text{C}$

LOW DENSITY POLYETHYLENE (0701)

$G(\text{Sec}^{-1})$	3.8	12.8	38.6	128
$\tau_w(\text{dynes/cm}^2 \times 10^{-5})$	1.36	2.80	4.52	7.40
$\dot{\gamma}_w(\text{Sec}^{-1})$	3.8	17.0	51.8	173.1
$B_0^{(*)}$	1.985	2.299	2.529	2.735
$B_\infty^{(**)}$	1.36	1.46	1.54	1.65
c	.14	.20	.19	.22

TABLE 6.2

LOW DENSITY POLYETHYLENE (0118) $\bar{M}_w = 53,500$ $\bar{M}_w/\bar{M}_n = 3.00$ $T = 150^\circ\text{C}$

$G(\text{Sec}^{-1})$	3.8	12.8	38.6	128
$\tau_w(\text{dynes/cm}^2 \times 10^{-5})$	1.8	3.14	5.09	8.08
$\dot{\gamma}_w(\text{Sec}^{-1})$	4.48	16.47	53.42	173.56
$B_0^{(*)}$	1.891	2.254	2.546	2.799
$B_\infty^{(**)}$	1.37	1.43	1.49	1.58
c	.200	.233	.224	.251

(*) Value obtained by regression

(**) Value obtained from experimental data

TABLE 6.3

HIGH DENSITY POLYETHYLENE (7930) $\bar{M}_w = 69,590$ $\bar{M}_w/\bar{M}_n = 4.17$ $T = 150^\circ\text{C}$

$G(\text{Sec}^{-1})$	3.8	12.8	38.6	128
τ_w (dynes/cm ² x 10 ⁻⁵)	1.11	2.54	4.97	9.13
$\dot{\gamma}_w$ (Sec ⁻¹)	3.89	14.92	45.97	161.21
$B_o^{(*)}$	1.804	1.986	2.325	2.850
$B_\infty^{(**)}$	1.367	1.492	1.618	1.777
c	.239	.284	.302	.280

TABLE 6.4

POLYPROPYLENE (PP.5820) $\bar{M}_w = 287,000$ $T = 180^\circ\text{C}$

$G(\text{Sec}^{-1})$	3.86	12.8	38.6	128
$\tau_w \times 10^{-5}$ (dynes/cm ²) ⁸³	1.57	2.82	4.76	
$\dot{\gamma}_w$ (Sec ⁻¹)	4.51	16.5	41.6	144.25
$B_o^{(*)}$	1.531	1.804	2.252	2.751 (cal.)
$B_\infty^{(**)}$	1.304	1.458	1.572	1.804
c	0.306	0.350	0.311	0.281

TABLE 6.5

POLYSTYRENE: (HF.55)

 $T=170^\circ\text{C}$ $\bar{M}_w = 320,000$ $\bar{M}_w/\bar{M}_n = 3.1$

$G(\text{Sec}^{-1})$	5.8	19.38	58
$\tau_w \times 10^{-5}$ (dynes/cm ²) ^{3.05}	5.09	7.31	
$\dot{\gamma}_w$ (Sec ⁻¹)	5.8	28.35	84.07
$B_o^{(*)}$	1.570	1.859	2.220
$B_\infty^{(**)}$	1.302	1.454	1.612
c	0.415	0.357	0.261

(*) Value obtained by regression

(**) Value obtained from experimental data.

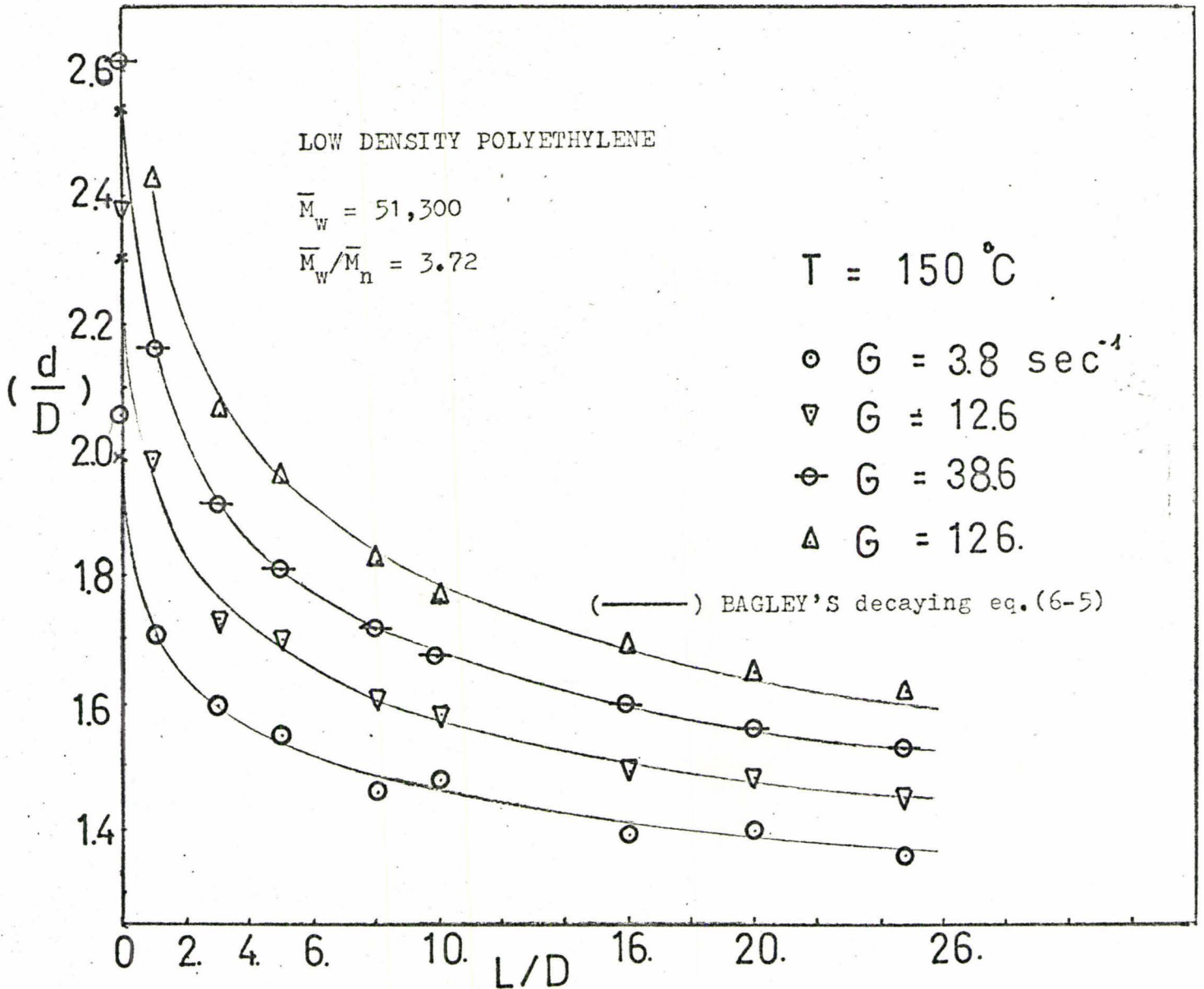


Fig. (6.1) Fitting of Bagley's equation (6-5) for low density polyethylene

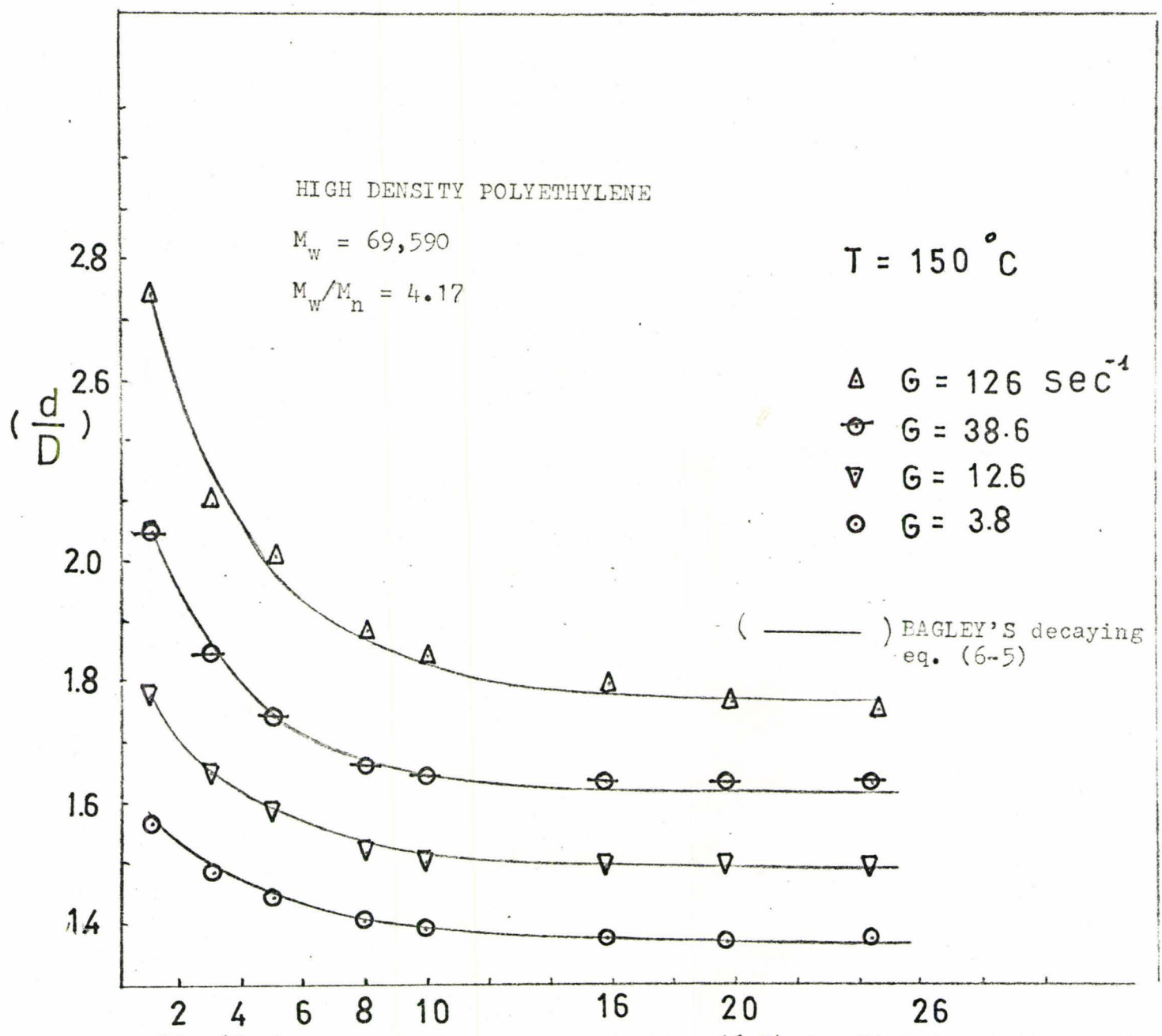


Fig.(6.2) Fitting of Bagley s equation (6-5) for High density polyethy lene.

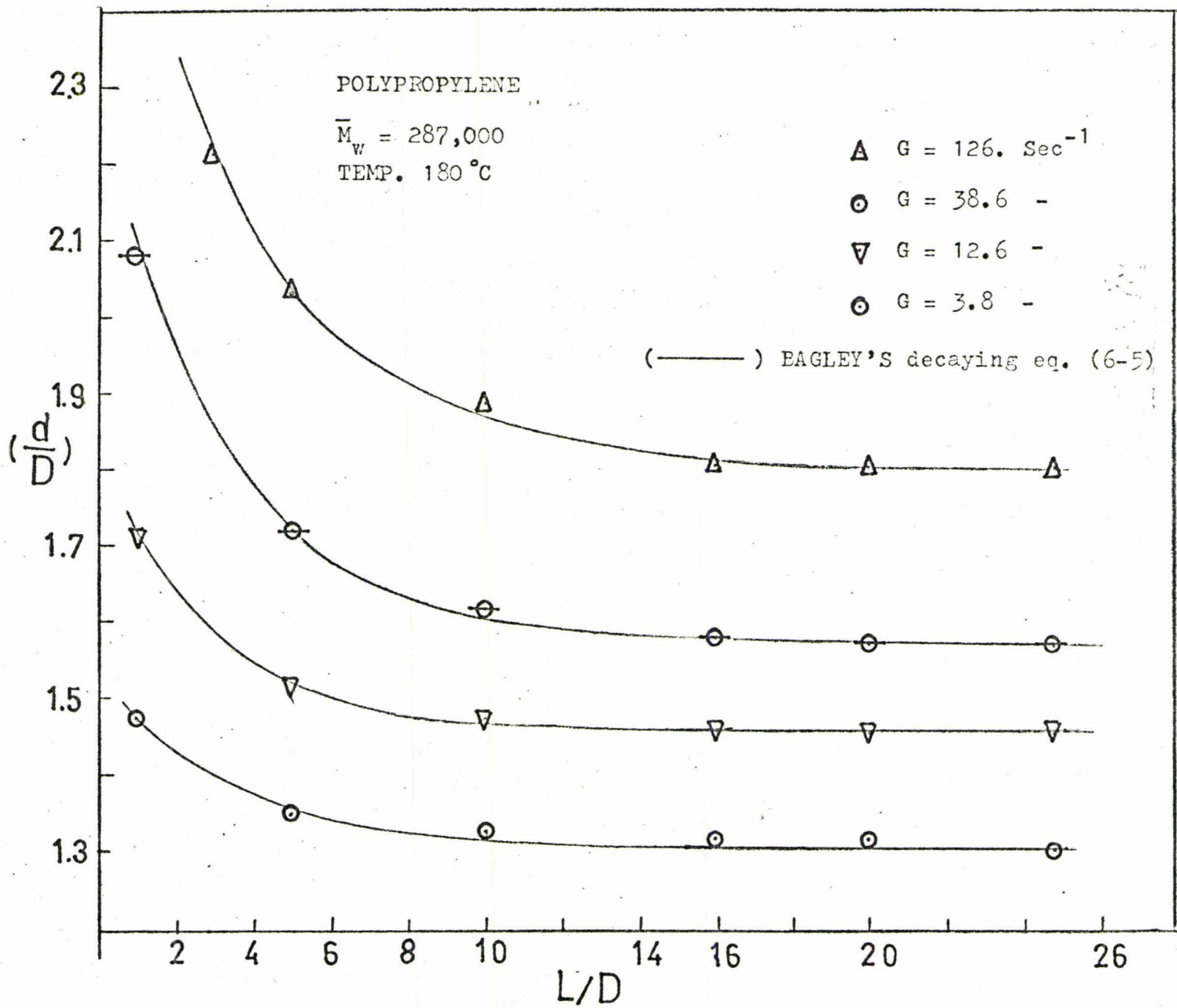


Fig.(6.3) Fitting of Bagley's decaying equation (6-5) for Polypropylene

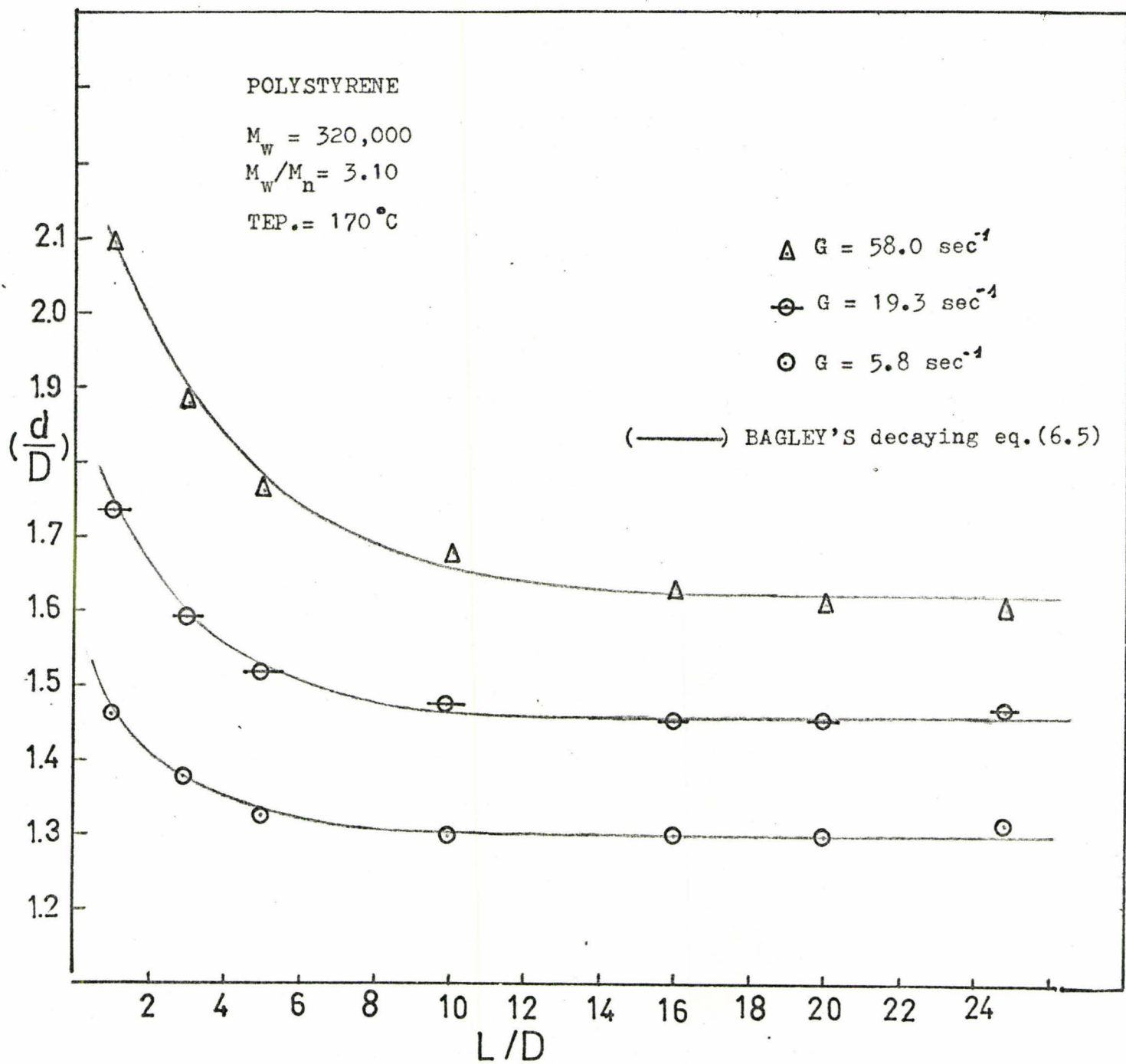


Fig. (6.4) Fitting of Bagley's decaying equation (6-5) for Polystyrene

TABLE 6.6

POLYSTYRENE: (HT 42.1)

T = 170°C

$G(\text{Sec}^{-1})$	5.8	19.38	58.
$\tau_w \times 10^{-5} (\text{dynes/cm}^2)$	4.49	6.99	9.30
$\dot{\gamma}_w (\text{Sec}^{-1})$	7.54	27.03	98.77
B_0	1.654	1.895	2.255
B_∞	1.319	1.436	1.592
c	0.569	0.330	0.300

The decay equation suggested by Bagley seems to fit our data very well for most of polymers studied, however, there are some pitfalls of significant importance.

- 1) The decay rate is not constant with respect to pseudo shear rate (Table 6.1 to 6.6). For some polymers, decay rate could be considered constant within experimental error, while in the case of polystyrene, it could hardly be constant but decreases with pseudo shear rate.
- 2) If the stored energy is dissipated along the capillary then this energy must convert to heat which changes the viscosity of the polymers. However, the apparent viscosity does not change, this is demonstrated by the straight line of the plot pressure versus die length.

Our future work could be more devoted to investigate the possibility of this dissipated energy.

Equation(6.5) suggested by Bagley would be useful in practical purpose when the equation parameters B , B_0 , c could be related

to the material properties and processing conditions. In future work, it would be worthwhile to investigate this relationship.

It is clear that the plot of die swell index, d/D , versus L/D decays exponentially, however, this shape of the curve could be fitted by many forms of equation. Accordingly, we do not have any fundamental equations at hand. Bagley's equation should be regarded only as a curve fitting at experimental data.

6.2 Effect of Deborah Number on Die Swell

6.2.1 Time Constant

The time constant of a material is defined in many ways in the literature. It may be defined for a particular theory such as the theories of Rouse⁽²⁸⁾ and Graessley⁽¹⁵⁾. It also may be defined as the inverse of the shear rate at which the viscosity decreases to some fixed percentage of the zero - shear rate viscosity. The following table summarizes all common definitions for time constant.

TABLE 6.2.1

Time constant	Where found	Remarks
θ_x	Harris ⁽¹⁸⁾	x represents viscosity (μ), or dynamic viscosity (μ'). For definition see Figure (6.5)
θ_o	Work by Graessley ^(16b) and co-workers	Defined in Graessley's theory ⁽¹⁵⁾ and is obtained by superimposing viscosity data on a master curve for viscosity versus shear rate.

θ_R	Rouse ⁽²⁸⁾	$\theta_R = \frac{6\mu_o M}{\Pi^2 CRT}$ defines the longest or largest time constant in the Rouse theory good only for dilute solutions. No "power law" region defined in this theory. The time constant is the same as that used by Bueche except for a constant multiple of 2.
θ_T	Tobolsky ⁽³⁴⁾ and co-workers	Obtained from stress relation work by Procedure X as described in work by Tobolsky and Murakami
θ_N	Graessley and co-workers (16b)	Obtained from a modification of Williams' work on dilute solutions ⁽³⁸⁾ .
θ_w	work by M.C. Williams ⁽³⁸⁾	Obtained from Williams' theory for intermediately concentrated solutions. θ_w is proportional to $\frac{\mu_o}{C^2}$

Harris⁽¹⁸⁾, working with solution of polystyrene at 25°C found that it is possible to relate the time constant θ_μ and θ_μ' to concentration and molecular weight for one and two components (blends) system.

$$\theta_\mu = 4.0 \times 10^{-16} C^{3.77} M_w^{3.27}$$

$$\theta_\mu = 4.16 \times 10^{-15} C^{2.63} M_w^{2.92}$$

where M_w and C are the weight average and polymer concentration.

Tobolsky found that for polymers having a narrow distribution of molecular weight θ_T varies with 3.5 power of the molecular weight.

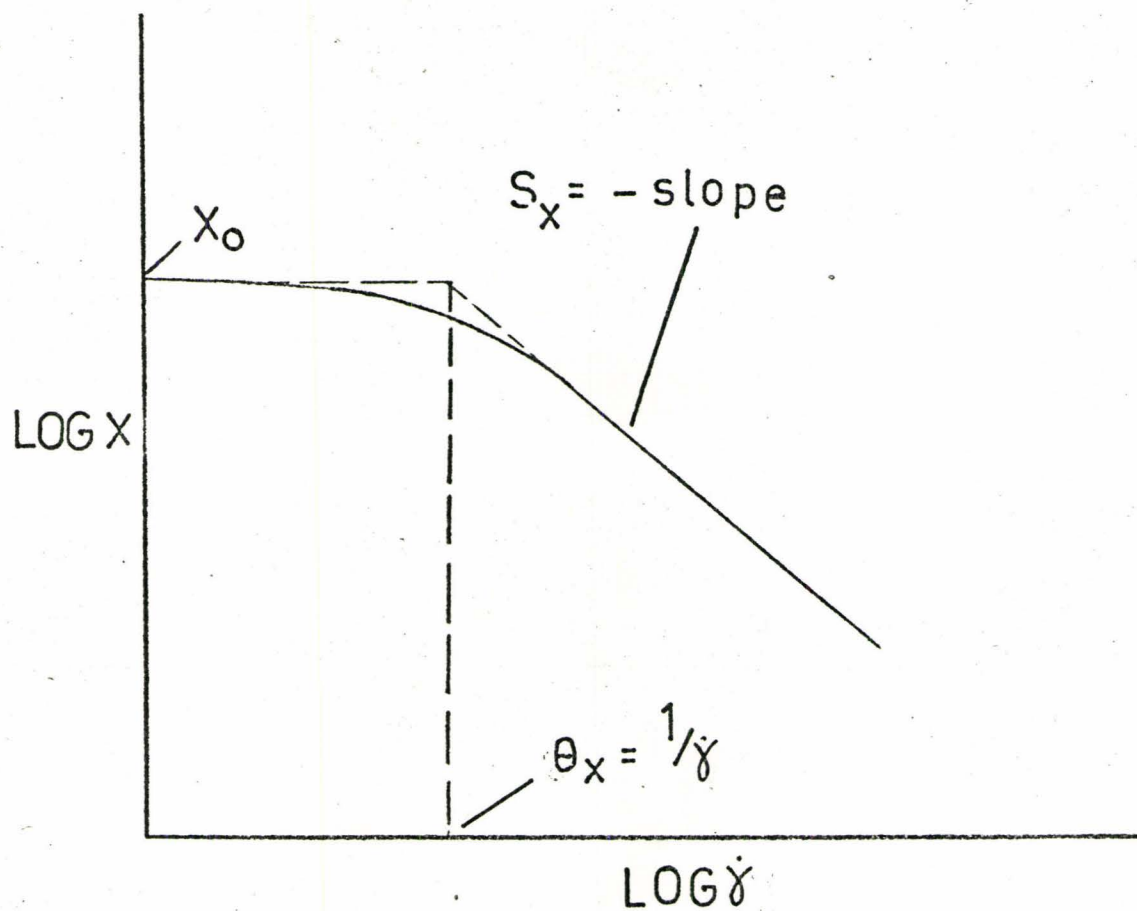


Fig.(6.5) Definition of time constant of a polymeric system.

6.2.2 Definition of Deborah number

Deborah number is defined⁽²⁵⁾ as the ratio of the natural time of the material to the duration time of a process:

$$N_{\text{Deb}} = \frac{\theta}{\theta_t} \quad \begin{array}{l} \text{(time constant of the material)} \\ \text{(processing time)} \end{array}$$

Metzner⁽²⁵⁾ used Tobolsky time constant to define Deborah number.

Processing time (θ_t) is used as the average residence time required for a particle of material to flow through the capillary which is:

$$\theta_t = \frac{\pi R^2 L}{Q} \quad (\text{Sec})$$

According to the definition of pseudo shear rate (G)

$$G = \frac{4Q}{\pi R^3}$$

hence:

$$\theta_t = \frac{8}{G} \left(\frac{L}{D} \right)$$

This definition of processing time has also been used by Bagley⁽⁵⁾, Metzner⁽²⁵⁾ and Roger⁽²⁸⁾ in investigating the effect of capillary dimensions on die swell. Processing time is also designated as t_a .

6.2.3 Effect of Deborah Number on Polymer Processing

Metzner⁽²⁵⁾ et al. has stressed the importance of this number on the extrusion of polymer melt through a capillary.. If the Deborah number is large i.e. if the time span of the fluid memory exceeds the residence time in the tube, the emerging extrudate is able to recall its state prior to entry into the tube. Conversely, as this dimensionless ratio approaches zero, the extrudate is able to recall only the flow conditions in the tube.⁽²⁵⁾ However the relationship

between Deborah number and die swell has not been proposed by former investigators.

To investigate the possible effect of processing time to die swell, the plots of die swell index, d/D , versus average residence time are shown in Figure (6.6) to Figure (6.9) for the polymers studied.

The following conclusions could be made from the plots:

- 1) At a fixed pseudo shear rate, die swell decreases with residence time to a equilibrium value depending on pseudo shear rate.
- 2) At a fixed residence time, die swell increases with pseudo shear rate.
- 3) The fact that all data points do not fall on the same curve means residence time or Deborah number is not the only factor determining die swell.

The importance of Deborah number as related to the phenomenon of die swell, is still unknown. Nevertheless, we can conclude that die swell is not solely dependent on the magnitude of this number.

6.3 Relationship Between Recoverable Shear Strain of a Short and Long Capillary

Hooke's law in shear is assumed to be obeyed by most of molten polymers

$$\sigma = J_o \tau_{12} \quad (5.1)$$

in which σ is the recoverable shear strain, τ_{12} are the shear stress and J_o the shear compliance ($J_o = 1/G_o$ where G_o is the shear modulus).

Following the model suggested by Bagley (Section 3.1) which relates the average coverable shear, $\bar{\sigma}$, to the die swell (Equation 3.22)

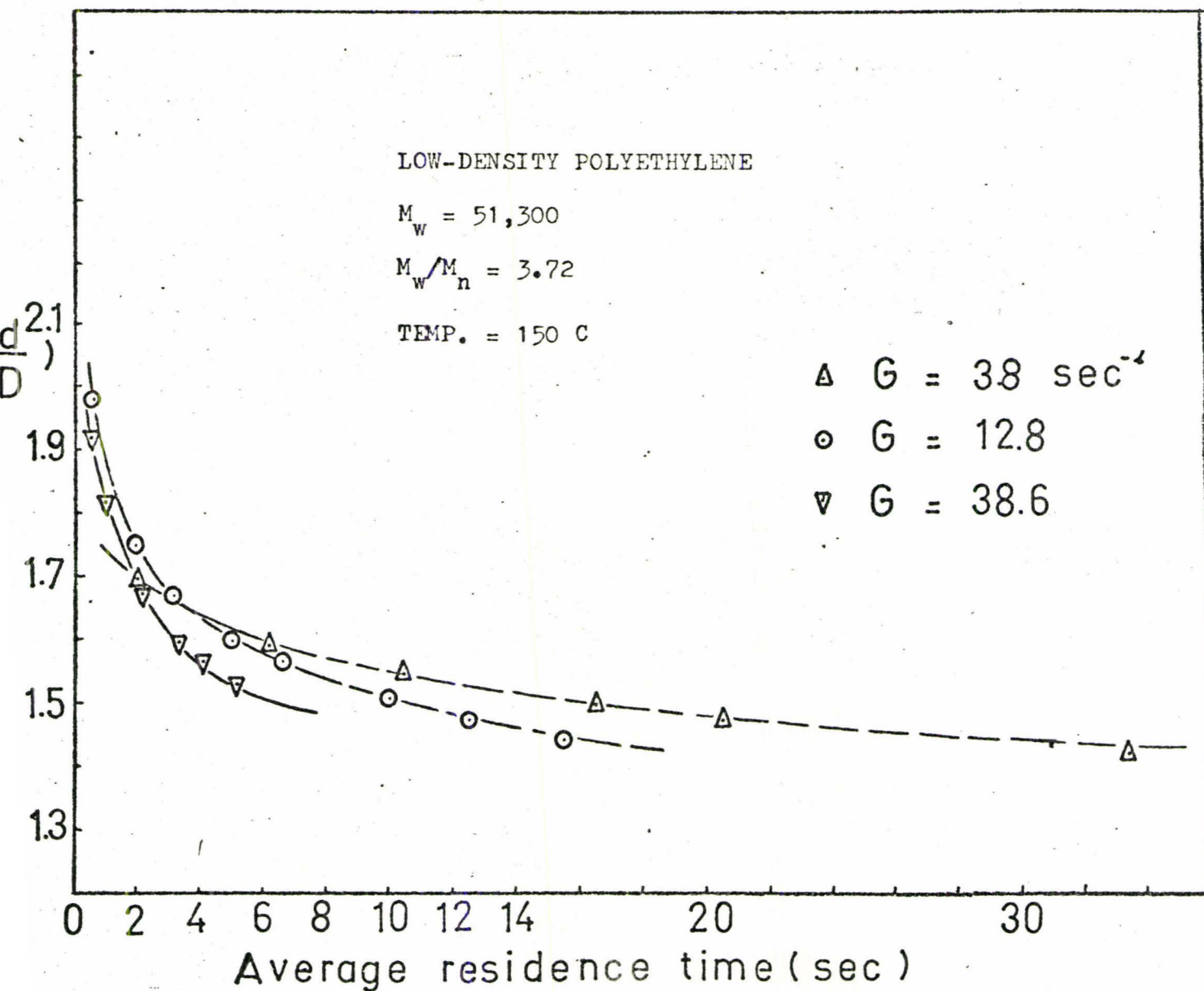


Fig. (6.6) plot of die swell vs. average residence time.

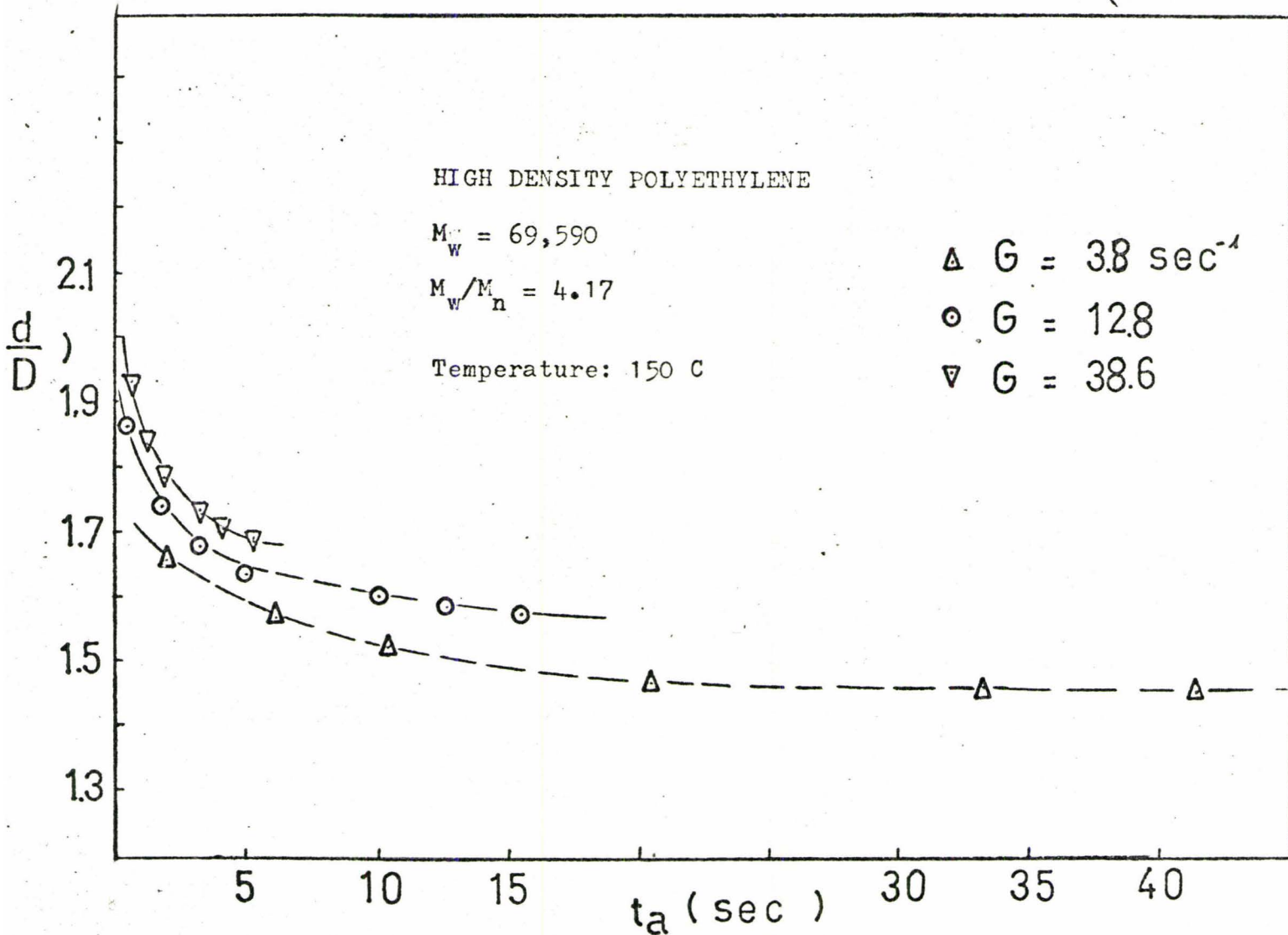


Fig. (6.7) Plot of die swell vs. average residence time.

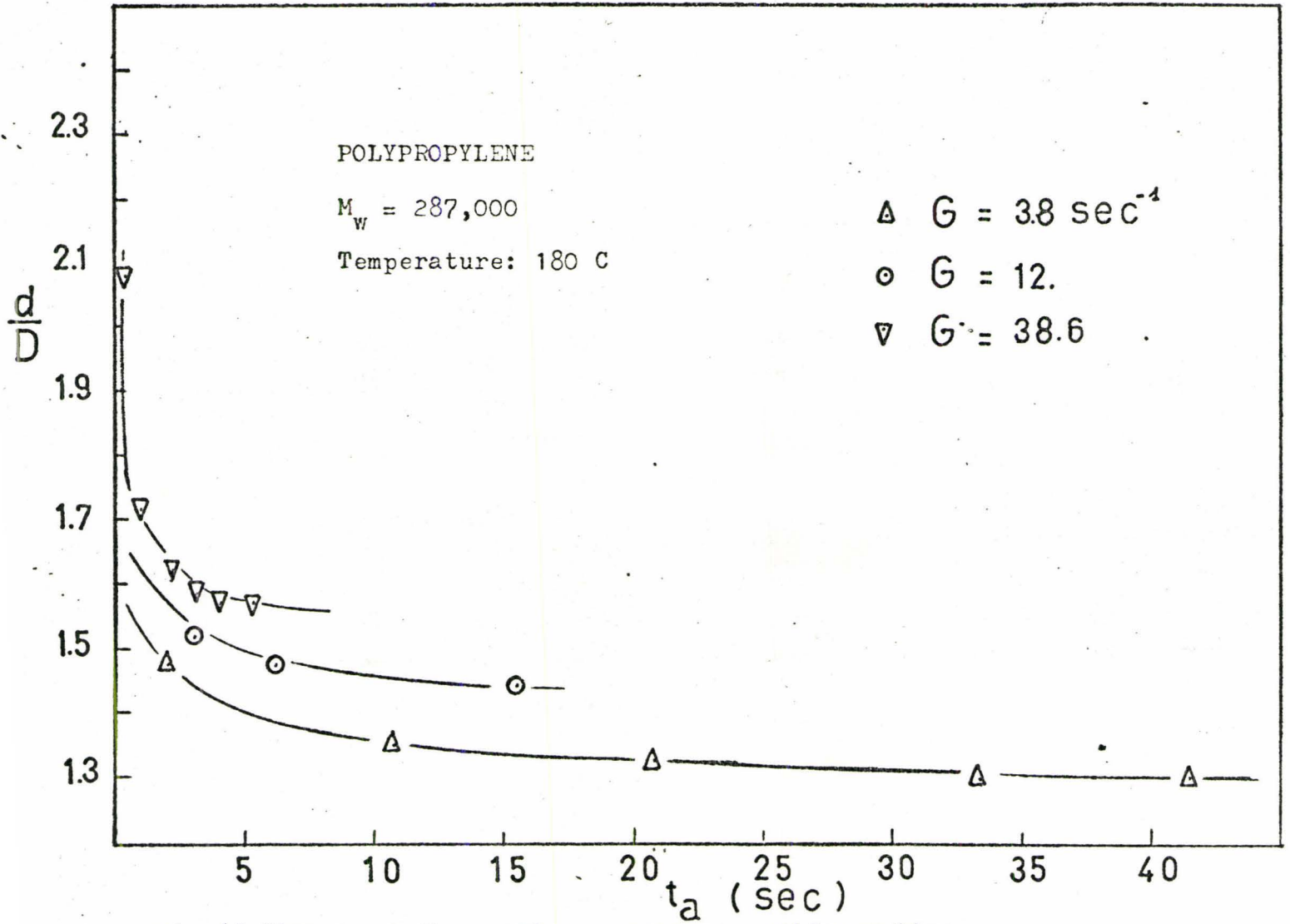


Fig.(6-8)Plot of die swell vs. average residence time.

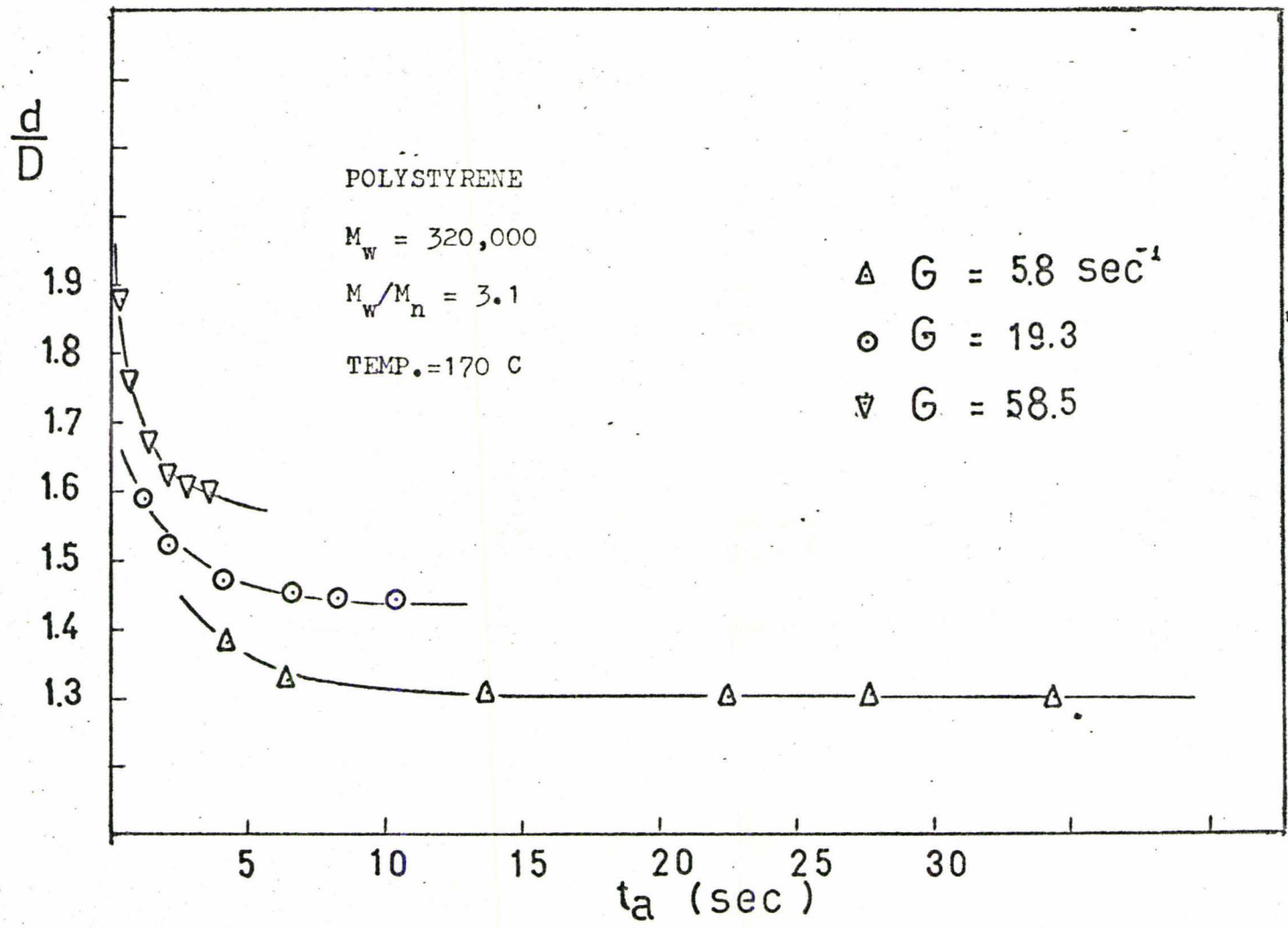


Fig. (6.9) Plot of die swell vs. average residence time.

$$\bar{\sigma} = \left[\left(\frac{d}{D} \right)^4 + \frac{2}{\left(\frac{d}{D} \right)^2} - 3 \right]^{1/2} \quad (3.22)$$

The relationship between average recoverable shear strain and its value at the wall has been derived in detail⁽²²⁾. The following relationship would hold in the case a parabolic velocity profile is assumed:

$$\sigma_w = \sqrt{3} \bar{\sigma} \quad (3.7)$$

In the case of very short capillary, a flat velocity profile is obtained, then the following relationship could be used⁽²²⁾:

$$\sigma_w = \sqrt{2} \bar{\sigma} \quad (3.8)$$

Combining (3.22) and (3.7), then replacing $\bar{\sigma}$ in (5.1) by σ_w we would obtain:

$$\sigma_w = \sqrt{3} \left[\left(\frac{d}{D} \right)^4 + \frac{2}{\left(\frac{d}{D} \right)^2} - 3 \right]^{1/2} = J_o \tau_w \quad (6.6)$$

It has been shown that (Section 4.4.4) in a short range of pseudo shear rate, molten polymer behaves as a power law fluid which means:

$$\tau_w = KG^n \quad (6.7)$$

Combining (6.6) and (6.7)

$$\sqrt{3} \left[\left(\frac{d}{D} \right)^4 + \frac{2}{\left(\frac{d}{D} \right)^2} - 3 \right]^{1/2} = J_o KG^n \quad (6.8)$$

Taking logarithm of both sides

$$\log \left[\left(\frac{d}{D} \right)^4 + \frac{2}{\left(\frac{d}{D} \right)^2} - 3 \right]^{1/2} = n \log G + (\log J_o K - \log \sqrt{3}) \quad (6.9)$$

According to Equation (6.9), the plot of $\left[\left(\frac{d}{D} \right)^4 + \frac{2}{\left(\frac{d}{D} \right)^2} - 3 \right]^{1/2} = \bar{\sigma}$

versus G on logarithmic paper would give a straight line with slope n .

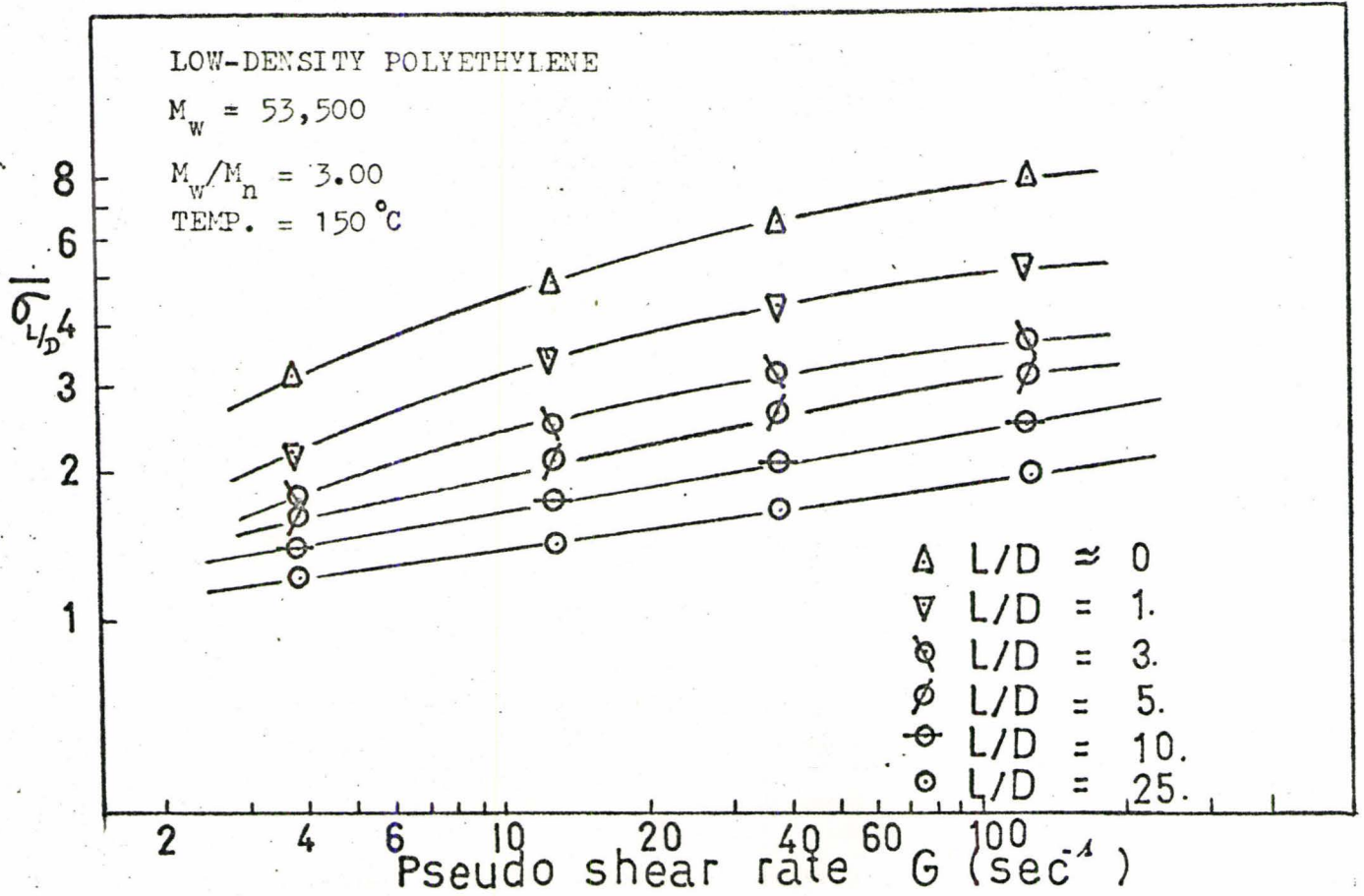


Fig.(6.10) Plot of average recoverable shear strain vs. pseudo shear rate.

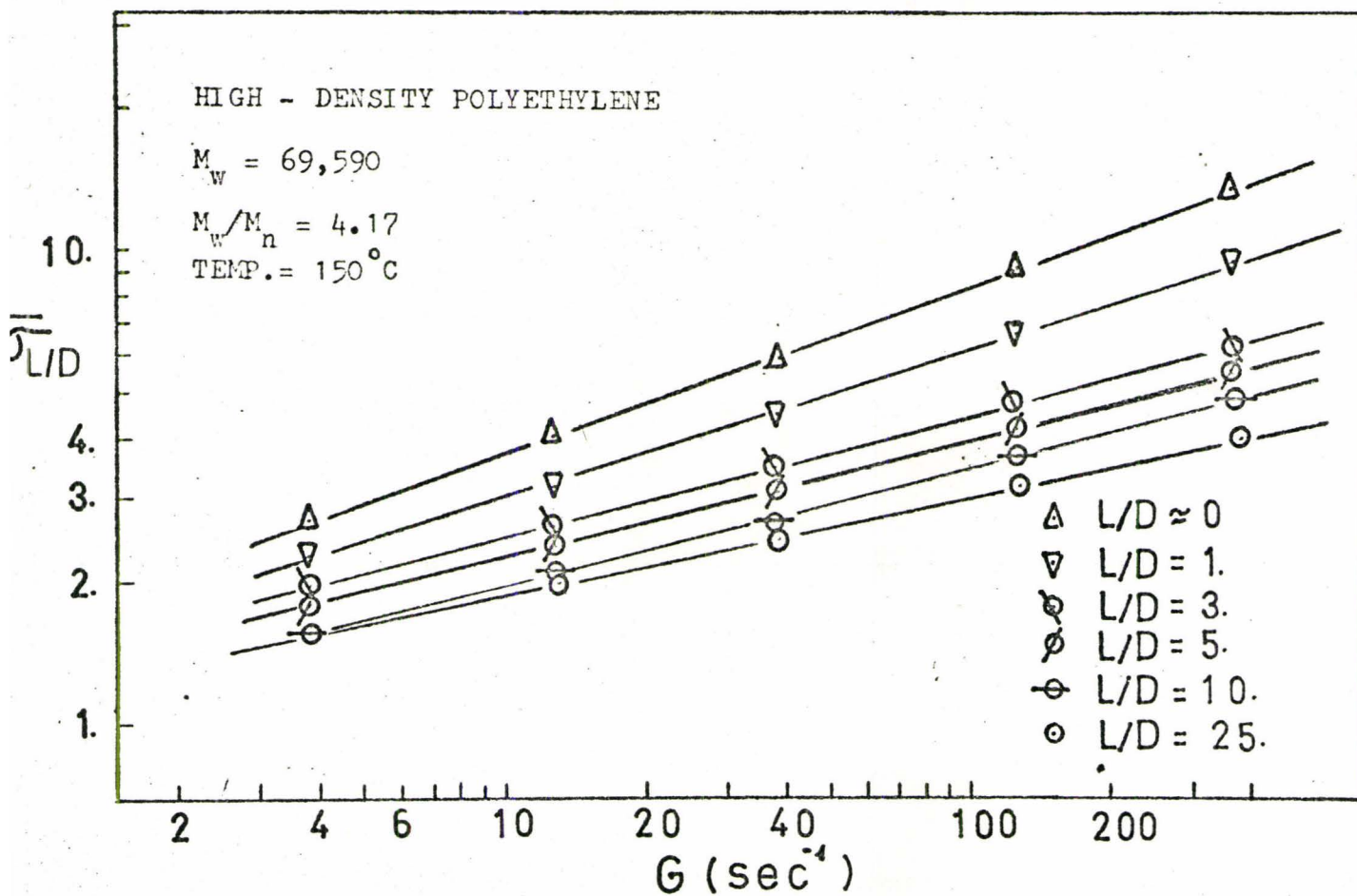
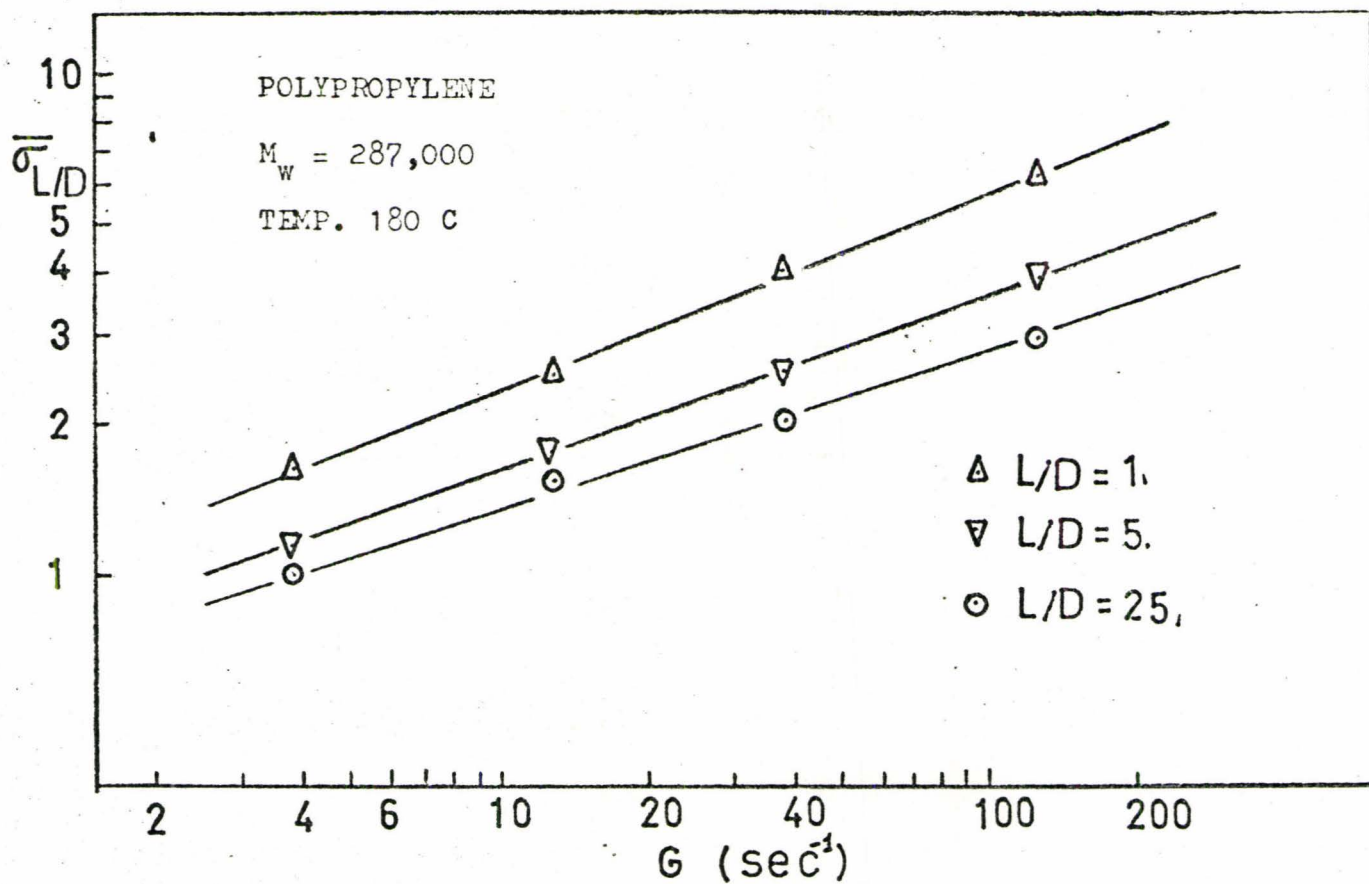


Fig. (6.11) Plot of average recoverable shear strain vs. pseudo shear rate.



Fig(6.12)Plot of γ_0 average recoverable shear strain vs. pseudo shear rate for Polypropylene

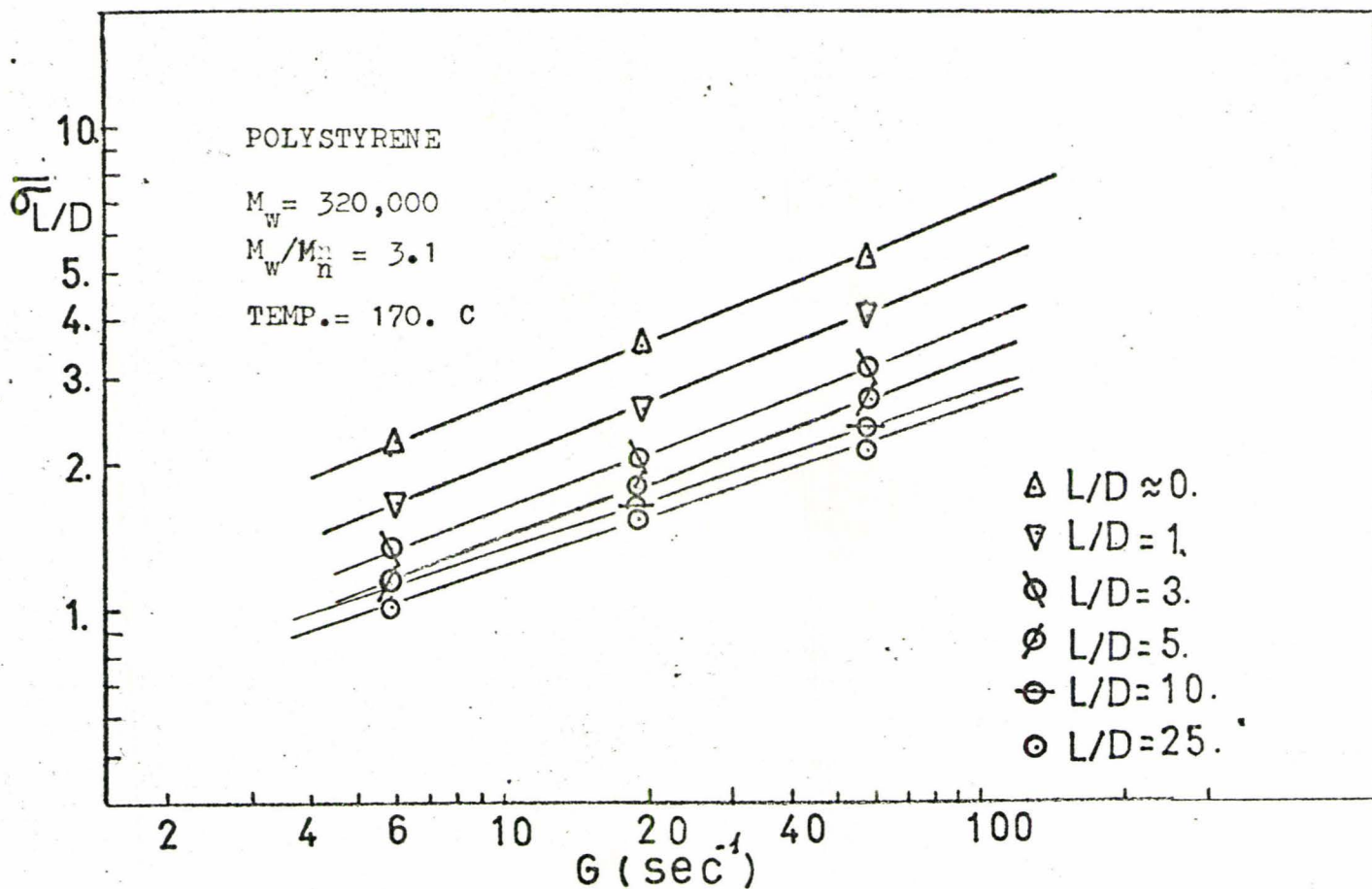


Fig.(6.13) Plot of average recoverable shear strain vs. pseudo shear rate for Polystyrene.

Figures (6.10) to (6.13) are the plots of $\bar{\sigma}_{L/D}$ versus G for polymers studied.

It appears that the plots do give the straight lines particularly for long capillaries (long enough to obtain a die swell index, d/D , at equilibrium value).

The values of the slopes of the plots $\bar{\sigma}_{L/D}$ versus G on logarithmic paper and the exponential values of the power law fluids are tabulated in Table (6.7). The difference between the two values may come from many sources. The molten polymers do not follow the power law exactly, hence $n^{(*)}$ is obtained with uncertainty. Secondly, because of the crudeness of the experimental determination of B , the recoverable shear strain obtained from die swell of extruded polymers is also an approximated value.

Table 6.7

	M_w	M_w/M_n	$n^{(*)}$	$n^{(**)}$
LDPE	53,500	3.0	0.44	0.37
HDPE	69,500	4.17	0.56	0.20
POLYPRO.	287,000	--	0.50	0.31
POLYSTYRENE	320,000	3.1	0.27	0.32

(*) Exponent of power law fluid obtained from the plot of τ_w versus G on logarithmic paper.

(**) Slope of the plot $\bar{\sigma}_{L/D}$ versus G on logarithmic paper for long capillary $L/D = 25$.

The plots of $\bar{\sigma}_{L/D}$ versus G for short capillaries have the tendency to shift upward (Fig 6.10 to 6.13). This phenomenon clearly indicates a change of recoverable shear strain along the capillary.

To elucidate the phenomenon, the relationship between recoverable shear strains for short and long capillaries is obtained as following:

Let $\bar{\sigma}_\infty$ and $\bar{\sigma}_{L/D}$ be the recoverable shear strains for infinitely long capillary and the one with dimensions ratio L/D respectively.

The plots of $\text{Ln}\left(\frac{\bar{\sigma}_{L/D}}{\bar{\sigma}_\infty}\right)$ versus (L/D) are shown in Figures (6.14)

to (6.15). The following equation is proposed for the relationship between $\bar{\sigma}_{L/D}$ and $\bar{\sigma}_\infty$

$$\text{Ln}\left(\frac{\bar{\sigma}_{L/D}}{\bar{\sigma}_\infty}\right) = A\left(\frac{L}{D}\right)^a \quad (6.10)$$

The data are best fitted by Equation (6.10). The constant A's and a's are tabulated in Tables (6.8) to (6.11)

It is interesting to notice that "a" depends only on polymer characteristics and nearly independent of pseudo shear rate (G)

"A" depends on shear rate (G) and equals to $\text{Ln}\left(\frac{\bar{\sigma}_{L/D}}{\bar{\sigma}_\infty}\right)_{L/D=1}$.

Equation (6.10) could be written as:

$$\text{Ln } \bar{\sigma}_\infty = \text{Ln}(\bar{\sigma}_{L/D}) - A\left(\frac{L}{D}\right)^a \quad (6.11)$$

TABLE 6.8

LDPE	$\bar{M}_w = 53,500$	$\bar{M}_w/\bar{M}_n = 3.00$	$T = 150^\circ\text{C}$	
G(Sec ⁻¹)	3.8	12.8	38.0	128.0
A	1.35	1.59	1.8	2.05
a	-.976	-.970	-.925	-.954

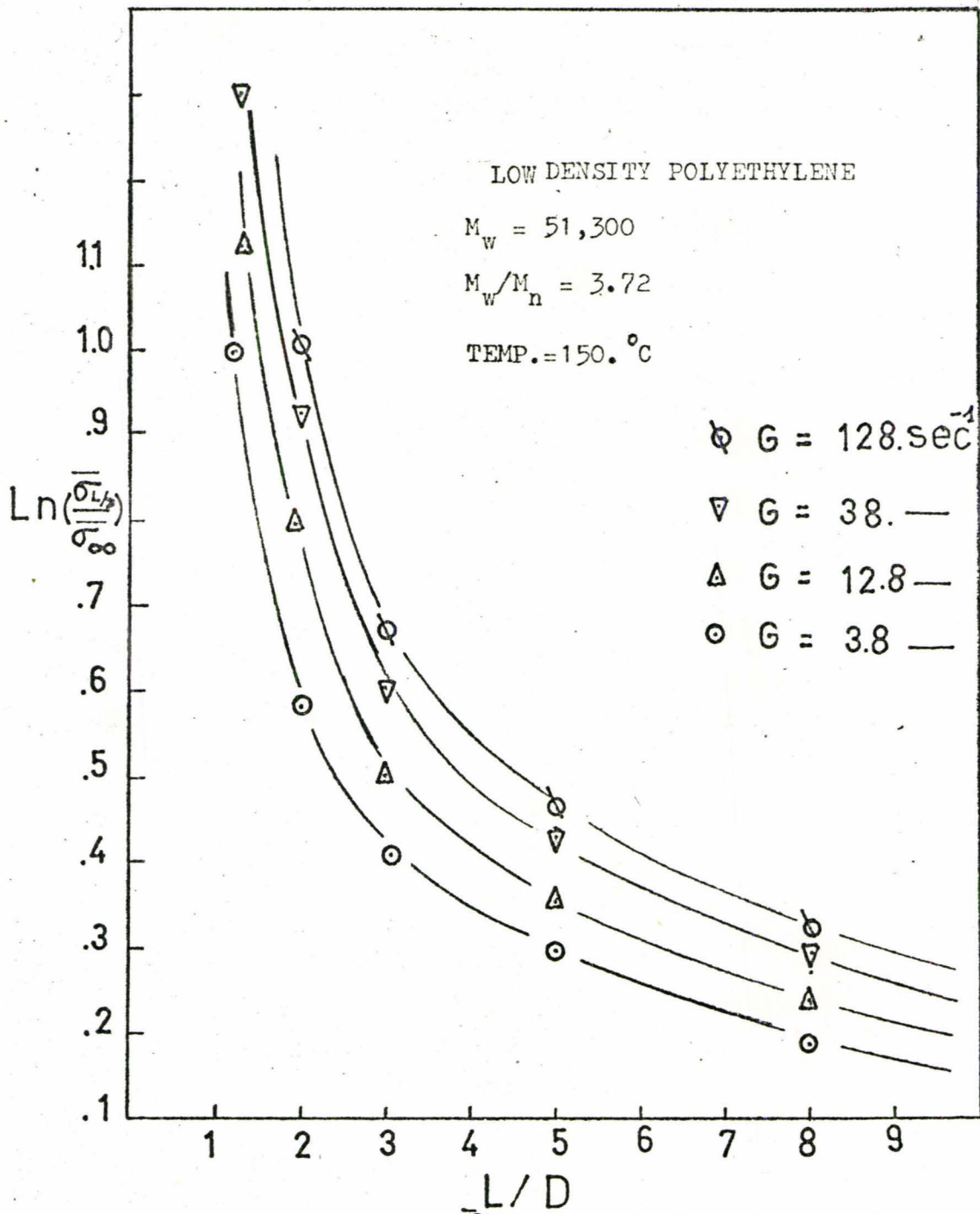


Fig. (6.14) Plot of $\text{Ln}\left(\frac{\sigma_{L/D}}{\sigma_{\infty}}\right)$ vs. L/D for High density polyethylene

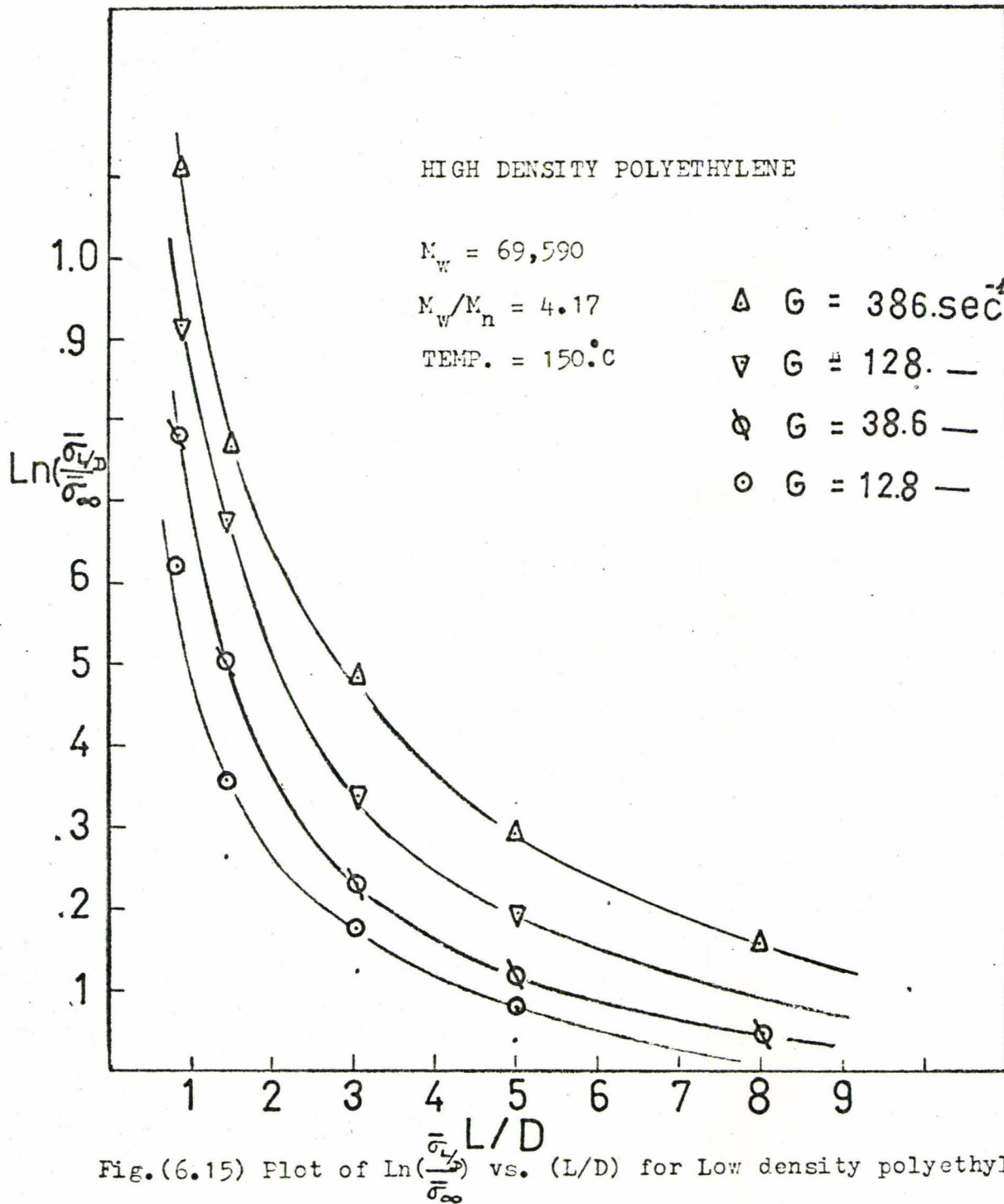


TABLE 6.9

HDPE: $\bar{M}_w = 69,590$ $\bar{M}_w/\bar{M}_n = 4.17$ $T = 150^\circ\text{C}$

$G(\text{Sec}^{-1})$	12.8	38.0	128.0	386.0
A	.64	.78	1.02	1.32
a	-.790	-.805	-.795	-.814

TABLE 6.10

POLYPROPYLENE: $\bar{M}_w = 287,000$ $T^\circ = 180^\circ\text{C}$

$G(\text{Sec}^{-1})$	12.8	38.8	128.0
A	1.35	2.2	2.8
a	-1.46	-1.39	-1.37

TABLE 6.11

POLYSTYRENE (HF-55) $\bar{M}_w = 320,000$ $\bar{M}_w/\bar{M}_n = 3.1$ $T = 170^\circ\text{C}$

$G(\text{Sec}^{-1})$	5.8	19.3	58.0
A	1.4	1.4	1.6
a	-1.7	-1.36	-1.22

The relationship between $\bar{\sigma}_{L/D}$ and $\bar{\sigma}_\infty$ could be used to estimate the die swell from short capillaries once "A" and "a" are obtained for a particular polymer. However, the relationships between "A" and "a" to polymer characteristics are still needed to be understood.

VII CONCLUSIONS

An INSTRON Rheometer has been used to study the polymer die swell. Based on the result of the experiment, the following conclusions could be made:

- 1) Die swell increases with shear rate
- 2) Die swell increases with shear stress
- 3) Die swell of low density polyethylene is not affected by temperature
- 4) Die swell strongly depends on the distribution of molecular weights; the broader the distribution, the larger the swelling ratio.
- 5) Swelling ratio decays exponentially with the ratio length to the diameter of the capillary for all polymers studied
- 6) The importance of Deborah number in polymer processing is still unknown, however, die swell is not solely dependent on this number.
- 7) Recoverable shear strain for short capillaries could be estimated from the knowledge of its value at equilibrium and polymer characteristic, thus die swell for short capillaries could be calculated backward through the model, $\bar{\sigma}_{L/D} = f(d/D)$, for die swell

VIII SUGGESTIONS

- 1) It is observed that frozen effect of extrudate has made the exact value of swell diameter impossible to obtain. To overcome this difficulty, the extrudate polymer should be annealed in an inert oil.
- 2) Further work could be devoted to investigate the effect of molecular weight and molecular weight distribution on the exponential decay curve of die swell versus L/D. Standard polystyrene could be used to carry out this work. The mechanism of swelling process could be complicated, however, clear understanding the effect of molecular weight and molecular weight distribution on the decay of swelling could somehow elucidate the answer for the problem.
- 3) As a good try, we could follow the line suggested by Kawasaki⁽²⁰⁾ by using a better model to explain the die swell phenomenon.
- 4) It is worthwhile to use standard polystyrene to investigate the effect of Deborah number on "die swell".

IX NOMENCLATURE

a	Constant defined by Equation (6.10)
A	Constant defined by Equation (6.10)
B	Die swell index (d/D)
B_0	Die swell index of zero length capillary
B_∞	Die swell index of infinite long capillary
c	Decay constant defined by Equation (6.5)
C	Polymer concentration
C_1	Constant in Mooney Equation (Eq. 3.7)
d	Extrudate diameter at extrusion temperature (inch)
d_0	Diameter of extrudate polymer at room temperature (inch)
D	Capillary diameter (inch)
E_0	Entanglement density at zero shear
f_b	Magnitude of force per unit cross-sectional area defined by Equation (3.12) (dynes/cm ²)
G	Pseudo shear rate (Sec ⁻¹)
G_0	Elastic shear modulus (dynes/cm ²)
I_1, I_2, I_3	Strain invariants defined by Equations (3.8) - (3.10)
J_0	Shear compliance (cm ² /dynes)
J_R	Rouse shear compliance defined by Equation (5.3)
K	Constant for power law fluid
k	Boltzmann's constant (erg molecule ⁻¹ °K ⁻¹)
L	Capillary length (inch)
L_e	Entrance length (inch)
L_s	Length of steady state region in capillary (inch)
M	Molecular weight
\bar{M}_n	Number average molecular weight
\bar{M}_w	Weight average molecular weight
\bar{M}_z	z average molecular weight
\bar{M}_{z+1}	(z+1) average molecular weight

N	End correction in capillary flow
Na	Concentration in molecules per unit volume (cm^{-3})
n	Exponent of power law fluid
P	Pressure (dynes/cm^2)
Q	Volume flow rate (inch^3/sec)
R	Capillary radius (inch)
R_g	Ideal gas constant ($\text{gm.cm}^2 \text{ sec}^{-2} \text{ g. mole}^{-1} \text{K}^{-1}$)
t_a	Average residence time (sec.)
t_{xx}	Tensional stress defined by equation (3.16)
T	Temperature ($^{\circ}\text{C}$ or $^{\circ}\text{K}$)
\bar{V}	Velocity vector
V_r, V_{θ}, V_z	Vector components of velocity (unit/sec)
W_i	Weight fraction of i - th component of polymer
\bar{W}	Stored energy function

GREEK LETTERS

$\dot{\gamma}_w$	True shear rate at the wall (sec^{-1})
Γ	Pseudo shear rate
μ	Non-Newtonian viscosity ($\text{gm/cm}\cdot\text{sec}$)
μ'	Dynamic viscosity
θ	Time constant, general
θ_μ	Viscosity curve time constant, see Figure 6.5
θ_μ	Dynamic viscosity time constant, see Figure 6.5
θ_R	Time constant, Rouse theory
θ_T	Tobolsky time constant
θ_w	Time constant, William's theory
θ_o	Time constant, Graessley's theory
θ_t	Average residence time (sec.)
λ	Extension ratio
$\lambda_1, \lambda_2, \lambda_3$	Principal extension ratios
ρ	Density (gm/cc)
ρ_o	Density of frozen polymer (gm/cc)
σ	Recoverable shear
$\bar{\sigma}$	Recoverable shear averaged over cross sectional area
$\bar{\sigma}_{L/D}$	Average recoverable shear strain of capillary having L/D dimensions
$\bar{\sigma}_\infty$	Average recoverable shear strain of infinite long capillary
τ_{12}	Shear stress (dynes/cm^2)
τ_{11}, τ_{12}	Normal stress (dynes/cm^2)
τ_t	Tensile stress (dynes/cm^2)
τ_w	True shear stress at the wall (dynes/cm^2)

X REFERENCES

- 1) Arai, T. and H. Aoyama
Trans. Soc. of Rheology., 7, 333 (1965)
- 2) Bagley, E. B.,
J. Appl. Phys., 28, 624 (1957).
- 3) Bagley, E. B. and H. J. Duffey,
Trans. Soc. of Rheology, 14 (4), 545 (1970).
- 4) Bagley, E. B., A. A. Mendelson and F. L. Finger,
Paper presented at National ACS Meeting, L.A.
March 29, April 2, 1971.
- 5) Bagley, E. B., S. H. Storey and D. C. West,
J. Appl. Polymer Science, 7, 1661 (1963).
- 6) Bernstein, E. B., A. Kersley and L. J. Zapas,
Trans. Soc. of Rheology, 7, 391 (1963).
- 7) Beynon, D. L. T. and B. S. Glyde,
Brit. Plastics, 33, 414 (1960).
- 8) Bradley, R. S. "The phenomenon of fluid motion"
Addison Wesley, Canada (1967).
- 9) Brydson, J. A., "Flow properties of polymer melts"
Van Nostrand Reinhold Co., New York (1970).
- 10) Burgess, H. and H. I. Lewis.
Brit. Plastics, 34 (3), 177 (1961).
- 11) Clegg, P. L.,
Brit. Plastics, 39, 96 (1966).
- 12) Coleman, B. D. and H. Markovitz,
J. Appl. Physics, 35, 1 (1964).
- 13) Dillon, J. H. and N. Johnston,
Physics, 4, 225 (1933).
- 14) Edwards, R, Tappi, J. of Polymer Science
49 (4), 55A (1966).
- 15) Graessley, W. W.,
J. Chem. Phys., 47, 1942 (1967).
- 16a) Goren, S. L., S. Middleman and J. Gavis,
J. Appl. Polymer Science, 3 (9), 367 (1960).
- 16b) Graessley, W. W. and L. Segal,
Macromolecules, 2, 49 (1969).

REFERENCES CONT'D

- 17) Graessley, W. W., S. D. Glasscock, and R. L. Crawley,
Trans. Society of Rheology, 14 (4), 519 (1970).
- 18) Harris, E. K.,
Ph. D. Thesis, University of Wisconsin, (1970).
- 19) Huseley, T. W. and C. G. Gogos,
Polymer Eng. Sci., 5 (3), 130 (1965).
- 20) Kawasaki, Tatsusaka and Ono,
Kokunski Kagaku, Vol. 30, No. 338, pp. 326-331 (1973).
- 21) Kruse, R. L.,
J. Polymer Science, 2 (9), 841 (1964).
- 22) Horie, M.
M. Eng. Thesis, McMaster University, Hamilton. (1972)
- 23) Lidorikis, S.,
M. Eng. Thesis, McMaster University, Hamilton.(1970)
- 24) McInstosh, "Elastic effects in the extrusion of polymer solutions",
Doctoral Thesis, Washington University, St. Louis, 1960.
- 25) Metzner, A. B., J. L. White and M. M. Denn,
Chemical Engineering Progress, 81, December 1966.
- 26) Mooney, M., "Rheology (F.R.Eirich, Ed.),
Vol. 11., Academic Press, New York (1958).
- 27) Nakajima, M., and M. Shida,
Trans. Soc. Rheol., 10 (1), 299 (1966).
- 28) Rogers, M. G.,
J. of Appl. Polymer Science, Vol. 14, 1679 (1970).
- 29) Seiglauff, C. K.,
Soc. Plastics Engrs. Transaction, 4 (2), 129 (1964).
- 30) Smelkov, R. E. and N. A. Kozulin,
Zh. Prikl. Khim 35 (12), 2698, (1962).
- 31) Spencer, R. S., R. E. Dillon,
J. Colloid Sci., 3, 163 (1948).
- 32) Tanner, R. I.,
J. Polymer Science (A2), 8, 2067 (1970).
- 33) Treloar, L. R. G,
"The physics of rubber elasticity", Oxford University Press,
(1967).
- 34) Tobolsky, A. V., H. Mark,
"Physical chemistry of High polymeric system", 2nd ed., Inter-
science, N. Y. (1950).

REFERENCES CONT'D

- 35) Vlachopoulos, J., M. Horie, S. Lidorikis, paper presented at the
? Knoxville meeting of the Soc. Rheol., (1971), to appear in *Tras. Soc. Rheol.*
(1972)
- 36) Wechsler, R. L. and T. H. Baylis,
Mod. Plastics, 36, 107 (1959).
- 37) Wilson, W. R. K.,
International Congress Technol.
Plastic Process, Proc. Discuss., Amsterdam (1960).
- 38) Williams, M. C.,
J. Chem. Phys., 42, 2988 (1965).

APPENDIX I

EXPERIMENTAL DATA
RESULTS OF EXPERIMENTAL MEASUREMENTS

Low Density Polyethylene (0701)

$$\bar{M}_w = 51,300$$

$$\bar{M}_w / \bar{M}_n = 3.72$$

Temperature = 150°C

L/D	$P \times 10^{-6}$ (Dynes/cm ²)	$4Q/\pi R^3$ (Sec ⁻¹)	d/D	(d/D)*=B	$(B^4 + \frac{2}{B^2} - 3)^{1/2}$
1	1.90	3.866	1.645	1.696	2.44
	3.62	12.880	1.924	1.984	3.60
	7.63	38.660	2.095	2.160	4.38
	14.75	128.000	2.362(MF)	2.435	5.67
	26.70	368.000	MF	---	--
2.99	2.86	3.866	1.543	1.591	2.04
	4.57	12.880	1.643	1.700	2.46
	9.53	38.660	1.857	1.915	3.31
	19.83	128.000	1.988	2.050	3.89
	31.79	386.000	MF	---	--
5.01	3.81	3.866	1.524	1.571	1.97
	7.44	12.880	1.666	1.718	2.52
	13.35	38.660	1.828	1.885	3.19
	27.46	128.000	1.933(MF)	1.993	3.98
	42.59	386.000	MF	---	--
9.9	6.35	3.866	1.438	1.483	1.65
	13.79	12.880	1.533	1.581	2.91
	23.20	38.660	1.613	1.663	2.28
	41.45	128.000	1.699	1.752	2.69
	53.69	386.000	MF	---	--
8	4.45	3.866	1.405	1.448	1.53
	8.71	12.880	1.545	1.593	2.05
	18.16	38.660	1.662	1.713	2.51
	32.55	128.000	1.766	1.820	2.91
	52.13	386.000	-MF	---	--

L/D POLYETHYLENE CONTINUED (0701)

L/D	$P \times 10^{-6}$ (dynes/cm ²)	$4Q/\pi R^3$ (Sec ⁻¹)	d/D	(d/D)*=B	$(B^4 + \frac{2}{B^2} - 3)$
16	0.954	3.866	1.334	1.425	1.45
	1.888	12.880	1.443	1.510	1.76
	3.179	38.660	1.542	1.589	2.04
	5.862	128.000	1.632	1.682	2.39
	9.219	386.000	MF	---	--
20	10.810	3.866	1.367	1.390	1.33
	22.060	12.880	1.443	1.487	1.67
	38.140	38.660	1.520	1.567	1.96
	68.790	128.000	1.600	1.649	2.26
	108.720	386.000	MF	---	--
24.8	14.300	3.866	1.324	1.365	1.24
	28.740	12.880	1.400	1.443	1.51
	48.950	38.660	1.474	1.520	1.78
	84.690	128.000	1.571	1.620	2.15
	127.160	386.000	1.625	1.676	2.36
20	1.270	3.866	1.985	2.047	3.87
	2.540	12.880	2.299	2.371	5.37
	6.350	38.660	2.529	2.608	6.60
	14.620	128.000	2.735	2.820	7.70
		386.000	---	---	--
	$\tau_w \times 10^{-5}$ (dyn/cm ²)	$\dot{\gamma}_w$ (Sec ⁻¹)			
	1.36	3.800			
	2.80	17.000			
	4.51	51.800			
	7.41	173.100			
	11.31	894.600			

(*) Corrected for temperature difference

Low Density Polyethylene (0118)

$$\bar{M}_w = 53,500$$

$$\bar{M}_w / \bar{M}_n = 3.00$$

$$\text{Temperature} = 150^\circ\text{C}$$

L/D	$P \times 10^{-6}$ (dynes/cm ²)	τ_w $\times 10^{-5}$	$4Q/\pi R^3$ (Sec ⁻¹)	d/D	d/D*	$(B^4 + \frac{2}{B^2} - 3)$
1	1.80	1.60	3.866	1.533	1.619	2.15
	4.50	3.30	12.880	1.815	1.917	3.31
	9.50	5.10	38.660	2.019	2.133	4.26
	5.00	6.25	128.000	2.190	2.813	5.09
	30.0'	1.31	386.600	MF	MF	--
2.99	2.6		3.866	1.436	1.517	1.77
	6.5		12.880	1.606	1.697	2.44
	12.0		38.660	1.748	1.847	3.03
	25.5		128.000	1.861	1.966	3.52
	40.2		386.600	MF	---	--
5.01	4.5		3.866	1.396	1.475	1.62
	9.8		12.880	1.520	1.605	2.10
	17.0		38.660	1.645	1.738	2.60
	33.5		128.000	1.730	1.827	2.94
	50.5		386.600	MF	---	--
8	7.1		3.866	1.350	1.426	1.45
	13.0		12.880	1.459	1.541	1.86
	23.1		38.660	1.550	1.637	2.22
	43.0		128.000	1.640	1.732	2.57
	63.5		386.600	MF	---	--
9.9	7.9		3.866	1.332	1.407	1.389
	15.4		12.880	1.422	1.502	1.71
	27.2		38.660	1.505	1.590	2.04
	51.5		128.000	1.590	1.680	2.38
	81.0		386.600	MF	---	--
6	13.5		3.866	1.300	1.373	1.27
	26.0		12.880	1.310	1.383	1.306
	89.5		38.660	1.447	1.528	1.81
	68.0		128.000	1.524	1.610	2.11
	108.0		386.600	MF	---	--

LOW DENSITY POLYETHYLENE (0118) CONTINUED

L/D	$P \times 10^{-6}$ (dynes/cm ²)	$4Q/\pi R^3$	d/D	d/D* = B	$(B^4 + \frac{2}{B^2} - 3)^{1/2}$
20	15.4	3.866	1.285	1.357	1.215
	28.0	12.880	1.345	1.420	1.430
	47.5	38.660	1.411	1.491	1.680
	81.5	128.000	1.489	1.573	1.980
	129.0	386.600	1.60C	1.690	2.410
24.8	18.5	3.860	1.282	1.354	1.20
	34.0	12.800	1.336	1.411	1.40
	57.0	38.600	1.390	1.468	1.59
	103.0	128.000	1.461	1.543	1.87
	157.0	386.600	1.563	1.651	2.26
20	.508	3.860	1.790	1.891	3.21
	2.54	12.800	2.134	2.254	4.81
	5.53	38.600	2.410	2.546	6.27
	16.84	128.000	2.650	2.799	7.66
	26.16	386.600	2.708	2.860	8.07
	$\tau_w \times 10^{-5}$ (Dyn/cm ²)	$\dot{\gamma}_w$ (Sec ⁻¹)			
	1.80	4.48			
	3.14	16.47			
	5.09	53.42			
	8.08	173.56			
	13.80	571.8			

(*) Corrected for temperature difference

High Density Polyethylene (7930)

$$\bar{M}_w = 69,590$$

$$\bar{M}_w / \bar{M}_n = 4.17$$

Temperature = 150°C

L/D	$P \times 10^{-6}$ (Dyn/cm ²)	$4Q/\pi R^3$	d/D	(d/D)*=B	$(B^4 + \frac{2}{B^2} - 3)^{1/2}$
0	0	3.866	1.804	1.906	2.65
	.47	12.880	1.986	2.098	4.09
	2.73	38.660	2.325	2.456	5.80
	8.26	128.000	2.850	3.010	8.90
	16.52	386.000	3.430	3.620	12.99
1	.31	3.860	1.571	1.660	2.29
	1.71	12.880	1.777	1.870	3.12
	4.45	38.600	2.057	2.170	4.41
	10.49	128.000	2.453	2.590	6.50
	20.98	386.000	2.886	3.050	9.15
2.99	1.59	3.860	1.491	1.575	1.99
	3.49	12.800	1.650	1.740	2.61
	8.45	38.600	1.830	1.930	3.36
	18.75	128.000	2.102	2.221	4.65
	33.69	386.000	2.541	2.684	6.15
5.01	3.05	3.860	1.448	1.529	1.82
	6.35	12.800	1.590	1.679	2.37
	12.07	38.600	1.740	1.840	3.00
	24.79	128.000	1.970	2.080	4.02
	43.61	386.000	2.362	2.498	5.30
8	4.45	3.860	1.410	1.560	1.93
	6.35	12.800	1.523	1.610	2.11
	14.62	38.600	1.693	1.788	2.80
	29.88	128.000	1.899	2.006	3.68
	50.23	386.000	2.175	2.290	4.98
9.9	4.45	3.860	1.390	1.468	1.60
	10.80	12.800	1.505	1.591	2.04
	22.25	38.600	1.652	1.740	2.61
	43.23	128.000	1.850	1.950	3.46
	74.38	386.000			4.65

HIGH DENSITY POLYETHYLENE (7930) CONTINUED

L/D	$P \times 10^{-6}$ (Dyn/cm ²)	$4Q/\pi R^3$	d/D	$(d/D)*=B$	$(B^4 + \frac{2}{B} - 3)^{1/2}$
16	6.99	3.860	1.385	1.463	1.58
	15.26	12.880	1.519	1.605	2.09
	20.88	38.600	1.638	1.730	2.57
	58.49	128.000	1.805	1.900	3.25
	97.28	368.000	2.000	2.112	4.16
20	12.71	3.860	1.375	1.450	1.54
	21.61	12.880	1.502	1.587	2.03
	38.78	38.600	1.620	1.710	2.49
	71.84	128.000	1.774	1.874	3.14
	120.08	368.000	1.961	2.070	3.97
24.8	12.71	3.860	1.375	1.468	1.60
	25.42	12.880	1.491	1.575	1.99
	47.68	38.600	1.600	1.690	2.42
	95.45	128.000	1.740	1.840	3.01
	157.00	368.000	1.940	2.050	3.89
	$\tau_w \times 10^{-5}$ (Dyn/cm ²)	$\dot{\gamma}_w$ (Sec ⁻¹)			
	1.11	3.890			
	2.54	14.920			
	4.97	45.970			
	9.13	161.210			
	14.68	595.200			

(*) Corrected for temperature difference

Polypropylene (PP-5820)

 $\bar{M}_w = 287,000$

Temperature = 180°C

L/D	$P \times 10^{-6}$ (Dyn/cm ²)	$4Q/\pi R^3$ (Sec ⁻¹)	d/D=B	$(B^4 + \frac{2}{B^2} - 3)^{1/2}$
0.99	1.27	3.860	1.472	1.61
	2.48	12.800	1.703	2.47
	4.45	38.600	2.082	4.02
	9.53	128.000	2.533	6.20
	17.80	386.000	3.133	9.67
5.01	2.09	3.860	1.350	1.16
	4.57	12.800	1.514	1.76
	8.90	38.600	1.716	2.52
	16.63	128.000	2.036	3.83
	27.33	386.000	2.577	6.43
9.9	3.49	3.860	1.330	1.12
	7.63	12.800	1.476	1.63
	13.98	38.600	1.620	2.15
	25.43	128.000	1.880	3.17
		386.000	---	
16	13.35	3.860	1.300	1.07
	21.61	12.800	1.409	1.39
	36.87	38.600	1.586	2.03
	58.48	128.000	1.807	2.87
20	6.99	3.860	1.300	1.016
	14.62	12.800	1.448	1.53
	25.43	38.600	1.565	1.95
	44.50	128.000	1.794	2.82
	69.29	386.000	---	--
24.8	8.90	3.860	1.300	1.01
	18.43	12.800	1.452	1.53
	31.78	38.600	1.575	1.99
	54.67	128.000	1.830	2.848
	83.91	386.000	---	--

 $\tau_w \times 10^{-5}$
(dynes/cm²)

0.83
1.57
2.60
4.64
6.90

 γ_w
(Sec⁻¹)

4.58
16.50
48.60
144.25
658.90

Polystyrene Commercial HF-55

$$\bar{M}_w = 320,000$$

$$\bar{M}_w/\bar{M}_n = 3.1$$

$$\text{Temperature} = 170^\circ\text{C}$$

L/D	$P \times 10^{-6}$ (Dynes/cm ²)	$4Q/\pi R^3$ (Sec ⁻¹)	(d/D)*=B	$(B^4 + \frac{2}{B^2} - 3)^{1/2}$
0	.318	5.80	1.640	2.23
	2.100	19.34	1.975	3.56
	4.190	58.00	2.361	5.36
	12.080	193.40	-MF	--
1	3.180	5.80	1.485	1.664
	6.420	19.34	1.733	2.585
	9.920	58.00	2.019	4.060
	19.720	193.40	-MF	---
3	5.090	5.80	1.382	1.302
	9.920	19.38	1.591	2.048
	15.650	58.00	1.875	3.151
	27.990	193.40	---	---
	44.530	580.00	---	---
5	5.720	5.80	1.330	1.122
	12.470	19.38	1.519	1.787
	20.740	58.00	1.758	2.770
	34.350	193.40	---	---
	52.160	580.00	---	---
10	12.720	5.80	1.310	1.053
	23.280	19.38	1.470	1.610
	36.000	58.00	1.670	2.340
	54.710	193.40	---	---
	76.330	580.00	---	---
16.1	17.100	5.80	1.295	1.002
	32.820	19.38	1.457	1.565
	51.910	58.00	1.626	2.178
	78.880	193.40	---	---
	108.800	580.00	---	---
20	22.900	5.800	1.291	.990
	42.360	19.380	1.445	1.520
	64.630	58.000	1.606	2.100
	96.690	193.400	---	---
	130.400	580.000	---	---

POLYSTYRENE COMMERCIAL HF-55 CONTINUED

L/D	$P \times 10^{-6}$ (Dyn/cm ²)	$\frac{4Q}{\pi R^3}$ (Sec ⁻¹)	(d/D)*=B	$(B^4 + \frac{2}{B^2} - 3)^{1/2}$
24.8	31.87	5.80	1.300	1.019
	53.81	19.38	1.450	1.540
	79.90	58.00	1.597	2.070
	117.68	193.40	---	---
	159.03	580.00	---	---
	$\tau_w \times 10^{-5}$ (Dyn/cm ²)	$\dot{\gamma}_w$ (Sec ⁻¹)		
	2.90 (3.05)	5.80		
	4.98 (5.09)	28.35		
	7.31	84.07		
	10.22 (10.32)	341.58		
	12.83 (13.30)	681.60		

(*) Corrected for temperature difference.

Commercial Polystyrene (HT42-1)
Temperature = 170°C

L/D	$P \times 10^{-6}$ (Dyn/cm ²)	$4Q/\pi R^3$	(d/D)*=B	$(B^4 + \frac{2}{B^2} - 3)^{1/2}$
0	1.59	5.80	1.753	2.660
	5.72	19.38	2.076	4.004
	9.86	58.00	2.461	5.830
	19.08	193.80	---	---
1	4.13	5.80	1.505	1.735
	9.54	19.38	1.762	2.770
	17.17	58.00	2.088	4.050
	29.89	193.80	---	---
50.89	580.00	---	---	
2.99	7.31	5.80	1.379	1.291
	13.99	19.38	1.599	2.080
	22.26	58.00	1.850	3.050
	36.26	193.80	---	---
8	14.31	5.80	1.312	1.060
	26.08	19.38	1.478	1.640
	40.07	58.00	1.659	2.300
	61.07	193.80	---	---
92.24	580.00	---	---	
9.9	20.67	5.80	1.320	1.088
	34.98	19.38	1.472	1.620
	50.25	58.00	1.643	2.242
	73.79	193.80	---	---
16.1	28.30	5.80	1.312	1.060
	48.98	19.38	1.441	1.508
	70.61	58.00	1.593	2.056
	102.40	193.40	---	---
20	34.66	5.80	1.310	1.053
	58.52	19.38	1.429	1.470
	85.88	58.00	1.581	2.010

COMMERCIAL POLYSTYRENE (HT42.1)

L/D	$P \times 10^{-6}$ (Dyn/cm ²)	$4Q/\pi R^3$	(d/D)*=B	$(B^4 + \frac{2}{B^2} - 3)^{1/2}$
24.8	42.30	5.80	1.310	1.053
	71.88	19.38	1.430	1.470
	106.87	58.00	1.593	2.056
	151.40	193.80	---	---
	$\tau_w \times 10^{-5}$ (Dyn/cm ²)	$\dot{\gamma}_w^{-1}$ (Sec ⁻¹)		
	4.13	7.54		
	6.80	27.03		
	9.51	98.77		
	12.70	485.30		
	17.10	892.80		

(*) Corrected for temperature difference

DATA TO INVESTIGATE TEMPERATURE EFFECT ON
DIE SWELL OF LOW DENSITY POLYETHYLENE

Low Density Polyethylene

$$\bar{M}_w = 53,500$$

$$\bar{M}_w / \bar{M}_n =$$

$$T = 150^\circ\text{C}$$

$$L/D = 40$$

	G (pseudo shear rate) Sec ⁻¹	Force (lb)	Die Swell (d/D)*
T=150°C	3.86	57.3	1.223
	12.80	98.0	1.245
	38.60	160.0	1.291
	128.00	273.0	1.323
	386.00	428.0	1.378
T=170°C	3.86	37.3	1.221
	12.80	71.0	1.243
	38.60	122.0	1.297
	128.00	212.0	1.327
	386.00	345.0	1.384
T=190°C	3.86	24.3	1.217
	12.80	52.0	1.245
	38.60	72.0	1.255
	128.00	165.0	1.291
	386.00	278.0	1.354
T=210°C	3.86	16.3	1.096
	12.80	36.0	1.100
	38.60	68.0	1.280
	128.00	126.0	1.315
	386.00	218.0	1.374

(*) Corrected for temperature difference